Title

Biotic Response to Paleoenvironmental Change in the Ediacaran and Early Cenozoic

Permalink

https://escholarship.org/uc/item/29402215

Author

Hall, Christine Meriwether Solon

Publication Date

2019

UNIVERSITY OF CALIFORNIA
RIVERSIDE

Biotic Response to Paleoenvironmental Change in the Ediacaran and Early Cenozoic

A Dissertation submitted in partial satisfaction
of the requirements for the degree of

Doctor of Philosophy

in

Geological Sciences

by

Christine Meriwether Solon Hall

June 2019

Dissertation Committee:
        Dr. Mary L. Droser, Co-Chairperson
        Dr. Sandra Kirtland Turner, Co-Chairperson
        Dr. Nigel Hughes

The Dissertation of Christine Meriwether Solon Hall is approved:

_____

_____

Committee Co-Chairperson

_____

Committee Co-Chairperson

University of California, Riverside

ACKNOWLEDGEMENTS

ABSTRACT OF THE DISSERTATION

Biotic Response to Paleoenvironmental Change in the Ediacaran and Early Cenozoic

by

Christine Meriwether Solon Hall

Doctor of Philosophy, Graduate Program in Geological Sciences
University of California, Riverside, June 2019
Dr. Mary L. Droser, Co-Chairperson
Dr. Sandra Kirtland Turner, Co-Chairperson

The effects of changes to environments on Earth in the past have been well

documented, and we have fossil evidence of how organisms responded to these

changes. In the past, possible responses to environmental change have ranged from

extinction and origination to migration to physical morphological changes. As we are

currently facing the prospect of dramatic alterations to Earth's environments,

understanding how life responded in the past may be one of our best opportunities to

gauge how future scenarios might play out.

Here I present new data detailing how two different groups of organisms were living in

fluctuating environments at two times in Earth's history. During the Ediacaran there was

a unique subset of organisms with three-fold symmetry that went extinct before the

beginning of the Cambrian. Although they were relatively abundant and diverse,

representing ~12-15% of the taxonomic diversity of the second (White Sea) Ediacaran

assemblage, no animals at any point afterwards have had tri-radially symmetric body

plans. I show that most of these tri-radial taxa share many morphological and ecological

similarities beyond their distinctive body plan and were likely related members of a tri-

radial clade. Furthermore, there is evidence that multiple tri-radial taxa were

generalists, able to survive in a wide variety of environments, indicating that a relatively

sharp environmental change would have been necessary to eliminate this group.

An almost opposite scenario is true for deep-sea ostracodes during Eocene Thermal

Maximum 2 (ETM2) in the equatorial and North Atlantic. Using high-resolution sampling

from ocean drill cores (ODP Site 1258 and IODP Site U1409) I show that, although this

was a relatively smaller event than the preceding Paleocene-Eocene Thermal Maximum,

ostracodes respond in noticeable ways. Ostracode diversity and abundance (as

measured by accumulation rate) remain low throughout the duration of ETM2.

Additionally, the dominant species in these cores exhibit a size decrease that is also

correlated with the event. Despite showing these clear signals of having been impacted

by ETM2, no ostracode genera disappear completely from either of the sites, indicating

that they were able to adapt and survive the environmental changes they faced.

Table of Contents

Chapter 2: Ostracode Response to an Early Eocene Warming Event in the North and Equatorial Atlantic

Chapter 3: Changes in Ostracode Body Size Across Eocene Thermal Maximum 2 at Two Deep-Sea Sites from the North and Equatorial Atlantic

List of Figures

List of Tables

INTRODUCTION

Our world is, and has been, a dynamic and changing place. Global climate change is one

of the biggest issues facing society today. The 2014 report of the Intergovernmental

Panel on Climate Change (IPCC) states that "in recent decades, changes in climate have

caused impacts on natural and human systems on all continents and across the oceans"

and that we are facing the prospect of severe, widespread, and irreversible impacts

globally. These impacts, encompassing a wide range of changes to local and global

environmental systems, will have consequences for all organisms, including humans,

living on Earth.

While climate change is undoubtedly occurring, the magnitude, timing, and scope both

of the environmental changes and the consequences these changes will have are less

certain. It is difficult to know exactly what scenario to expect and even then how to

prepare for it. In order to make informed decisions about how to proceed, it is

important to understand as many of the possible effects climate change will have as

possible. By evaluating all the possible impacts, ranging from extinctions to smaller

effects on individual organisms, we will be able to better constrain the possible future

situations.

It is no surprise then that lot of research has been focused on predicting how, and how

quickly, environments will change and what the impact of these changes will be on the

organisms living in these environments. The reality is that we have run similar experiments on this planet in the past. While the rates of change we are currently experiencing are unprecedented, environments have been changing since Earth's formation. The geologic and fossil records document these changes and how life, once it evolved, responded to them. By investigating these records of change in the past, we can begin to understand what the future might hold for life on Earth in the midst of global climate change.

The Ediacaran Period

Before the Ediacaran Period, life on Earth was largely composed of small, simple organisms, and fossil evidence for these organisms is very limited (Erwin et al., 2011; Knoll, 2011). Arising approximately 575 million years ago, the Ediacara Biota represents the oldest communities of macroscopic metazoan fossils preserved on Earth (Droser and Gehling, 2015). This unique fauna is composed of generally soft-bodied, morphologically diverse organisms whose taxonomic affinities relative to life from later periods in Earth's history remain largely enigmatic (Xiao and Laflamme, 2009).

The evolution of complex metazoan life, including the Ediacara Biota, is thought to be, at least partially, the result of changing environmental conditions, notably oxygen levels, in the ocean-atmosphere system (Canfield et al., 2007; Knoll, 2011; Lyons et al., 2014). The Ediacara Biota has been divided into three main temporal-geographic assemblages,

each composed of a relatively unique set of taxa (Boag et al., 2017; Droser et al., 2017; Waggoner, 2003). As with the emergence of the fauna as a whole, the differences in taxa between the three assemblages have been related to fluctuations in oxygen levels during the Ediacaran. These fluctuations were likely responsible both for the emergence of new taxa with higher oxygen demands as oxygen levels increased, and for the loss of those organisms as oxygen levels later dropped (Evans et al., 2018). These taxa, which are not found again in the fossil record, largely seem to represent early evolutionary experiments that went extinct after failing to cope with changes to their environment. While not considered one of the 'big five' mass extinctions, the disappearances of Ediacara taxa signify an early example of how changes to the environment can greatly impact the composition and diversity of life on Earth. Indeed, the uniqueness of the taxa of this time, relative to any other time before or after, is largely responsible for the difficulty we have today with even identifying how these groups fit in to the evolutionary tree.

By studying these organisms, we can investigate how early complex communities interacted with their environment and how successful different groups were. Their lack of well-defined taxonomic affinities forces us to look more closely at other aspects of these organisms, such as their morphology and ecology, and how changes in these areas specifically were related to other factors. The exceptional preservation of these

assemblages provides the unique opportunity to look at 'snapshots' in time of life on the seafloor, giving us rare insight into these enigmatic fossil communities.

The Early Cenozoic Era

Several hundred millions of years' worth of environmental change following the Ediacaran led to a very different composition of life on Earth in the Cenozoic (Sepkoski, 1981). In the Paleogene, about 55 million years ago, Earth was experiencing multiple climatic shifts (Kirtland Turner et al., 2014). The most well-known of these, the Paleocene-Eocene Thermal Maximum (PETM), represents a time in Earth's history where the rapid input of a large amount of isotopically light carbon to the ocean and atmosphere systems resulted in a relatively rapid rise in global temperatures, along with a host of other environmental shifts (Dunkley Jones et al., 2013; Greene et al., 2019; Kirtland Turner, 2018; McInerney and Wing, 2011). Because of this, the PETM, and the several other similar but smaller hyperthermal events that followed in the several million years afterwards, are often considered some of the best analogs we have for understanding the changes we are causing today, and how they might impact life on Earth (Norris et al., 2013).

As a result, these events, particularly the PETM, have received a lot of research attention in the last couple decades. The effects of these large carbon inputs into the ocean-atmosphere, including temperature changes, ocean acidification, changing sea

level and circulation, and changing nutrient and dissolved ion levels, have been well

documented, as have organisms' responses to them (Brierley and Kingsford, 2009;

Doney et al., 2012; Norris et al., 2013). Extinctions, originations, migrations, and changes

in organisms' biologies and in how they interact have all been correlated with these

events (Norris et al., 2013). These combined efforts have shown that hyperthermal

events have had an impact on the biosphere in the past, and there is every reason to

think that similar changes will continue to impact how organisms live.

By investigating the biotic consequences of hyperthermal events in the past, we are able

to make predictions about the future. Using the different events in the early Cenozoic,

with their varying magnitudes and timescales, enables us to evaluate different possible

future scenarios by looking at the differences in animal responses to a variety of

alternative environmental shifts. This approach can facilitate efforts to understand the

different potential outcomes associated with different magnitudes of environmental

change.

Scope of This Work

In this dissertation, I will investigate how animals responded in two different changing

marine environments at these very different times in Earth's history. Chapter 1

examines the occurrence, ecology, and morphologic diversity of tri-radial taxa, a subset

of organisms with a body plan unique to the Ediacaran that thrived during the 'second-

wave' of the Ediacara Biota, but are not found in later Ediacaran assemblages following

a drop in oxygen. Chapter 2 assesses the impact of changing environmental conditions

during a Paleogene hypothermal event on the diversity and abundance of ostracodes

(small, bivalved crustaceans) at two localities in the deep sea. Chapter 3 then

investigates more specifically how the most abundant groups of ostracodes in these

assemblages responded to these changes by studying the morphological changes in

these groups across the event. By studying how life responded to environmental

perturbations at a variety of different scopes and scales, we may be able to begin to

elucidate the possible responses that we may observe in life today and in the future to

the changing environmental conditions that we are currently facing.

References

Boag, T.H., Darroch, S.A.F., and Laflamme, M., 2016, Ediacaran distributions in space and time: testing assemblage concepts of earliest macroscopic body fossils: Paleobiology, v. 42, p. 574–594.

Brierley, A.S., and Kingsford, M.J., 2009, Impacts of climate change on marine organisms and ecosystems: Current Biology, v. 19, R602-R614.

Canfield, D.E., Poulton, S.W., and Narbonne, G.M., 2007, Late-Neoproterozoic deep-ocean oxygenation and the rise of animal life: Science, v. 315, p. 92-95.

Doney, S.C., Ruckelshaus, M., Emmett Duffy, J., Barry, J.P., Chan, F., English, C.A., Galindo, H.M., Grebmeier, J.M., Hollowed, A.B., Knowlton, N., and Polovina, J., 2012, Climate change impacts on marine ecosystems: Annual Review of Marine Science, v. 4, p. 11-37.

Droser, M.L., and Gehling, J.G., 2015, The advent of animals: the view from the Ediacaran: Proceedings of the National Academy of Sciences, v. 112, p. 4865-4870.

Droser, M.L., Tarhan, L.G., and Gehling, J.G., 2017, The rise of animals in a changing environment: global ecological innovation in the Ediacaran: Annual Review of Earth and Planetary Sciences, v. 45, p. 593–617.

Dunkley Jones, T., Lunt, D.J., Schmidt, D.N., Ridgwell, A., Sluijs, A., Valdes, P.J., and Maslin, M., 2013, Climate model and proxy data constraints on ocean warming across the Paleocene-Eocene Thermal Maximum: Earth-Science Reviews, v. 125, p. 123-145.

Erwin, D.H., Laflamme, M., Tweedt, S.M., Sperling, E.A., Pisani, D., and Peterson, K.J., 2011, The Cambrian conundrum: Early divergence and later ecological success in the early history of animals: Science, v. 334, p. 1091–1097.

Evans, S.D., Diamond, C.W., Droser, M.L., and Lyons, T.W., 2018, Dynamic oxygen coupled with biological and ecological innovation during the second wave of the Ediacara Biota: Emerging Topics in Life Sciences, v. 2, p. 223-233.

Greene, S.E., Ridgwell, A., Kirtland Turner, S., Schmidt, D.N., Pälike, H., Thomas, E., Greene, L.K., and Hoogakker, B.A.A., 2019, Early Cenozoic decoupling of climate and carbonate compensation depth trends: Paleoceanography and Paleoclimatology.

IPCC, 2014, Climate change 2014: Synthesis Report. Contribution of Working Groups I, II, and III to the Fifth Assessment Report of the Intergovernmental Panel on Climate Change [Core Writing Team, Pachauri, R.K., and Meyer, L.A., eds.]: Geneva, Switzerland, IPCC, 151 pp.

Kirtland Turner, S., 2018, Constraints on the onset duration of the Paleocene-Eocene Thermal Maximum: Philosophical Transactions of the Royal Society A, v. 376, p. 1-16.

Kirtland Turner, S., Sexton, P.F., Charles, C.D., Norris, R.D., 2014, Persistence of carbon release events through the peak of early Eocene global warmth: Nature Geoscience, v. 7, p. 748-751.

Knoll, A.H., 2011, The multiple origins of complex multicellularity: Annual Review of Earth and Planetary Sciences, v. 39, p. 217-239.

Lyons, T.W., Reinhard, C.T., and Planavsky, N.J., 2014, The rise of oxygen in Earth's early ocean and atmosphere: Nature, v. 506, p. 307-315.

McInerney, F.A., and Wing, S.L., 2011, The Paleocene-Eocene Thermal Maximum: A perturbation of carbon cycle, climate, and biosphere with implications for the future: Annual Reviews of Earth and Planetary Science, v. 39, p. 489-516.

Norris, R.D., Kirtland Turner, S., Hull, P.M., and Ridgwell, A., 2013, Marine ecosystem responses to Cenozoic global change: Science, v. 341, p. 492-498.

Sepkoski, J.J., 1981, A factor analytic description of the Phanerozoic marine fossil record: Paleobiology, v. 7, p. 36-53.

Waggoner, B., 2003, The Ediacaran biotas in space and time. Integrative and Comparative Biology: v. 43, p. 104–113.

Xiao, S. and Laflamme, M., 2009, On the eve of animal radiation: phylogeny, ecology, and evolution the Ediacara biota: Trends in Ecology and Evolution, v. 24, p. 31-40.

CHAPTER 1: THE SHORT-LIVED BUT SUCCESSFUL TRI-RADIAL BODY PLAN: A VEIW FROM THE EDIACARAN OF AUSTRALIA

Abstract

There are multiple tri-radially symmetric taxa amongst the Ediacara Biota, but the tri-radial body plan is unique to this time; taxa with threefold symmetry go extinct by the beginning of the Cambrian. Many of these taxa are included in a morphogroup referred to as Trilobozoa or Triradialomorpha. Abundant specimens of these tri-radial taxa exist at the Nilpena National Heritage Ediacara fossil site and at other sites throughout Australia. Here, we review the occurrence and diversity of tri-radial genera from the Australian Ediacaran, including *Albumares*, *Anfesta*, *Coronacollina*, *Hallidaya*, *Rugoconites*, *Skinnera*, and *Tribrachidium* and evaluate the possibility that their shared symmetry unites them phylogenetically. We find that, with the exception of *Coronacollina*, these taxa are morphologically similar enough to justify considering them a clade of related organisms. The diversity and abundances of these taxa in South Australia provide a unique venue for research investigating the relationships among these Ediacaran taxa.

Introduction

The Ediacara Biota and Tri-Radial Symmetry

The Ediacara Biota represents one of the first major radiations of large, morphologically

complex eukaryotes. It includes a suite of about 50 described genera (Laflamme et al.,

2013) of soft-bodied organisms that vary widely in size and morphology (Narbonne,

2005) and are globally distributed (Fedonkin et al., 2007; Waggoner, 2003). The Ediacara

Biota has been divided into three assemblages, the Avalon, the White Sea, and the

Nama, based on similar age and shared taxa (Boag, 2016; Waggoner, 2003). The

transition between the Avalon and White Sea assemblages has been termed the 'second

wave' of the Ediacara Biota, because of the appearance of new ecological and biological

innovations (Droser et al., 2017).

There is general acceptance that the Ediacara Biota includes stem-group metazoans

(Budd and Jensen, 2015; Droser et al., 2017; Erwin, 2015; Laflamme et al., 2013) in

addition to a number of enigmatic taxa, but determining phylogenetic relationships has

proven problematic. Despite this, some taxa have well-constrained affinities. For

example, *Kimberella* is broadly interpreted as a stem-group mollusk (Fedonkin and

Waggoner, 1997). Taxa are typically identified to the species and genus level but not

into higher categories which is indicative of the difficulty of classifying these organisms;

however, groupings proposed by Xiao and Laflamme (2009; see also Erwin et al., 2011;

Laflamme et al., 2013) provide a useful starting point for comparison. Multiple taxa of

the Ediacara Biota exhibit tri-radial symmetry (Ivantsov and Fedonkin, 2002; Xiao and

Laflamme, 2009). With few exceptions, these taxa are only found in the White Sea

assemblage and disappear by the beginning of the Nama assemblage. There are no

known organisms from the Cambrian onwards that exhibit tri-radial symmetry. The lack

of Phanerozoic tri-radial organisms suggests that the Triradialomorph morphogroup

went extinct at the end of the Ediacaran Period and that threefold symmetry was a

failed evolutionary experiment in animal body plans.
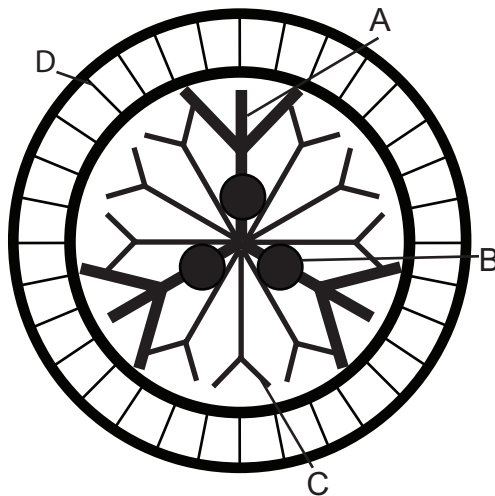
Figure 1.1. Diagram of a hypothetical tri-radial fossil. A,B: The main feature that dictates the three-fold symmetry can be ridges or canals (A) or bumps (B). C: There may be other features between the main tri-radial features. D: Some specimens have an outer "fringe".

Tri-radial symmetry, in this case, indicates the presence of three, relatively evenly

spaced features arranged around a circle (Figure 1.1). There may also be other features

that branch from or surround the three main features. Diagnoses are based on features

that include bumps, ridges and/or canals that are arranged with some element of

threefold symmetry (Xiao and Laflamme, 2009). Taxa that have been identified as tri-

radial also share other characteristics, such as a conical or disc-like shape and similar

diameter size ranges. These tri-radial forms have been tentatively grouped into a 'clade'

known as Trilobozoa (Fedonkin 1985a; Ivantsov and Fedonkin, 2002) or

Triradialomorpha (Erwin et al., 2011; Laflamme et al., 2013; Xiao and Laflamme, 2009).

While previous work has described these groups as 'clades', it is worth noting that this

term implies a phylogenetic relationship that has not yet been demonstrated. Here, we

refer to the groupings as 'morphogroups'. Fedonkin (1985a) distinguishes Trilobozoa as

a class of coelenterates based on "a unique threefold radial symmetry" and gives

Tribrachidium, Skinnera, Anfesta, and *Albumares* as example taxa; Ivantsov and

Fedonkin (2002) also include *Hallidaya* and "probably *Rugoconites*" in the Trilobozoa.

Erwin et al. (2011) describe the Triradialomorph morphogroup as being characterized by

three planes of symmetry or three independent arm-like structures where each branch

is typically composed of smaller branching structures. They propose that the group

includes the genera *Albumares*, *Anfesta*, *Pomoria*, *Skinnera*, *Tribrachidium*, and

Triforillonia. The proposed grouping provides a useful starting point for comparisons of

tri-radial taxa. While most Ediacaran organisms with tri-radial symmetry have been

included in this morphogroup, not all are. In particular, *Rugoconites* (Seilacher, 1989)

and *Coronacollina* (Clites, Droser, and Gehling, 2012) have also been described as having

threefold symmetry, but are not consistently included in lists of tri-radial taxa. Few

other taxa, such as *Pteridinium*, also have body plans with three main elements, but these are excluded from this and other tri-radial groupings because the three elements are not arranged radially, and because they are perhaps more distinguished by the presence of modular, repeated units in their body plans than by the three main elements.

In this paper, we review and compare taxa that express tri-radial symmetry occurring in the Ediacaran of Australia. We further discuss their diversity, abundance, and distribution in the Ediacara Member, and examine them as a potential extinct clade.

Australian Occurrences

The taxa discussed here occur commonly in the White Sea assemblage in the Flinders Ranges area and are part of the 'second wave' of the Ediacara Biota (Droser et al., 2017). There are over 750 tri-radial fossils at the Nilpena field site alone, and many others at other sites throughout the Flinders. Several of the taxa are also found in the White Sea region of Russia and in Ukraine and the Northern Territory.

The Ediacara Member of the Rawnsley Quartzite crops out throughout the Flinders Ranges area and is the uppermost Ediacaran unit in the Neoproterozoic-middle Cambrian succession of South Australia (Gehling, 2000). It is uniquely characterized by dense and exceptionally preserved fossil assemblages of the Ediacara fossils of the
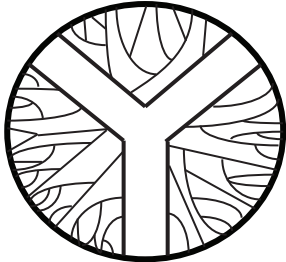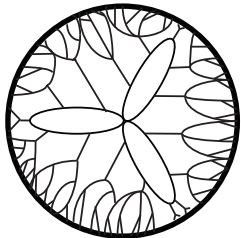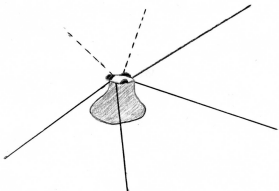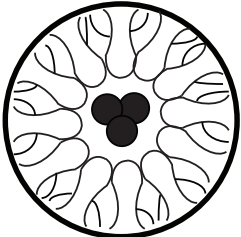
White Sea assemblage (cf. Waggoner, 2003). The Ediacara Member consists of a siliciclastic, sandstone-dominated sequence interpreted to have been deposited across a range of shallow marine and deltaic settings. Fossils typically occur as hyporelief external and internal molds on the base of sandstone beds.
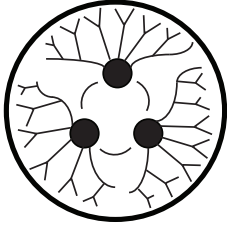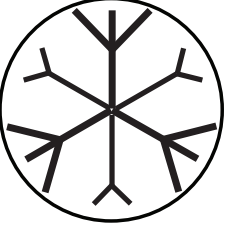
At the National Ediacara Fossil Heritage site at Nilpena Station, 34 beds varying in size have been excavated revealing thousands of fossils preserved *in situ* (Droser et al., 2017). At Nilpena, the Ediacara Member is comprised of five distinct facies: the Shoreface Sandstone facies, the Oscillation-Rippled Sandstone facies, the Flat-Laminated to Linguoid-Rippled Sandstone facies, the Planar-Laminated and Rip-Up Sandstone facies, and Channelized Sandstone and Sand-Breccia facies (Gehling and Droser, 2013; Tarhan et al., 2017). The excavated bedding planes at the Nilpena field site come from the Oscillation-Rippled Sandstone facies (rippled sandstones representing shallow marine deposition settings) and the Planar-Laminated and Rip-Up Sandstone facies (canyon fill beds characterized by planar lamination and tool marks) (Gehling and Droser, 2013).

Tri-Radial Taxa from the White Sea Assemblage

The tri-radial genera present in Australia, *Albumares*, *Anfesta*, *Coronacollina*, *Hallidaya*, *Skinnera*, *Rugoconites*, and *Tribrachidium*, represent the range of observed tri-radial morphologies (Table 1.1).

Table 1.1. Summary of tri-radial taxa.

Taxon	Depiction	Size and Brief Description	Localities
Albumares	After Seilacher, 1992	Approximately 13mm in diameter. Flattened tri-lobate "bell", divided into 3 rays with 3 thin radiating ridges that bifurcate 4 times. Numerous thin tentacles around edge.	Onega Peninsula, Russia South Australia
Anfesta	After McMenamin, 2000	Up to 18mm in diameter. Flattened discoid umbrella with 3 elongated radiating ridges truncated before the edge of the specimen surrounded by thinner branching ridges.	White Sea region, Russia; South Australia
Coronacollina	After Clites et al., 2012	Truncated cone up to 22mm in diameter with narrow, ruler-straight spicules up to 37cm in length. Cone rim threefold. Smaller specimens have 3 separate nodes instead of a continuous cone rim.	South Australia
Hallidaya		Diameter ranges from 5-50mm; most specimens are 10-30mm. Disc-shaped with discrete, ringed, inflated "nuclei" usually near the center of the organism, but sometimes scattered.	Northern Territory, Australia

Taxon	Depiction	Size and Brief Description	Localities
Skinnera	After Seilacher, 1999	Diameter ranges from 4-32mm. Round with a ring of 3 main depressions around the center, sometimes with a ring of up to 15 smaller depressions surrounding these.	Northern Territory, Australia; South Australia
Rugoconites		Diameter ranges from 10-60mm. Round with branching ridges that radiate outward from the center of the organism, terminating sharply at the outer edges.	South Australia; Russia; Wernecke Mts., Canada(?)
Tribrachidium		Diameter ranges from 3-40mm. Slightly conical with three "arms" that radiate from the center and bend 90° clockwise. "Tentacular fringe" from bend in arms to edge.	South Australia; White Sea region, Russia; Podolia, Ukraine
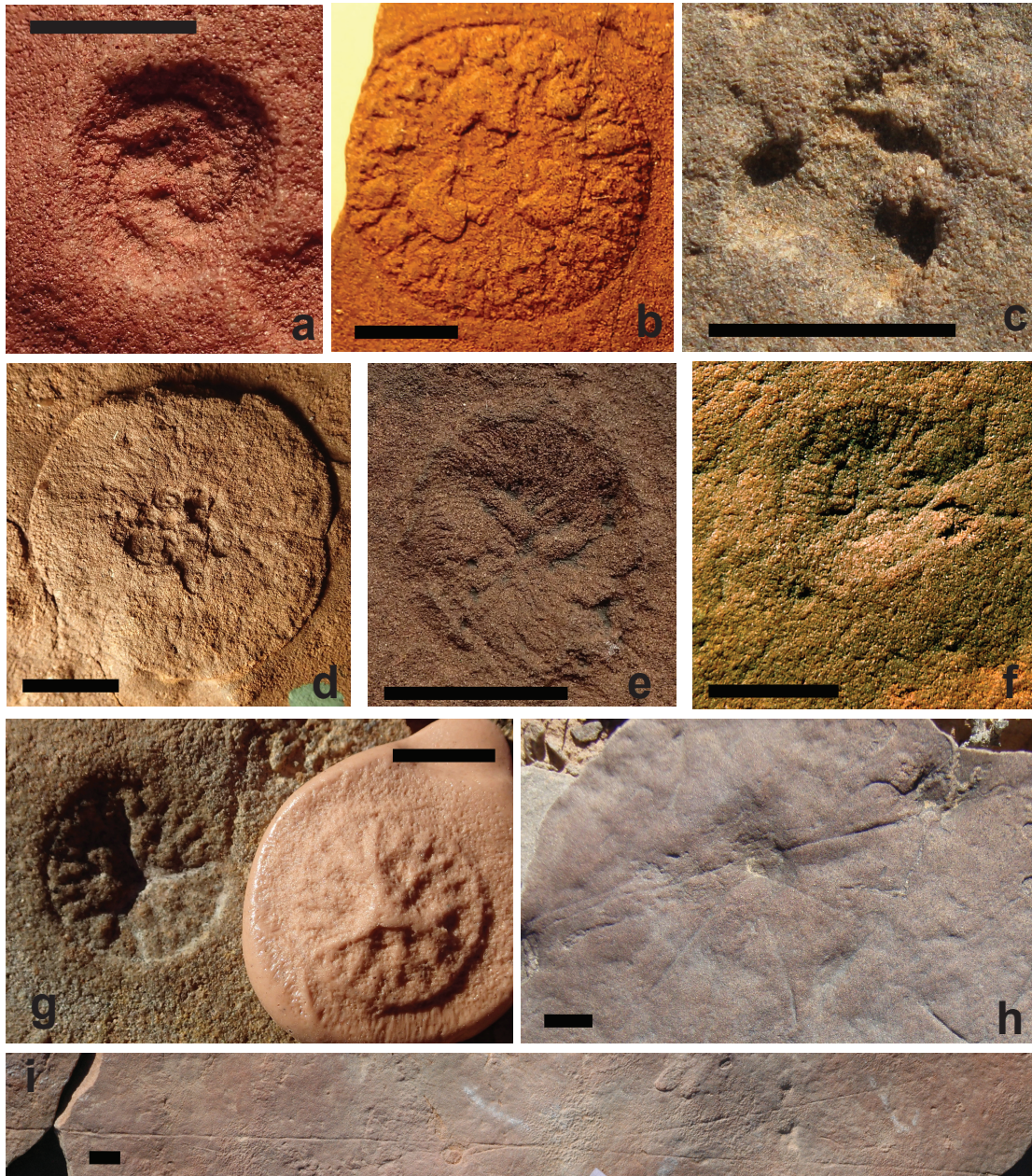
Figure 1.2. Tri-radial taxa from the Ediacaran of South Australia. a: *Tribrachidium* (SAM P42662). b: *Skinnera* (SAM F16473) c: *Coronacollina* 'tripod' with three nodes instead of a continuous rim (TBEW 95/113). d: *Hallidaya* (SAM F16464a) e: *Albumares* (SAM P42554) f: *Anfesta* (SAM P36588c) g: *Rugoconites enigmaticus*. Also note the silly putty mold that shows how the organism would have looked sitting on the sea floor. (STC-J 560/493) h: *Coronacollina* with several spicules radiating out from cone. i: *Coronacollina* with long spicules (TBEW 222/350). All scale bars are 1 cm.

Tribrachidium

Tribrachidium (Figure 1.2a) was originally described from South Australia (Glaessner and

Daily, 1959), where it is relatively common (Hall et al., 2015), but it also occurs in the

White Sea region of Russia (Laflamme et al., 2013; Martin et al., 2000) and Podolia,

Ukraine (Fedonkin et al., 2007). *Tribrachidium* specimens are circular in plane view, but

can have up to about 2 mm of vertical relief, resulting in a slightly conical shape (Hall et

al., 2015). *Tribrachidium* is chiefly distinguished by three ridges that radiate from the

center of the specimen and bend 90° clockwise, giving the genus its distinctive tri-radial

symmetry (Glaessner and Daily, 1959). Well-preserved specimens have 'tentacular

fringe', or numerous, fine ridges that extend from the bend in the three main ridges out

to the edge of the specimen (Glaessner and Daily, 1959). This fringe or 'caul' covers the

entire specimen, including the arms, in some larger *Tribrachidium* (Jenkins, 1992). Near

the bend in each arm is a 'bulla', or slightly convex bump that has been interpreted,

albeit without other evidence, as a possible reproductive structure (Jenkins, 1992).

Additionally, a Y-shaped groove found near the center of some specimens has been

interpreted as a mouth structure (Glaessner and Wade, 1966). Recent work also

suggests that the shape of *Tribrachidium* was able to passively direct water to the apex

of the organism, possibly signifying that *Tribrachidium* employed a suspension feeding

strategy to obtain nutrients (Rahman et al., 2015).

Based on examination of nearly 300 specimens from the Ediacara Member, *Tribrachidium* ranges in size from about 3 to 38 mm (Hall et al., 2015). Of these, larger specimens typically appear to be scaled-up versions of the smaller specimens, with some minor differences: specimens with diameters less than 15 mm commonly lack the tentacular fringe that is typically present in larger specimens. However, on bedding planes with a grainsize greater than fine-medium-grained, tentacular fringe cannot be distinguished on larger specimens. Thus, the presence or absence of fringe may be more related to taphonomy than to growth. This also underscores the importance of collecting as many specimens as possible; analysis of too few specimens may result in difficulty determining which of the observed patterns are attributable to growth, as opposed to other factors such as taphonomic processes.

As is the case with all taxa of the Ediacara Biota, it is difficult to assess the meaning of preserved height because of compaction and the scale of measurement. However, the height of *Tribrachidium* appears to increase linearly with diameter, but there is scatter in the data and only about 2 mm of range in specimen heights. There is also a weak correlation between the distance from the center of a specimen to the bend in the arms and the distance from the bend in the arms to the outer edge of a specimen (Figure 1.3). As a *Tribrachidium* grew, the distance from the center to the bend in the arms appears to have grown faster than the distance from the bend in the arms to the edge. Thus,

although the overall shape and appearance of *Tribrachidium* remain similar throughout

an organism's life, growth was not isometric.
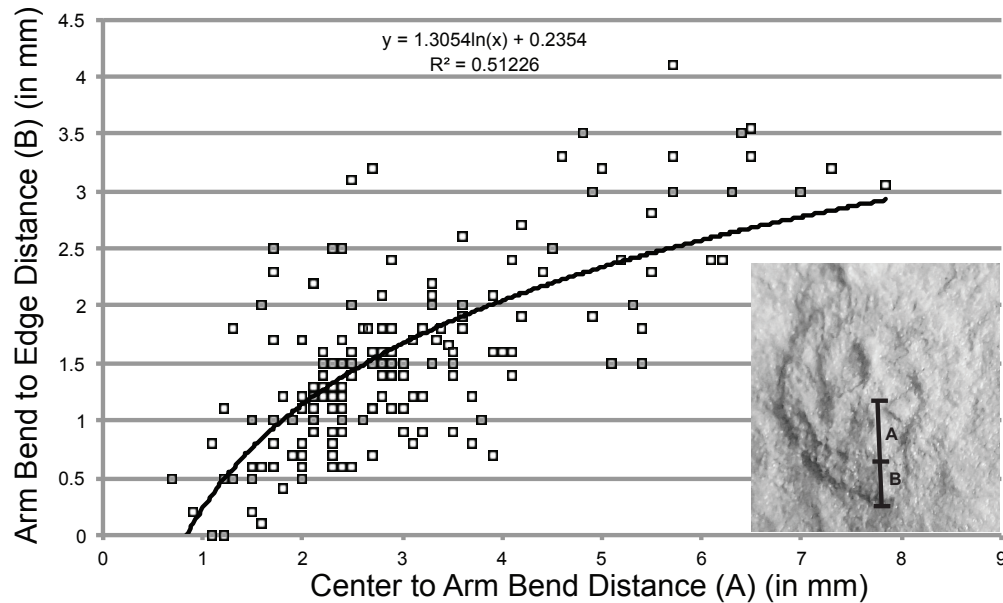
Figure 1.3. *Tribrachidium* arm bend measurements. A graph of the distances from the center of specimens to the bend in the arms vs. the distances from the arm bends to the edge of the organisms for the *Tribrachidium* at Nilpena. In the inset, (A) shows an example distance from the center to the arm bend, and (B) shows an example distance from the arm bend to the edge of the specimen. The distance from the center to the arm bend is larger and likely continued to grow even as the growth of the outer edge slowed.

Rugoconites

Rugoconites (Figure 1.2g), described from South Australia, is a circular to oval-shaped

fossil with a diameter of 1-6 cm (Glaessner and Wade, 1966). Specimens vary in relief

from nearly flat to about 1 cm high, and specimens with higher relief appear conical in

cross-section. The genus is distinguished by the branching ridges that radiate from a

central point and end sharply at the periphery of the organism (Glaessner and Wade, 1966). *Rugoconites* is one of few described Ediacaran genera that is not monospecific (Wade, 1972); however, *Rugoconites enigmaticus* is much more common than *Rugoconites tenuirugosus*. *Rugoconites tenuirugosus* has been differentiated from *Rugoconites enigmaticus* on the basis of thinner, more numerous ridges (Wade, 1972). The known specimens of *R. tenuirugosus* tend to be larger in diameter but have no vertical relief other than the minimal relief of the thin ridges (Wade, 1972).

Rugoconites is relatively common in the Ediacara Member, and specimens have also been found in Russia (Fedonkin et al., 2007) as well as possibly the Wernecke Mountains of Canada (Narbonne and Hofmann, 1987). Interestingly, *Rugoconites* has been inconsistently included in groups of tri-radial Ediacaran taxa. Seilacher (1989) is the first reference to "tri-radiate" symmetry with regard to *Rugoconites*, and Xiao and Laflamme (2009) refer to them as "possibly" tri-radial, but Erwin et al. (2011) group them with poriferans rather than triradialomorphs.

Analyses of 200 *Rugoconites* specimens reveal insight into how this organism may have grown and developed. *Rugoconites* specimens are composed of "main" ridges that go from the center to the edge of the organism and "sub-branches" that extend off of the main ridges, but do not go through the center of the organism (Hall et al., 2018). Well-preserved *Rugoconites* specimens have either six, nine, twelve, or fifteen main ridges,

suggesting that new main ridges appear together in threes throughout the development

of *Rugoconites*. The number of main ridges increases in concert with diameter.

Specimens with different numbers of main ridges do not overlap in size (Hall et al.,

2018). All specimens with six main ridges are smaller than those with nine main ridges,

none with nine main ridges are larger than those with twelve, and specimens with

fifteen main ridges are larger than all other specimens. The number and arrangement of

the sub-branches, those that do not go through the center of the organism, is generally

less clear and varies more from specimen to specimen, but the total number of sub-

branches seems to increase with increasing diameter (Hall et al., 2018). Specimens with

six main ridges are the most similar to one another of any group, and consistently

alternate three thick main ridges with three sub-branches and three thinner main ridges

with two sub-branches. Specimens with nine main ridges are slightly less consistent, but

generally have six main ridges with two sub-branches and three main ridges without

sub-branches. It is suggested that this indicates that *Rugoconites* may have added main

ridges by differing rates of growth of certain sub-branches; in each stage of growth

three sub-branches grew into main ridges (Hall et al., 2018).

Coronacollina

Coronacollina is only known from South Australia (Clites et al., 2012; Reid et al, 2017). It

consists of a truncated cone 1-22 mm in diameter associated with narrow straight

spicules <2 cm to 37 cm in length (Clites et al., 2012). Multiple ruler-straight spicules

diverge radially from cone (Figure 1.2h) and commonly disarticulate. The cone is thimble-shaped and possesses a threefold rim. Smaller specimens have three separate nodes instead of a continuous rim (Figure 1.2c; Clites et al., 2012). Though the body of the organism is tri-radial and the spicules have a radial arrangement, the highest number of spicules observed associated with a body is four. More spicules may have been attached during life, but were disarticulated before being preserved. There are 32 specimens with articulated spicules. It is apparent from articulated specimens that the spicules were attached at the top of the rim. Given this, it is not surprising that spicules disarticulated during a storm or burial.

Articulated spicules do not cross, while disarticulated spicules can cross (Clites et al., 2012). Spicules can be quite long (up to 37 cm; Figure 1.2i), and it is likely that longer spicules, once disarticulated from the cone, broke into small sections (Figure 1.4). The majority of spicules are ruler-straight, including 37 of 45 spicules on Sub bed (GSA Data Repository Item 2012088, Table DR3). Those that are not are only slightly curved. These spicules make *Coronacollina* the only tri-radial genus to have skeletonized elements.

Spicule Length Frequency
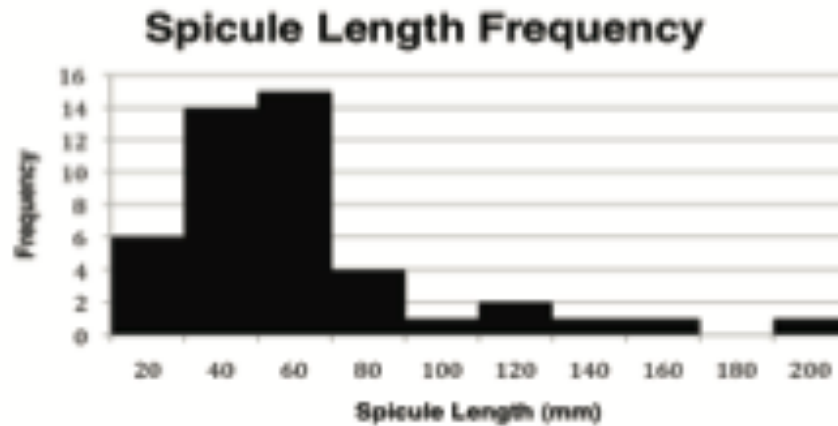
Figure 1.4. Frequency of spicules of different lengths on Sub bed at Nilpena. The abundance of short spicules and fewer long spicules suggests that long spicules broke while being transported (GSA Data Repository Item 2012088, Fig. DR3).

Coronacollina also exhibits apparent growth series, from specimens with an average cone diameter of <1 mm to those greater than 1 cm in size. In addition, the smaller form of *Coronacollina* is preserved as three separate nodes rather than one continuous body. The association of these three nodes with spicules confirms it is a form of *Coronacollina*. It is not clear exactly how these three-node forms developed and whether they are simply a juvenile form of *Coronacollina* or a distinct yet still closely related form. *Coronacollina* bears morphological resemblance to *Choia*, a Burgess Shale taxon interpreted as a demosponge (Clites et al., 2012).

Skinnera

Skinnera (Figure 1.2b) is a relatively common fossil where it was discovered at Mt. Skinner in the Northern Territory of Australia, but it is uncommon in South Australia and

not known from any other localities (Fedonkin et al., 2007). *Skinnera* fossils are round

with three main depressions in the center (Wade, 1969). In larger and well-preserved

specimens, a ring of up to 15 smaller depressions surrounds these three main

depressions (Wade, 1969). Some fossils of *Skinnera* also have a series of paired canals

that radiate from the center (Wade, 1969). Specimens are slightly dome-shaped, with

larger specimens exhibiting a markedly lower height-to-width ratio than smaller

specimens (Wade, 1969). Specimens have a maximum vertical relief of about 2 mm

(Wade, 1969).

Hallidaya

Hallidaya (Figure 1.2d) is a relatively uncommon genus that was originally described

from the Northern Territory of Australia (Wade, 1969) but has also been found in South

Australia (Retallack, 2013). *Hallidaya* is described as disc-shaped with "nuclei" that are

typically at the center of the specimen, although they are sometimes scattered. Some

Hallidaya with centrally-located nuclei also have dichotomously branching radial

furrows, though these are not commonly well preserved. Unlike other taxa included in

this study, *Hallidaya* are typically preserved as positive features on the base of

sandstone beds (Wade, 1969). The diameters of the nuclei are directly related to the

diameter of the specimen, with larger nuclei present in larger specimens (Wade, 1969).

Albumares

Albumares (Figure 1.2e) was first described from the Onega peninsula in the White Sea

region of Russia (Keller and Fedonkin, 1977), but has since also been found in South

Australia (Fedonkin et al., 2007). *Albumares* is described as a flattened, hemispherical

umbrella (or 'bell'), divided into three rays that are separated by three small ridges that

were interpreted as mouth lobes (Keller and Fedonkin, 1977). Although the organism

appears round as a fossil, it is thought that the umbrella of the organism may have been

more tri-lobate, but flattened into a round shape upon burial (Fedonkin, 1985b). Each of

the rays contains three thin ridges that radiate out from the center and bifurcate four

times toward the periphery of the specimen. This ridge system has been interpreted as

a gastrovascular system (Keller and Fedonkin, 1977). Specimens also show more than

100 short, thin tentacles along the edge of the bell (Keller and Fedonkin, 1977).

Anfesta

Anfesta (Figure 1.2f) was also first described from the White Sea region of Russia

(Fedonkin, 1984). Although not common, it is also known from South Australia

(Fedonkin et al., 2007). It is preserved as a shallow negative impression on the bases of

beds (Fedonkin, 1984), and is quite similar to *Albumares*, with a main difference being

an originally discoid, rather than tri-lobate umbrella (Fedonkin, 1985b). *Anfesta* has

three elongated ridges with rounded ends that radiate from its center at 120° angles,

but do not quite reach the edge of the specimen (Fedonkin, 1985b). These ridges are

surrounded by thinner branching ridges that extend to the outer margin of the fossil

(Fedonkin, 1984). These ridges can be up to 5 mm in length and up to 1.3 mm in width

(Fedonkin, 1984).

Distribution in the Flinders Ranges and elsewhere in Australia

The tri-radial taxa in Australia do not all share similar distribution patterns. Some genera

(*Albumares*, *Anfesta*, *Hallidaya*, and *Skinnera*) occur relatively rarely in Ediacaran-aged

rocks from Australia, while others (*Coronacollina*, *Tribrachidium*, and *Rugoconites*) are

very common and even dominate bedding planes in the Ediacara Member. Only a few

specimens of *Albumares* and *Anfesta* are known at all from Australia; most of these are

now housed at the South Australia Museum. Published reports indicate that *Hallidaya*

and *Skinnera* are also relatively uncommon in Australia; however, unpublished reports

indicate that they may be slightly more common than previously thought (P. Haines,

pers. comm. 2016). *Hallidaya* is only known from the Northern Territory. *Skinnera* is

more common in the Northern Territory (Wade, 1969), but has also been found in the

Ediacara Member in the Flinders Ranges (Fedonkin et al., 2007) (Table 1.2).

Table 1.2. Abundances of tri-radial taxa.

Taxon	Recorded Occurrences
Albumares	10
Anfesta	10
Coronacollina	370
Hallidaya	33
Skinnera	10
Rugoconites	200
Tribrachidium	286

In contrast, *Coronacollina*, *Rugoconites*, and *Tribrachidium* are each the dominant taxon

of least one excavated bed at Nilpena (Figure 1.5), and occur in varied abundances on

others. *Coronacollina*, as identified by a single cone, dominates one excavated bed, Sub,

where it makes up about 72% of the organisms on the bed. It also occurs in smaller

numbers on nine of the 34 other beds. Disarticulated spicules are also found abundantly

on Sub Bed, and uncommonly on others. While *Coronacollina* occurs most commonly in

the Planar-Laminated and Rip-Up Sandstone facies, interpreted as sub-wave base

canyon fill (Clites et al., 2012), it also occurs in the Oscillation-Rippled Sandstone facies

and the Flat-Laminated to Linguoid-Rippled Sandstone facies (Gehling and Droser, 2013;

Tarhan et al., 2017). *Coronacollina* is unique to the Ediacara Member in South Australia;

it has thus-far only been identified at Nilpena.
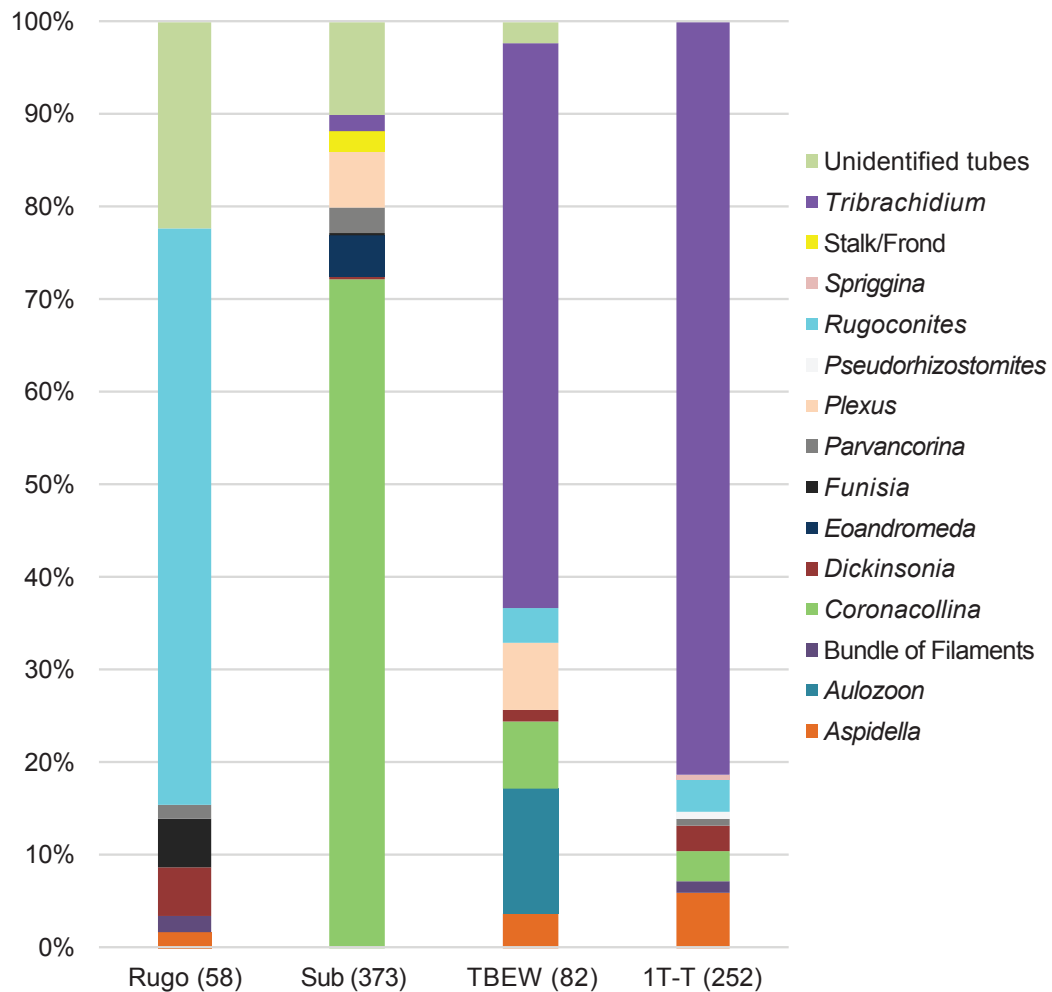
Figure 1.5. Stacked-bar histogram of fossils on Nilpena bedding planes dominated by a tri-radial fossil. Numbers in parentheses are the total numbers of fossils on the bedding planes.

Rugoconites is the dominant genus on one bed from the Oscillation-Rippled Sandstone facies (between fair- and storm-weather wave base) at South Ediacara. On this bed, *Rugoconites* makes up about 62% of the fossil specimens on the bed. Additionally, *Rugoconites* occurs on 12 other excavated beds, always as 10 or fewer specimens per bed. It is by far most commonly found in the Oscillation-Rippled Sandstone facies, but

also occurs in the Planar-Laminated and Rip-Up Sandstone facies, Flat-Laminated to

Linguoid-Rippled Sandstone facies, and the Cross-Bedded Sandstone facies

representative of deposition at fair-weather wave base (Gehling and Droser, 2013). It is

likely that while *Rugoconites* was most able to thrive in environments between fair- and

storm-weather wave base with oscillatory water flow, it was able to adapt well enough

to at least survive in a variety of other environments.

Tribrachidium is unique among the tri-radial genera in that it dominates two beds from

different facies. On 1T-T in the Oscillation-Rippled Sandstone facies, *Tribrachidium*

makes up 81% of the organisms on the bed; on TBEW in the Planar-Laminated and Rip-

Up Sandstone facies it makes up about 61% of the organisms known from the bed. In

addition to these beds, it is found on eight of the other excavated beds. It is also found

relatively commonly at the South Ediacara site. Like *Rugoconites*, it has been found in

four of the fossiliferous facies of the Ediacara Member. Because it was able to dominate

beds in different facies, we know that it was able not just to live but to thrive in

different environmental conditions.

Coronacollina, *Rugoconites*, and *Tribrachidium* are all found relatively commonly in the

Ediacara Member. Although *Rugoconites* and *Tribrachidium* are known from other

localities around the world, the best opportunities to study these taxa are from the Ediacara Member.

Discussion

Other Tri-Radial Taxa

Although many tri-radial taxa are present in South Australia, there are other tri-radial and tri-radial-like taxa known from other localities that are not known from Australia. *Triforillonia* is the only tri-radial genus known from the earlier Avalon Assemblage. It is preserved in shallow positive hyporelief and described as having three rounded lobes radiating from a central rosette at equal angles, with a diameter of 20-26 mm (Gehling, Narbonne, and Anderson, 2000). Its preservation as a relatively flat cast has been used to suggest that *Triforillonia* was less resilient than other tri-radial forms such as *Tribrachidium* (Fedonkin et al., 2007). Like *Anfesta* and *Albumares*, *Triforillonia* is a relatively uncommon genus, with about 10 known specimens. It is also included in the Erwin et al. (2011) Triradialamorpha grouping.

There are two tri-radial taxa known only from the White Sea region of Russia. *Pomoria* is a small discoidal form, about 16-20 mm in diameter. It has bent processes that extend radially from the center and two rows of smaller, tentacle-like projections in the middle and along the margin of the organism (Fedonkin et al., 2007). It is an uncommon genus, but is included in the Erwin et al. (2011) Triadialamorpha grouping, and in other lists of

tri-radial taxa (e.g. Droser et al., 2017; McCall, 2006). *Ventogyrus* also occurs only in the White Sea region. Originally described as a *Pteridinium*-like organism (Ivantsov and Grazhdankin, 1997), *Ventogyrus* is in fact composed of three modules, each with several transverse septa, arranged around an axial rod into an egg-shaped capsule (Fedonkin and Ivantsov, 2007).

Comparison of Taxa: Morphologies and Taphonomy

The preserved morphology of fossils of soft bodied organisms is a function of both taphonomic processes and the biology of the organism. The most consequential taphonomic concerns for preservation are the environment in which the organisms were living and buried in and the grain size of the casting sand. Different environments may lead to differences in preservation that, if not considered in a taphonomic context, could be perceived as differences in the actual organisms. Additionally, finer grained sands are capable of resolving finer details in the fossils that may have been biologically present but not preserved in fossils preserved in larger grained sand. Thus, it is necessary to analyze as many specimens as possible, particularly those from different lithologies or facies. This is particularly important for comparing fossils with apparent similar morphology. Because the Ediacara Member in South Australia is composed of fossiliferous rocks from five facies and rocks with different grain sizes, we are able to begin to control for taphonomy in studies of several of these taxa.

Tri-radial fossils have several characters, including ridges, rays, bulges, spicules, and depressions, that can be counted and measured. These features are the basis for identification of particular taxa; however, because these taxa are soft-bodied, features can be obscured. For example, very few specimens of *Rugoconites* are well preserved. Usually only part of a given specimen is clear, and in some fossils, the entire specimen lacks well-defined detail. It does become valid, then, to question whether similar, rarer, taxa such as *Anfesta* and *Albumares* are in fact distinct genera, or if instead they are merely taphomorphs of *Rugoconites*.

To answer this, we can consider the range of preservation in fossils that have been identified as *Rugoconites*. Despite the common poor preservation, the consistency in the features observed in these fossils, even across different depositional environments, and the consistent differences between *Rugoconites* and *Anfesta* and *Albumares* make it likely that these are valid, distinct taxa. Unlike in *Anfesta* and *Albumares*, there is always evidence, even in poorly preserved *Rugoconites*, that all of the ridges branch at least once. *Rugoconites* is thus distinguishable from *Anfesta* or *Albumares* because the large, main ridges in these two taxa do not branch. Furthermore, because there are abundant *Rugoconites* from four different facies in the Ediacara Member, we can confidently say that *Albumares* and *Anfesta* are not taphomorphs of *Rugoconites*.

Albumares and *Anfesta* share a number of features. These taxa are distinguished by the more tri-lobate shape of *Albumares* (vs. rounder *Anfesta*) and a greater number of bifurcating ridges in *Albumares*. While it is possible that with the discovery of more specimens of these taxa that they may more appropriately be considered as separate species of the same genus, but that is not clear at this time. They are, however, at least clearly separate species.

With this possible exception, we find that all of the other taxa we investigate here are distinct genera. The bent arms of *Tribrachidium* are particularly distinctive, but in some specimens of *Tribrachidium*, particularly smaller ones, the arms are less clear and are sometimes just preserved as three bulb-like features. Yet, these fossils are readily distinguished from *Skinnera* and *Hallidaya*, both of which have round, bulbous primary features. *Tribrachidium* fossils have more vertical relief and are more conical than the relatively flat *Skinnera* and *Hallidaya*. The round features in *Skinnera* and *Hallidaya* are different enough to distinguish between the genera. In *Hallidaya*, the 'nuclei' are grouped tightly together in the center; in *Skinnera*, the round features are spread slightly apart around the center.

Of these taxa, *Rugoconites* is the only one with more than one described species. The main species, *R. enigmaticus*, is quite abundant in the Ediacara Member. However, *R. tenuirugosus* is known from fewer than 10 specimens, and most of these are

incomplete. Based on our observations of these and other *Rugoconites* specimens, we

find that *R. tenuirugosus* may not be a valid, distinct species and thus, requires a closer

examination.

We agree with other authors (Erwin et al., 2011; Ivantsov and Fedonkin, 2002; Laflamme

et al., 2013; Xiao and Laflamme, 2009) that the tri-radial morphogroup is justified. The

fact that these genera are so similar, and yet still distinct from one another, supports

the hypothesis that these groups likely represent a clade of closely related taxa, which

we propose be defined on the basis of an overall disc-like body shape with tri-radially

symmetric elements. Based on what is preserved, we find no reason that this set of

characters should not have a shared evolutionary origin. We further suggest that, within

this grouping, some taxa do appear more similar than others. For example, *Rugoconites*,

Anfesta, and *Albumares* all share a main threefold element with surrounding branching

features. *Rugoconites* has not previously been consistently included in this

morphogroup but should be. Well-preserved specimens clearly show elements of

threefold symmetry, and its similarities to *Albumares* and *Anfesta*, taxa consistently

included in tri-radial groupings, are striking. It is unlikely that such similar taxa are not

closely related to one another.

Based on their morphologies, *Hallidaya* and *Skinnera* should also be included in this tri-

radial clade. Their round features make them morphologically distinct enough to be

valid genera, and they share radial branching features with *Anfesta*, *Albumares*, and *Rugoconites*. *Tribrachidium* certainly has very clear threefold symmetry, and the fringe that is present on some well-preserved specimens helps to further unite it with some of the otherwise slightly dissimilar other taxa. Still, we propose that while *Tribrachidium* should be included this tri-radial clade, it was likely slightly less closely related to the other taxa. It is the only genus with features that bend instead of extending straight out, and it lacks branching features.

Triforillonia is likely not closely related to these taxa because it is does not share the overall round, disc-shaped body that the other taxa have. *Coronacollina* is also likely not closely related. It is the only tri-radial genus with skeletonized elements, and its overall shape, while clearly possessing elements of threefold symmetry, is different from the other disc-like taxa. It seems unlikely that *Ventogyrus* is as closely related to the other taxa, but more analysis is needed to determine the similarity of both *Ventogyrus* and *Pomoria* to the other taxa.

Tri-radial taxa have been hypothesized as members of a variety of phyla, most commonly Porifera, Cnidaria, and Echinodermata. There is no evidence that any of these taxa were mobile; they all appear to have lived immobile lifestyles on the seafloor. *Coronacollina* is the only genus with skeletonized elements in its body plan. There is evidence that *Tribrachidium* was a suspension feeder (Rahman et al., 2015), and it

seems likely that this was the case for the other members of the tri-radial clade. Thus, these taxa were benthic, immobile, likely-suspension feeders. Given this ecology, it is likely that these taxa were poriferan-grade organisms, but it not clear that they were even stem-group poriferans.

Ongoing further morphometric analyses will help to clarify the relationships between these taxa. The characters described here, such as the presence and nature of branching features, and the presence of round internal features, can be used to help distinguish between sub-groupings of tri-radial taxa. These analyses can, in turn, elucidate patterns of growth and development that may also aid comparisons among these taxa. Growth patterns and ecological roles are both features that are commonly shared by related taxa (*e.g.* Fink, 1982). Biologically important criteria, such as patterns of growth and development and aspects of ecology including feeding and reproductive methods, will provide a better basis for constraining the relationship of these taxa to one another, and even to other taxa from later geologic periods, such as the recently-discovered, modern *Dendrogramma* (Just et al., 2014), than superficial morphologic similarities.

Conclusions

Tri-radially symmetric organisms were relatively common in the Ediacaran of Australia; they have been preserved extensively in the Ediacara Member of South Australia, and are also found in the Northern Territory and other White Sea assemblage sites. This

body plan is, with one exception, completely unique to this assemblage. Apart from the rare occurrence of a single genus in the Avalon assemblage, tri-radial body plans are only known from the second wave of the Ediacara Biota. During the second wave, organisms with this body plan were relatively successful. They were abundant, diverse, and able to thrive in a variety of environments. Some of these genera were even the dominant taxon in some communities. Despite their success, they apparently disappear by the time of the Nama assemblage, and tri-radial body plans are not found again in the fossil record or today. This time period is a unique window for this symmetry that does not occur again in the history of life on Earth.

These taxa, while sharing a symmetry, are morphologically diverse. They are all morphological distinct from one another and are valid taxa. They were abundant and are found in several different facies representing a range of depositional environments. We find that based on their morphologies *Rugoconites*, *Anfesta*, *Albumares*, *Skinnera*, *Hallidaya*, and *Tribrachidium* likely formed a clade of related tri-radial organisms. Because these, along with *Coronacollina*, are all valid, distinct taxa, it is clear that tri-radial body plans comprised a significant proportion of the diversity of the Ediacara Biota.

Understanding the relationships among these enigmatic taxa, and, even more so, their relationship to modern clades, has proved to be a difficult task (Xiao and Laflamme,

2009). Clarifying fundamental biological properties, such as growth and development, and the ecological roles of these taxa, is the most realistic and plausible method we have for understanding what these organisms were and how they lived. Determining how these organisms grew, and which, if any, growth strategies are shared among different taxa will also provide a more concrete basis for defining higher taxonomic groupings of these organisms. Because of the diversity and abundance of these taxa, Australia provides a unique venue for further research of this extinct body plan.

References

Boag, T.H., Darroch, S.A.F., and Laflamme, M., 2016, Ediacaran distributions in space and time: testing assemblage concepts of earliest macroscopic body fossils: Paleobiology, v. 42, p. 574–594.

Budd, G.E. and Jensen, S., 2015, The origin of the animals and a 'Savannah' hypothesis for early bilaterian evolution: Biological Reviews, v. 92, p. 446-473.

Clites, E.C., Droser, M.L., and Gehling, J.G., 2012, The advent of hard-part structural support among the Ediacara biota: Ediacaran harbinger of a Cambrian mode of body construction: Geology, v. 40, p. 307–310.

Droser, M.L., Tarhan, L.G., and Gehling, J.G., 2017, The rise of animals in a changing environment: global ecological innovation in the Ediacaran: Annual Review of Earth and Planetary Sciences, v. 45, p. 593–617.

Erwin, D.H., 2015, Early metazoan life: Divergence, environment and ecology: Philosophical Transactions of the Royal Society of London B, v. 370(1684), 20150036.

Erwin, D.H., Laflamme, M., Tweedt, S.M., Sperling, E.A., Pisani, D., and Peterson, K.J., 2011, The Cambrian conundrum: Early divergence and later ecological success in the early history of animals: Science, v. 334, p. 1091–1097.

Fedonkin, M.A., 1984, Promorphology of Vendian Radalia, *in* Ivanovsky, A.B.. and Ivanov, A.B., eds., Stratigraphy and Paleontology of the Most Ancient Phanerozoic: Moscow, Nauka, p. 27–45.

Fedonkin, M.A., 1985a, Precambrian metazoans: the problems of preservation, systematics and evolution: Philosophical Transactions of the Royal Society of London B, v. 311 (1148), p. 27–45.

Fedonkin, M.A., 1985, Systematic description of Vendian metazoan, *in* Sokolov, B.S., and Iwanowski, A.B., eds., The Vendian System, Volume 1 Paleontology: Berlin, Springer-Verlag, p. 71–120.

Fedonkin, M.A., Gehling, J.G., Grey, K., Narbonne, G.M., and Vickers-Rich, P., 2007, The Rise of Animals: Evolution and Diversification of the Kingdom Animalia: Baltimore, Maryland, The Johns Hopkins University Press, 326 p.

Fedonkin, M.A., and Ivantsov, A.Y, 2007, *Ventogyrus*, a possible siphonophore-like trilobozoan coelenterate from the Vendian Sequence (late Neoproterozoic), northern Russia, *in* Vickers-Rich, P. and Komarower, P., eds., The Rise and Fall of the Ediacaran Biota: Geological Society Special Publications, Vol. 286: London: Geological Society, p. 187–194.

Fedonkin, M.A., and Waggoner, B.M., 1997, The Late Precambrian fossil *Kimberella* is a mollusc-like bilaterian organism: Nature, v. 388, p. 868–871.

Fink, W.L., 1982, The conceptual relationship between ontogeny and phylogeny: Paleobiology, v. 8, p. 254–264.

Gehling, J.G., 2000, Environmental interpretation and a sequence stratigraphic framework for the terminal Proterozoic Ediacara Member within the Rawnsley Quartzite, South Australia: Precambrian Research, v. 100, p. 65–95.

Gehling, J.G. and Droser, M.L., 2013, How well do fossil assemblages of the Ediacara biota tell time?: Geology, v. 41, p. 447–450.

Gehling, J.G., Narbonne, G.M., and Anderson, M.M., 2000, The first named Ediacaran body fossil, *Aspidella terranovica*: Palaeontology, v. 43, p. 427–456.

Glaessner, M.F. and Daily, B., 1959, The geology and late Precambrian fauna of the Ediacara Fossil Reserve: Records of the South Australia Museum, v. 13, p. 396–401.

Glaessner, M.F. and Wade, M., 1966, The late Precambrian fossils from Ediacara, South Australia: Paleontology, v. 9, p. 599–628.

Hall, C.M.S., Droser, M.L., and Gehling, J.G., 2018, Sizing up *Rugoconites*: A study of the ontogeny and ecology of an enigmatic Ediacaran genus: Australasian Palaeontological Memoirs, v 51, p. 7-17.

Hall, C.M.S., Droser, M.L., Gehling, J.G., and Dzaugis, M.E., 2015, Paleoecology of the enigmatic *Tribrachidium*: New data from the Ediacaran of South Australia: Precambrian Research, v. 269, p. 183–194.

Ivantsov, A.Yu. and Fedonkin, M.A., 2002, Conulariid-like fossil from the Vendian of Russia: a metazoan clade across the Proterozoic/Palaeozoic boundary: Palaeontology, v. 45, p. 1219–1229.

Ivantsov, A.Yu. and Grazhdankin, D.V., 1997, A new representative of the Petalonamae from the Upper Vendian of the Arkhangelsk Region: Palaeontological Journal, v. 31, p. 1–16.

Jenkins, R.J.F., 1992, Functional and ecological aspects of Ediacaran assemblages, *in* Lipps, J.H. and Signor, P.W., eds., Origin and Early Evolution of the Metazoa: New York, Plenum Press, p. 131–176.

Just, J., Kristensen, R., and Olesen, J., 2014, *Dendrogramma*, new genus, with two new non-bilaterian species from the marine bathyal of Southeastern Australia (Animalia, Metazoa incertae sedis) – with similarities to some medusoids from the Precambrian Ediacara: PLoS ONE, v. 9(9), 1–11.

Keller, B.M. and Fedonkin, M.A., 1977, New organic finds in the Precambrian Valday series along the Syuz'ma River: International Geology Review, v. 19, p. 924–930.

Laflamme, M., Darroch, S.A.F., Tweedt, S.M., Peterson, K.J., and Erwin, D.H., 2013, The end of the Ediacara: extinction, biotic replacement, or Cheshire Cat?: Gondwana Research, v. 23, p. 558–573.

Martin, M.W., Grazhdankin, D.V., Bowring, S.A., Evans, D.A.D., Fedonkin, M.A., and Kirschvink, J.L., 2000, Age of Neoproterozoic bilaterian body and trace fossils, White Sea, Russia: implications for metazoan evolution: Science, v. 288, p. 841–845.

McCall, G.J.H., 2006, The Vendian (Ediacaran) in the geological record: Enigmas in geology's prelude to the Cambrian explosion: Earth-Science Reviews, v. 77, p. 1–229.

McMenamin, M.A.S., 2000, The garden of Ediacara: Discovering the first complex Life: New York, Columbia University Press.

Narbonne, G.M., 2005, The Ediacara biota: Neoproterozoic origin of animals and their ecosystems: Annual Review of Earth and Planetary Sciences, v. 33, p. 421–442.

Narbonne, G.M. and Hofmann, H.J., 1987, Ediacaran biota of the Wernecke Mountains, Yukon, Canada: Palaeontology, v. 30, p. 647–676.

Rahman, I.A., Darroch, S.A.F., Racicot, R.A., and Laflamme, M., 2015, Suspension feeding in the enigmatic Ediacaran organism *Tribrachidium* demonstrates complexity of Neoproterozoic ecosystems: Science Advances, v. 1(10), e1500800.

Reid, L.M., García-Bellido, D.C., Payne, J.L., Runnegar, B., and Gehling, J.G., 2017,
Possible evidence of primary succession in a juvenile-dominated Ediacara fossil
surface from the Flinders Ranges, South Australia: Palaeogeography,
Palaeoclimatology, Palaeoclimatology, v. 476, p. 68–76.

Retallack, G.J., 2013, Ediacaran life on land: Nature, v. 493, p. 89–92.

Seilacher, A., 1989, Vendozoa: Organismic construction in the Proterozoic biosphere:
Lethaia, v. 22, p. 229–239.

Seilacher, A., 1992, Vendobionta and Psammocorallia: Lost constructions of
Precambrian evolution: Journal of the Geological Society, v. 149, p. 607–613.

Seilacher, A., 1999, Biomat-related lifestyles in the Precambrian: Palaios, v. 14, p. 86–93.

Tarhan, L.G., Droser, M.L., Gehling, J.G., and Dzaugis, M.P., 2017, Microbial mat
sandwiches and other anactualistic sedimentary features of the Ediacara
Member (Rawnsley Quartzite, South Australia): Implications for interpretation of
the Ediacaran sedimentary record: Palaios, v. 32, p. 181–194.

Wade, M., 1969, Medusae from uppermost Precambrian or Cambrian sandstones,
central Australia: Palaeontology, v. 12, p. 351–365.

Wade, M., 1972, Hydrozoa and Scyphozoa and other medusoids from the Precambrian
Ediacara fauna, South Australia: Palaeontology, v. 15, p. 197–225.

Waggoner, B., 2003, The Ediacaran biotas in space and time. Integrative and
Comparative Biology: v. 43, p. 104–113.

Xiao, S. and Laflamme, M., 2009, On the eve of animal radiation: phylogeny, ecology,
and evolution the Ediacara biota: Trends in Ecology and Evolution, v. 24, p. 31–
40.

CHAPTER 2: OSTRACODE RESPONSE TO AN EARLY EOCENE WARMING EVENT IN THE NORTH AND EQUATORIAL ATLANTIC

Abstract

Earth's climate in the late Paleocene and early Eocene was characterized by multiple hyperthermal events, including the Paleocene-Eocene Thermal Maximum (PETM) and Eocene Thermal Maximum 2 (ETM2). These events have been identified by global carbon and oxygen isotope excursions. Eocene Thermal Maximum 2 (ETM2) occurred about two million years after the PETM. The isotope excursions that identify it are about half the magnitude of those corresponding to the PETM, indicating that ETM2 was a less extreme hyperthermal event. Single-celled microfossils, such as forams, have been used extensively to characterize these early Cenozoic climate events. Ostracodes (small, bivalved crustaceans) provide an opportunity to characterize and evaluate how multicellular animals responded to these changing environments. Here, we investigate patterns of ostracode abundance and diversity across EMT2 at two deep marine sites: ODP Site 1258 in the equatorial Atlantic and IODP Site U1409 in the north Atlantic. We evaluate patterns of ostracode accumulation rates and diversity as they correspond to the bulk and benthic foraminifera carbon and oxygen isotope excursions. At both sites, ostracode accumulation rate and diversity decrease at ETM2, but recover to pre-ETM2 conditions within the recovery period of the isotope excursions. Ostracode accumulation rates after ETM2 are similar to those before the excursions, and the

ostracode genera present after ETM2 are, with only a couple exceptions, the same as those present before ETM2.

Introduction

Extensive warming that coincided with input of large amounts of carbon to the atmosphere and ocean at the Paleocene-Eocene boundary (Kennett and Stott, 1991), provides a possible analogue for modern climate change. This event of relatively rapid warming coupled with an atmospheric and oceanic carbon isotope excursion has been termed the Paleocene-Eocene Thermal Maximum (PETM), and it has since been recognized from localities world-wide. The PETM occurred approximately 55-56 million years ago, and is marked by a global warming of ~5° C (Dunkley Jones et al., 2013; McInerney and Wing, 2011; Zachos et al., 2010), as can be identified by the associated excursion in stable oxygen isotopes. The PETM is characterized by a negative carbon isotope excursion of greater than 2‰ and extensive dissolution of seafloor carbonate sediments; furthermore, these effects have been noted globally (Dunkley Jones et al., 2013; Zachos et al., 2007).

There is still significant disagreement concerning many of the specifics of the PETM, but there is increasing consensus that the carbon release that triggered the PETM occurred quite rapidly, likely over a only few thousand years (Kirtland Turner et al., 2017; Kirtland Turner, 2018). The PETM was an extreme event that introduced what is likely to be at

least several thousand petagrams of carbon into the ocean-atmosphere system (Gutjahr et al., 2017; Dickens et al., 1997). The source(s) of this carbon is also still controversial, but suggestions have included volcanic flood basalts, such as those associated with the North Atlantic Igneous Province (Gutjahr et al., 2017; Storey et al., 2007), remobilization of methane hydrate deposits (Dickens et al., 1995), thawing permafrost (DeConto et al., 2012) and oxidation of organic carbon (Higgins and Schrag, 2006).

Unsurprisingly, these massive environmental changes over a relatively short time period impacted the organisms living at that time. Notably, there is an extinction event of benthic foraminifera that coincides with the PETM. It has been suggested that this extinction was likely in response to variations in the temperature of the deep ocean, pH, and/or dissolved oxygen (Thomas, 2003). Conversely, it appears that ostracodes, although they still experienced changes in community structures, were less stressed than deep-sea benthic foraminifera (Webb et al., 2009).

Eocene Hyperthermal Events

Although the PETM is the largest and most well-studied hyperthermal event, there are multiple other, similar albeit smaller, events that occur episodically throughout the early to middle Eocene. The Early Eocene Climate Optimum (EECO) is an interval in which multiple hyperthermal events occurred (Zachos et al., 2008). Like the PETM, these events were also rapid, global, can be identified by negative carbon and oxygen isotope

excursions (Littler et al, 2014), and were likely associated with elevated levels of silica

burial (Penman et al., 2019). However, in addition to being smaller in magnitude than

the PETM, the early Eocene hyperthermal events also had shorter recovery intervals,

perhaps suggesting that the carbon was re-sequestered by the ocean (though not

recorded by foraminiferal or carbonate records) or that carbon cycle feedbacks other

than silicate weathering were able to speed up recovery times (Sexton et al., 2011).

Similarly, the regularity with which these intervals recurred indicates that the source of

the carbon may have differed from that of the PETM as well, and was possibly

something more regular such as carbon dioxide ventilation (Sexton et al., 2011).

Although the PETM was clearly an exceptional event, it has been suggested that the

subsequent early-to-middle Eocene hyperthermals may have been a relatively regular

feature of the early Cenozoic warm period (Kirtland Turner et al., 2014; Littler et al.,

2014; Sexton et al., 2011). Furthermore, these early Eocene hyperthermal events appear

to be paced by orbital forcings (Kirtland Turner et al., 2014; Sexton et al., 2011; Zachos

et al., 2010).

The first of these smaller hyperthermal events is Eocene Thermal Maximum 2 event

(ETM2, also sometimes referred to as the ELMO or H1 event) which occurred between

53-54 million years ago. ETM2 was a hyperthermal event marked by roughly half the

magnitude of the PETM. It is shorter in duration and characterized by a negative carbon

isotope excursion of ~1‰ and roughly 2° C of warming (Lauretano et al., 2015; Kirtland

Turner et al., 2014; Cramer et al., 2003). Ostracodes represent an opportunity to examine the impact that this event had on multicellular animal life. In this paper, we compare patterns of ostracode diversity and abundance across Eocene Thermal Maximum 2 from two deep-sea ocean drilling sites, IODP Site U1409 in the north Atlantic off the coast of Newfoundland and ODP Site 1258 in the tropical Atlantic off the coast of Suriname, in order to begin to develop a global record of how these animals responded changing climates and environments in the early Eocene.

Ostracode Records

Ostracodes are a class of small, bivalved animals in the subphylum Crustacea of the phylum Arthropoda that form an important part of the marine biota (Benton and Harper, 2009). Ostracodes are characterized by their shrimp-like body plan housed within a small, seed-shaped calcium carbonate shell (Horne et al., 2002). They are very small, typically not more than a few millimeters in length, although they are commonly only a few hundred microns (Benson, 1981).

In addition to being abundant in modern oceans and lakes, ostracodes also have a very rich fossil record, originating in the early Paleozoic, which makes them ideally suited to paleontological research. Ostracodes are abundant in the fossil record (Horne and Martens, 2000), typically preserved as single, separated valves.

Ostracodes provide an ideal study system for understanding past environmental conditions. First, because ostracodes have shells composed of calcium carbonate, they are commonly preserved in the fossil record (Boomer, 2002). Secondly, because they are microfossils, it is possible to have large numbers of them in relatively small amounts of sediment, such as from cores. And thirdly, in the case of ostracodes recovered from core sediments, it is possible to create high-resolution records of ostracodes and their environment through millions of years (Boomer, 2002). Finally, because of their small size, ostracodes represent an ideal opportunity for investigating the response of more complex, multicellular animals to environmental change in high-resolution ocean drill core records.

Past studies have investigated how marine ostracodes respond to environmental changes around the PETM and the Cretaceous-Paleogene (K/Pg) extinction. Yamaguchi and Norris (2015) found that on Allison Guyot in the Central Pacific, ostracodes underwent a large extinction during the PETM; a 64% loss of species richness and 94% loss of abundance in ostracodes were recorded. On the guyot, the extinction lasted for about 1.1 million years before a 200 thousand-year-long recovery. This is in contrast to a 25-38% extinction on continental margins followed by a relatively rapid recovery. The authors suggest that guyot extinction may have been caused by a combination of acidification, metabolic limitations resulting from increased temperature, and faster bottom-water currents, and that the long recovery was due to the isolation of guyot

populations. Boomer and Whatley (1995) also describe high levels of endemism in ostracode species on guyots as well as ostracode extinction events on guyots during the PETM. Steineck and Thomas (1996) found that during the PETM the ostracode assemblage on the Maud Rise in the Weddell Sea experienced a large turnover coincident with a strong decrease in benthic foraminiferal $\delta^{18}O$ that indicates a 4-6° C increase in deep water temperature. During this event, ostracode diversity and abundance fell to the lowest levels recorded in the study, and an opportunistic, thin-walled ostracode fauna replaced the previously stable, dominant, heavily calcified fauna. After a recovery of 25-40 thousand years, the previously dominant taxa returned, but were smaller than before. Yamaguchi et al. (2017a; and see also Yamaguchi et al., 2017b and 2017c) found that ostracodes showed varied responses to environmental change events earlier in the Paleocene. Near the K/Pg boundary, deep-sea ostracodes from the north Atlantic (IODP Site U1407) show a rate of extinction similar to that of background extinction levels, which was notably lower than that calculated for shallow marine sites in Texas and Brazil, and also different from other deep-sea and coeval North Atlantic sites. During the Latest Danian Event (LDE), there was an increase in benthic ostracode accumulation rate followed by a decrease in taxonomic diversity and changes in taxonomic composition, but no ostracode extinction event. Following the LDE, they found the appearance of faunas with tolerance to warm, acidified water. Furthermore, Yamaguchi et al. (2012) noted that ostracodes from a North Atlantic core decreased in size during the PETM, and that the correlation between ostracode body

size and benthic foraminiferal oxygen isotope data suggests that this decrease was the

result of increased temperatures. Importantly, the authors also note that, although both

ostracodes and benthic foraminifera show decreased body-size during the PETM, the

ostracodes show a decrease in lifetime metabolic rate, while benthic foraminifera

metabolic activity has been shown to increase with higher temperature (*e.g.* Alegret et

al., 2010; Thomas, 2007). Thus, different benthic taxa responded differently to the

changing environmental conditions of the PETM, but responses to ETM2 remain

enigmatic.

Sites

IODP Site U1409: Expedition 342 of the Integrated Ocean Drilling Program (IODP) was

designed to target Paleogene-aged sedimentary sequences from a wide range of

paleodepths with high deposition and microfossil accumulation rates (Expedition 342

Scientists, 2012). Site U1409 of Expedition 342 is located on the Southeast

Newfoundland Ridge off the coast of Newfoundland, Canada, around 41°N, 49°W

(Figure 2.1), and was recovered from a present sea floor water depth of 3503 m (Norris

et al., 2014). The paleodepth of the site is about 3050 meters below sea level (Tucholke

and Vogt, 1979), and the site was more shallow than the Paleogene carbonate

compensation depth. Coring at the site recovered deep-sea pelagic sediment ranging

from the Pleistocene to the early Paleocene (Norris et al., 2014). The sedimentary

sequence recovered is approximately 200 m thick and is composed of four

lithostratigraphic units (Norris et al., 2014). Sedimentation rates for the Paleocene and

Eocene sections of the core, representing ~15 Ma, range from 0.47-1.80 cm/kyr (Norris

et al., 2014). Benthic foraminifera are mostly rare in the Paleocene and Eocene

sediments, but the preservation of their tests is typically good (Norris et al., 2014).
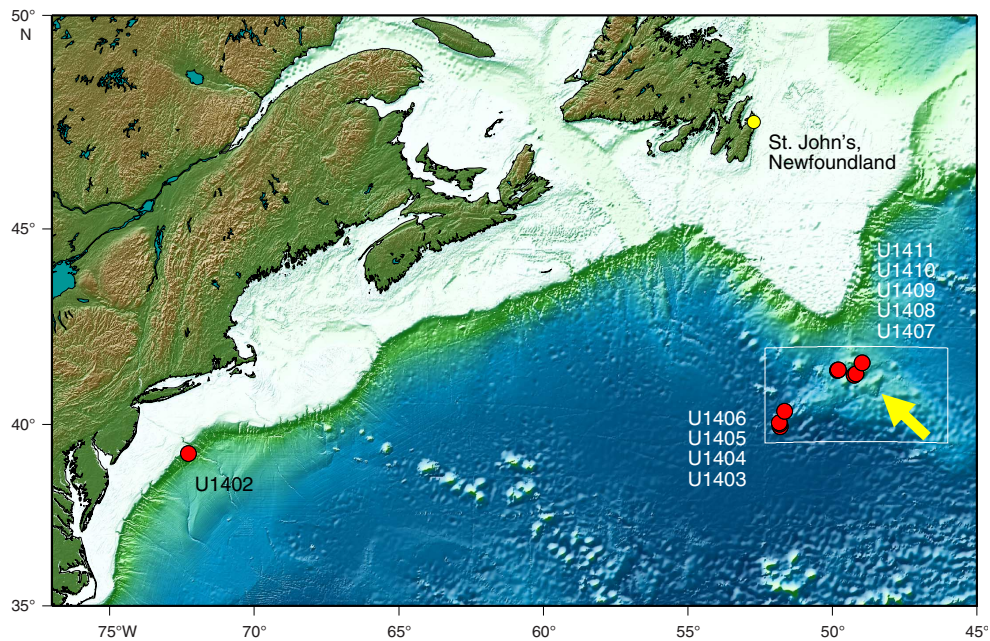
Figure 2.1. IODP Site U1409. Map of sites from IODP expedition 342, including U1409.
Modified from Expedition 342 Scientists, 2012.

ODP Site 1258: Ocean Drilling Program (ODP) Leg 207 was designed to obtain a high-

resolution Paleogene oceanographic record from a location in tropical latitudes in order

to evaluate paleoenvironmental changes and the biotic response to them (Erbacher et

al., 2004). Site 1258 is the deepest site of the paleoceanographic depth transect

conducted by ODP Leg 207 (Figure 2.2). Site 1258 is located on the western slope of the

Demerara Rise, about 380 km north of Suriname in the tropical Atlantic, at about 9°N,

54°W (Shipboard Scientific Party, 2004), and was recovered from a present sea floor water depth of 3192 m (Erbacher et al., 2004). The paleodepth of the site during the Eocene was around 2500-3200 m (Sexton et al., 2006). The material recovered from this site ranges from early Albian to Miocene in age, though there are some hiatuses in the record (Shipboard Scientific Party, 2004). The five distinct hiatuses may represent periods of slow deposition or erosion, and, based on biostratigraphic evidence, appear to range from approximately 1-32 million years in duration (Shipboard Scientific Party, 2004). Five lithostratigraphic sequences were recognized from the cores. The Paleocene- and Eocene-aged material is in Unit II, a 325 m thick, greenish gray sequence composed of nannofossil and calcareous chalk with foraminifera (Shipboard Scientific Party, 2004). Middle Eocene- late Paleocene (~20 Ma) sedimentation rates are described as average for pelagic chalks and oozes, at about 1.5 cm/ kyr (Shipboard Scientific Party, 2004). Preservation of foraminifera in the Paleocene and Eocene sediments ranges from poor to good (Shipboard Scientific Party, 2004).

This research examines records from both of these sites in order to directly compare conditions during ETM2 at different regions of the Atlantic Ocean. By comparing data from the North Atlantic to data from the equatorial region, we begin to create a more global record, and it becomes possible to begin to determine how universal changes in the paleoenvironment were and whether life in different locations responded to changes in the same way.
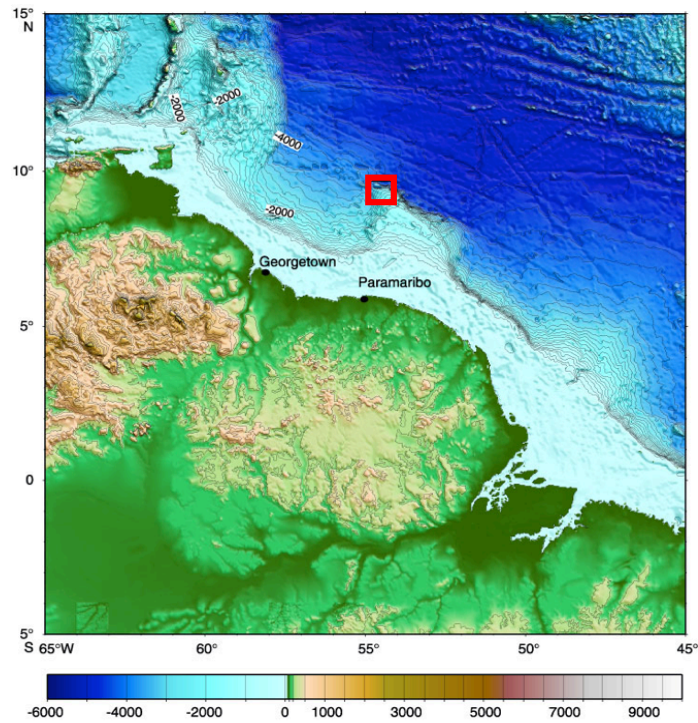
Figure 2.2. ODP Site 1258. Map showing location of ODP Site 1258. Modified from Erbacher et al., 2004.

Methods

We used δ¹³C and δ¹⁸O isotope records to target ETM2-aged sediments in the cores. For ODP Site 1258, bulk carbonate δ¹³C and δ¹⁸O records have been generated for about 4.25 million years of carbonate core sediment spanning the Early Eocene Climate Optimum (Kirtland Turner et al., 2014). This record includes the isotope excursions that identify ETM2.

For IODP Site U1409, we generated bulk carbonate $\delta^{13}C$ and $\delta^{18}O$ isotope records for late Paleocene and early Eocene. The bulk carbonate was run on a Kiel IV carbonate perception device coupled to a DELTA V dual-inlet mass spectrometer. Samples were run with known standard, and the results converted into delta values internally and reported relative to Vienna PeeDee Belemnite (VPBD).

For both sites, ostracodes were picked from samples across the identified isotope excursions in order to develop the ostracode record across the ETM2 hyperthermal event. We picked ostracodes from samples at a high resolution before the excursions as well as during the excursions and following the recoveries. At IODP Site U1409, the samples picked were at a resolution of about every 3 cm. At ODP Site 1258, the samples picked were at a resolution of about every 9 cm.

Sample Processing and Picking

Core sediments from both sites was washed and sieved through a 63 μm mesh with deionized water, dried, and weighed to obtain the coarse fraction. All of the ostracodes in the greater than 180 μm size fraction were picked using a binocular microscope. Photographs were taken using a TESCAN MIRA3 GMU scanning electron microscope in CFAMM at UC Riverside. The number of ostracodes collected from each sample was recorded to calculate the ostracode accumulation rates through the cores. To ensure that the number of ostracodes was not overestimated, the number of left and right

valves of each genus in a sample was counted, and the smaller of these two numbers was added to the number of articulated ostracodes in that sample to give a minimum number of individuals for each sample.

Ostracode Accumulation and Diversity

After they were picked, all of the ostracodes were identified to the genus level (Figures 2.3-2.5). The presence of the different genera from the samples throughout the cores, as well as the numbers of individuals present from each genus, were recorded to generate a record of ostracode assemblages for each of the cores.

Ostracode abundance is reported here as ostracode accumulation rate, in order to correct for changes in sedimentation and differences in sediment sample sizes. The ostracode accumulation rates for the sites was calculated by multiplying sedimentation rate, dry bulk density, and number of ostracodes per gram for each sample to generate a record of ostracodes per kyr cm^2.
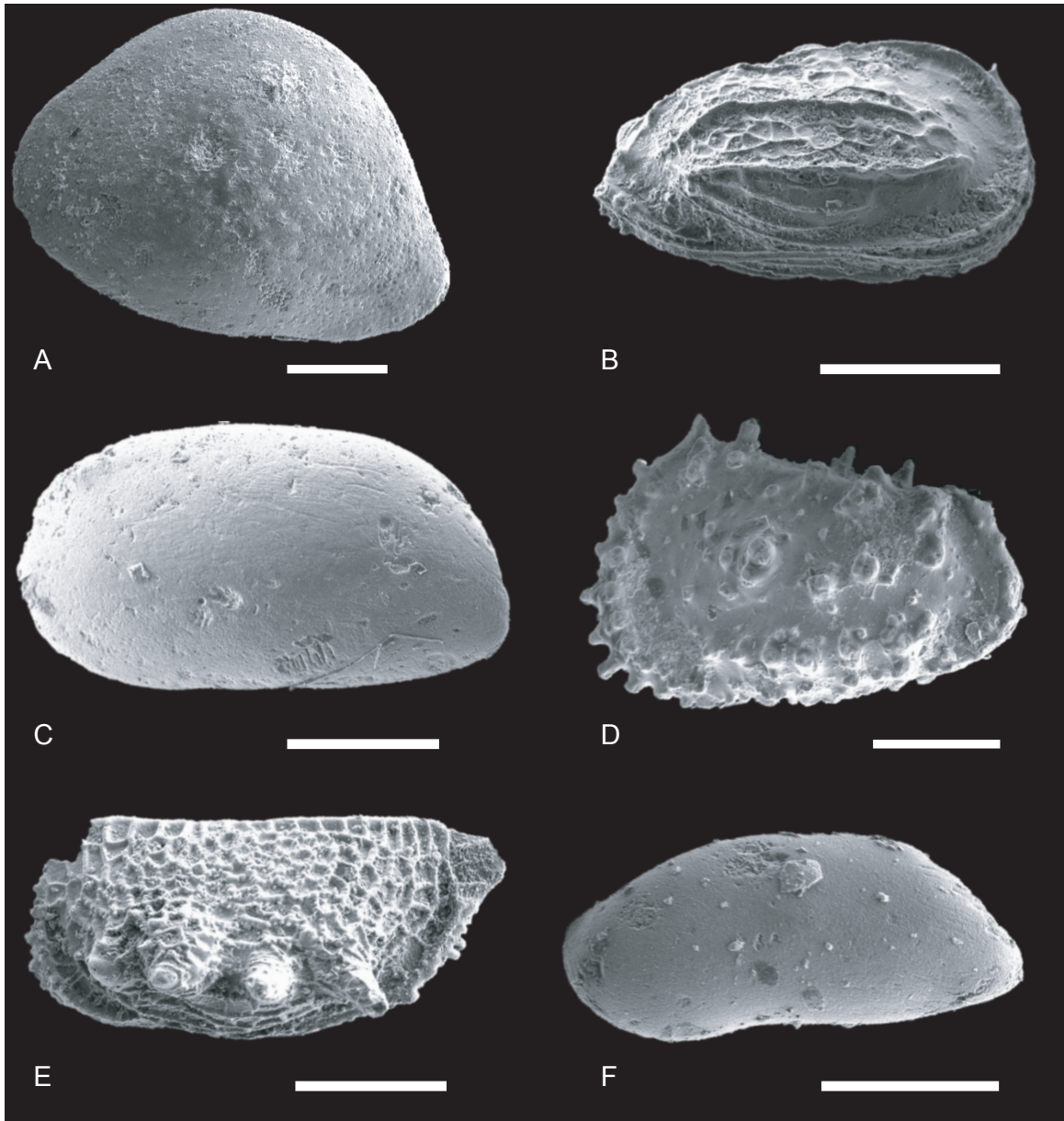
Figure 2.3. Plate 1. SEM images of external views of ostracodes from this study. All scale bars are 200 μm. A. *Neonesidea* left valve from 1258; B. *Ambocythere* right view of carapace from 1258; C. *Krithe* left valve from 1258; D. *Croninocythereis* left valve from 1258; E. *Nemoceratina* left valve from U1409; F. *Argilloecia* left valve from U1409.
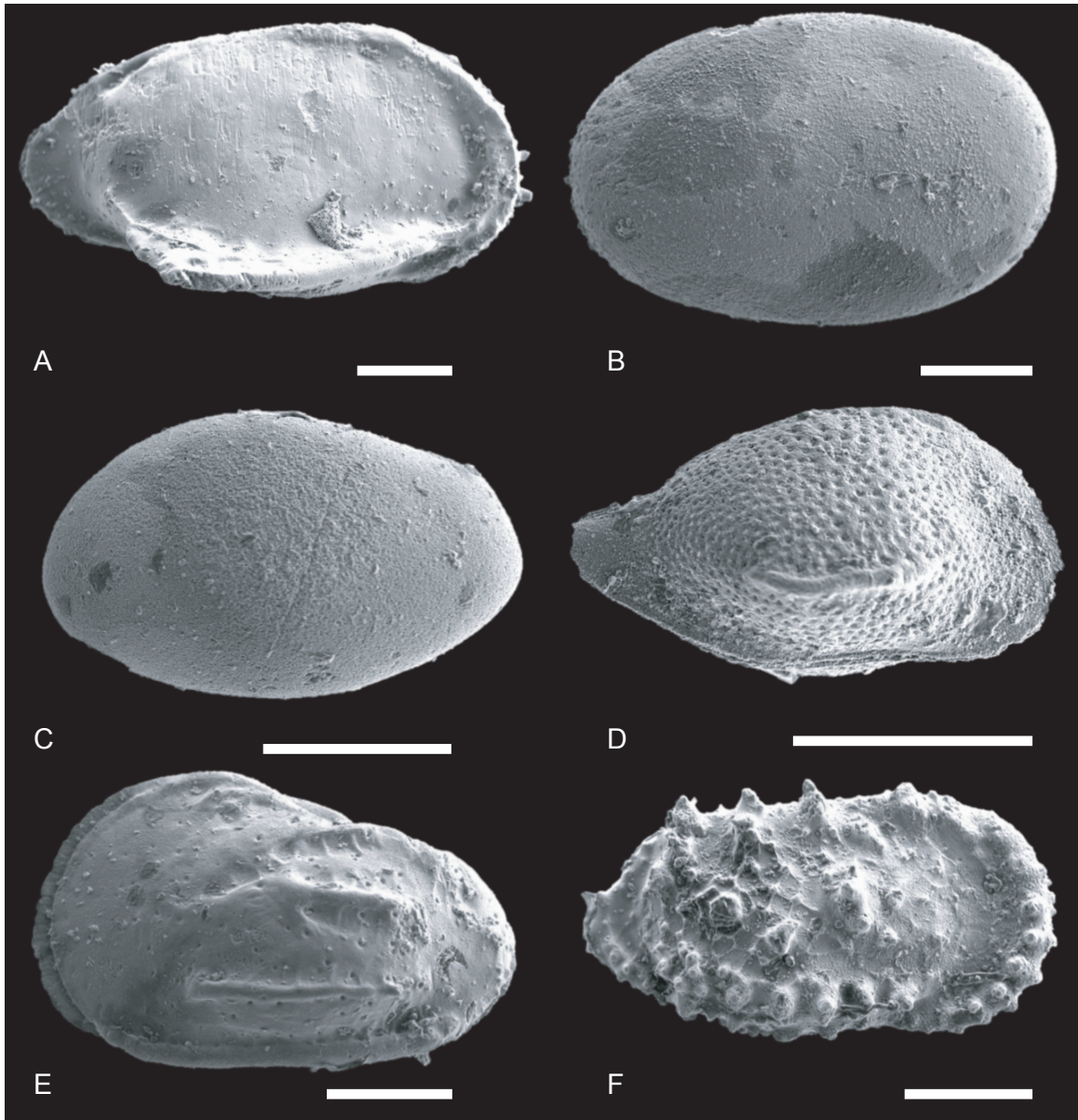
Figure 2.4. Plate 2. SEM images of external views of ostracodes from this study. All scale bars are 200 μm. A. *Pterygocythereis* right valve from U1409; B. *Cytherella* right valve from U1409; C. *Cardobairdia* left valve from U1409; D. *Rimacytheropteron* right valve from U1409; E. *Phacorhabdotus* left valve from U1409; F. *Croninocythereis* right valve from U1409.
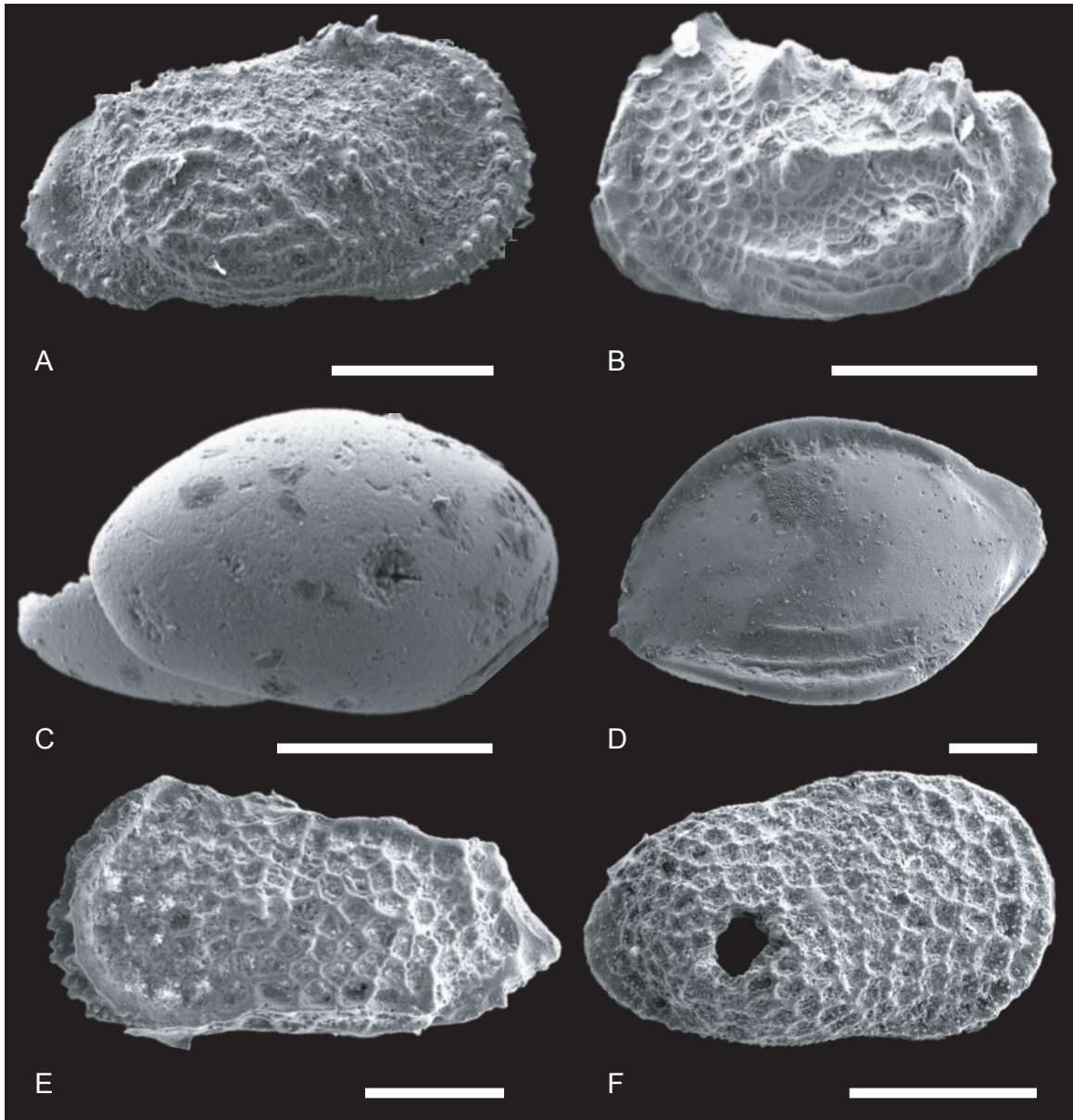
Figure 2.5. Plate 3. SEM images of external views of ostracodes from this study. All scale bars are 200 μm. A. *Pennyella* right valve from 1258; B. *Herrigocythere* left valve from 1258; C. Xestoleberidae gen. et sp. right valve with associated left valve from 1258; D. *Pelecocythere* left valve from U1409; E. *Trachyleberidea* left valve from U1409; F. *Rugocythereis* right valve from U1409.

Results

Isotope Results

We examined a ~400 kyr interval of IODP Site U1409 that includes the ~150 kyr ETM2.
The carbon isotope excursion interval that identifies ETM2 has been located between
174.46 and 172.26 mcd. We find about a 0.62‰ drop in carbon isotope values and
about a 0.6‰ drop in oxygen isotope values at ETM2, followed by a partial recovery in
the carbon isotopes and a full recovery in the oxygen isotopes.

For Site 1258, we used the bulk carbon and oxygen isotope data generated by Kirtland
Turner et al. (2014). The carbon isotope excursion that identifies ETM2 has been located
between 133.42 and 132.12 mcd. There is about a 1.56‰ drop in carbon isotope values
and about a 0.61‰ drop in oxygen isotope values followed by a recovery of each.

IODP Site U1409

Ostracode accumulation rate was calculated across the picked interval for IODP Site
1409 in the north Atlantic (Figure 2.6). During the time periods after and especially
before ETM2 ostracode accumulation rate was variable, with relatively large changes
from sample to sample. During ETM2, ostracode accumulation rate stays noticeably and
consistently lower than pre- and post-ETM2 times. Multiple samples during ETM2 did
not contain any ostracodes. The timing of the onset of the decrease and the recovery
back to more variable, slightly higher ostracode accumulation rates correlates with the

onsets and recoveries of the carbon and oxygen isotope excursions (Figure 2.6). Relative to pre-ETM2, post-ETM2 ostracode accumulation rates are slightly lower and less variable, while still being higher and more variable than ostracode accumulation rates during ETM2.
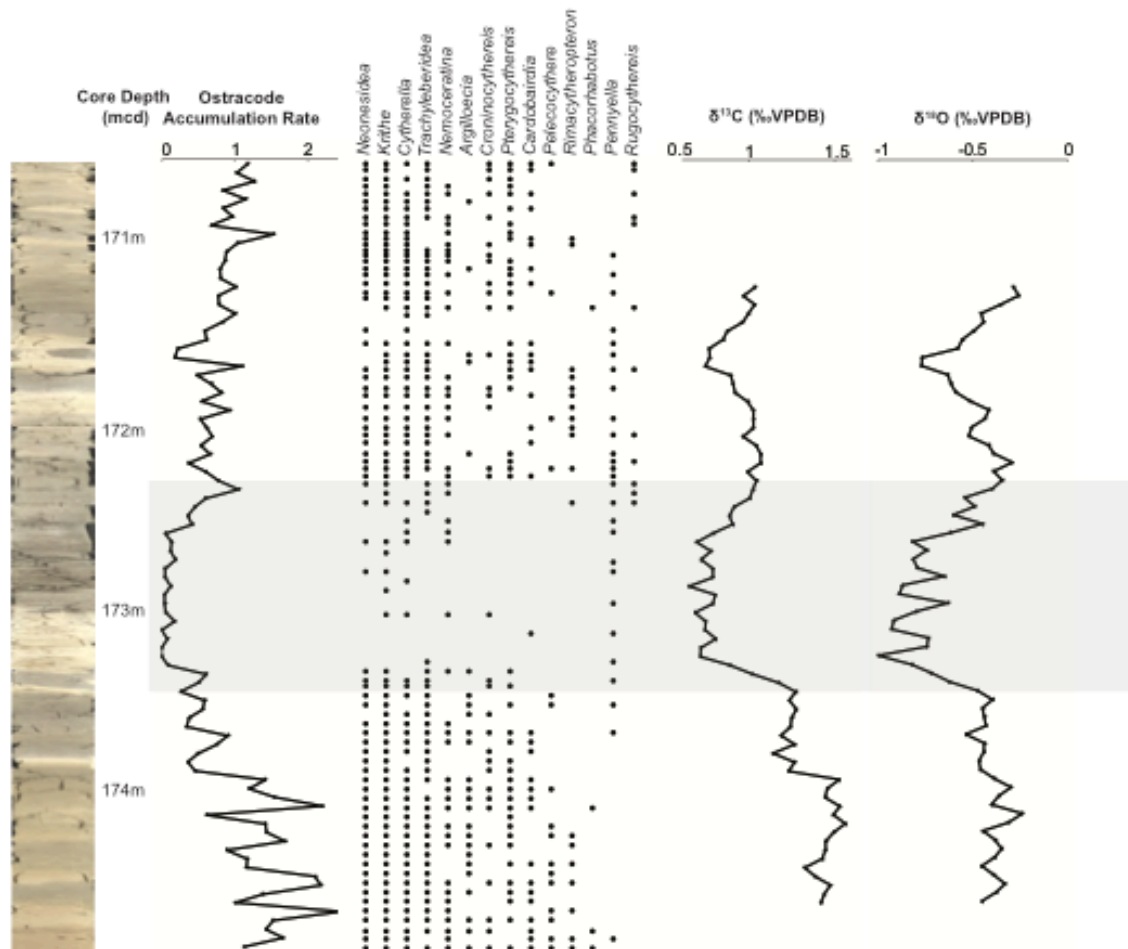
Figure 2.6. U1409 Accumulation rate, diversity and isotope results. Ostracode accumulation rate and diversity from Site U1409 shown with core depth and bulk carbon and oxygen isotopes. Horizontal gray bar identifies ETM2. Ostracode accumulation rate given in ostracodes per kyr cm^2. Diversity given in presence or absence of each genus in each sample.

There are 14 total genera in the samples from the picked interval from IODP Site U1409 (Figure 2.6). During ETM2, the average genus diversity per sample drops to about 3 genera, as compared to about 7 genera before ETM2 and 8 after ETM2. Two genera, *Pelecocythere* and *Phacorhabdotus*, are not present in any samples during ETM2, but both of these genera are generally relatively rare throughout the picked interval. A few other genera are also only present towards the beginning or end of ETM2, despite being present in several samples both before and after. The assemblages before and after ETM2 are similar to one another. *Krithe* and *Neonesidea* are the most abundant throughout the interval, and are the dominant genera both before and after ETM2. Other genera, notably *Cytherella* and *Trachyleberidea,* are also present in most samples before and after ETM2. All genera present before ETM2 are also present in at least one sample after ETM2. One genus, *Rugocythereis* is present only in samples during and after ETM2. It appears for the first time in the picked interval towards the end of ETM2 and then continues to be moderately common through the end of the picked interval. *Pennyella* first appears at this site just before ETM2, and remains common throughout ETM2 and afterwards, but disappears before the end of the picked interval. Only *Krithe* is found in more samples during ETM2, but the temporal distribution of *Krithe* throughout ETM2 is more patchy, with larger gaps between appearances than observed in *Pennyella*. Some genera, including *Argilloecia* and *Pelecocythere*, were markedly more common before ETM2 than after.

ODP Site 1258

Ostracode accumulation rate was calculated across the picked interval for ODP Site 1258 in the tropical Atlantic (Figure 2.7). Before ETM2, ostracode accumulation rate was relatively variable. During ETM2 ostracode accumulation rate is less variable, and stays mostly lower relative to the time periods before and after the isotope excursion. This period of sustained relatively lower ostracode accumulation rates correspond to the timing of the carbon and oxygen isotope excursions, with an initial drop beginning at the onset of the isotope excursions and a recovery to the highest ostracode accumulation rate in the picked interval roughly correlating to the end of the recoveries in the isotope excursions (Figure 2.7). Following a spike at the end of ETM2, ostracode accumulation rate slowly decreases and has less variation from sample to sample. Despite the slow decrease, the ostracode accumulation rates after ETM2 are still mostly higher than the rates during ETM2.
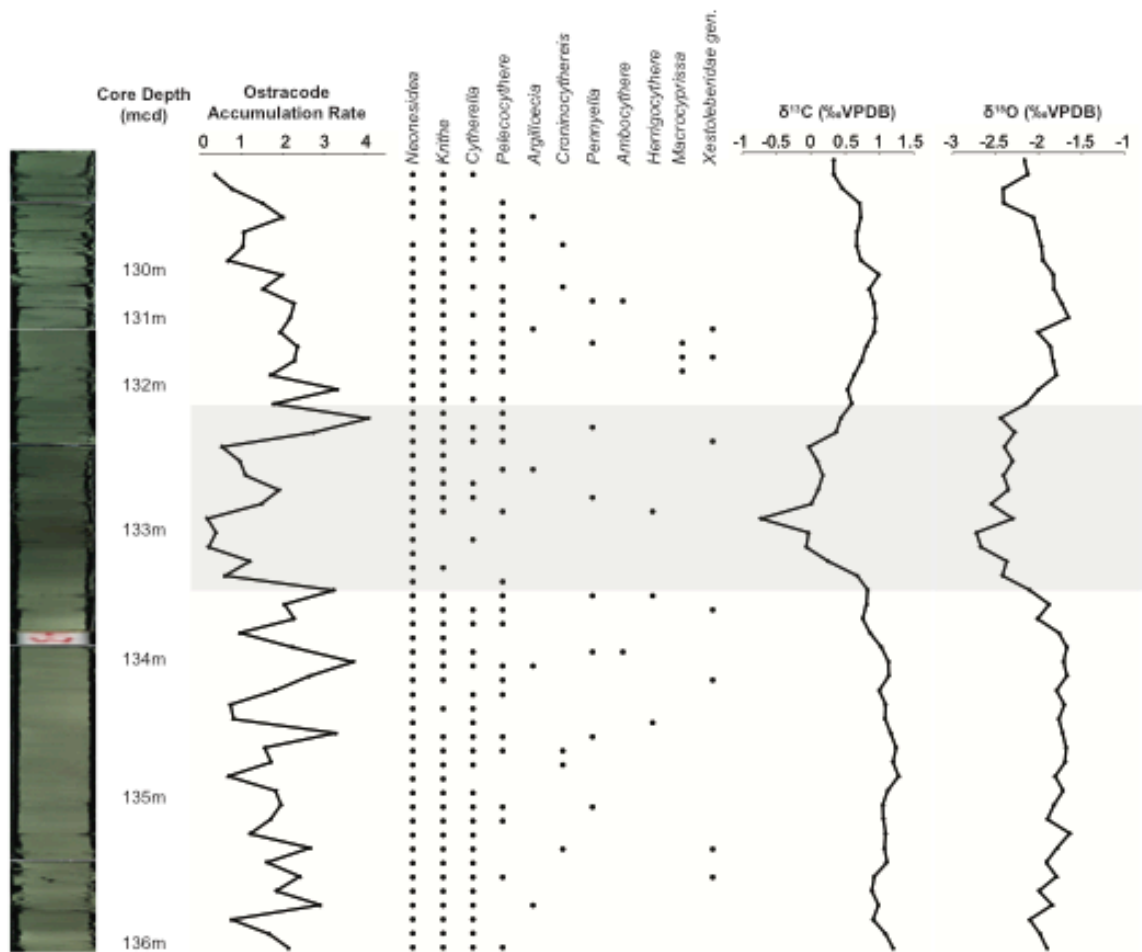
Figure 2.7. 1258 Accumulation rate, diversity and isotope results. Ostracode accumulation rate and diversity from Site 1258 shown with core depth and carbon and oxygen isotopes. Bulk isotope data from Kirtland Turner et al., 2014. Horizontal gray bar identifies ETM2. Ostracode accumulation rate given in ostracodes per kyr cm^2. Diversity given in presence or absence of each genus in each sample.

There are a total of 11 genera in the samples from the picked interval from ODP Site

1258 (Figure 2.7). During ETM2 the average genus diversity per sample drops slightly to

about 3 genera, as compared to about 4 genera before ETM2 and 4 after ETM2. Only

three genera are not present at all in any samples during ETM2: *Croninocythereis* and

Ambocythere, are generally rare genera, with *Ambocythere* only appearing in one

sample before and one sample after ETM2, and *Macrocyprissa* is also rare, present in only three samples, all after ETM2. *Macrocyprissa* is one of only two genera not present in samples both before and after ETM2. The second, *Herrigocythere*, is also rare-represented in only three samples, two before and one during ETM2. Every sample from the picked interval contained at least one ostracode, even through the duration of ETM2. *Neonesidea* is the only genus present in every sample during ETM2, and, in fact, is present in all but one sample throughout the entire picked interval. *Neonesidea* and *Krithe* are the most dominant genera throughout the interval. *Krithe* disappears from a few samples at the beginning of ETM2, but returns and subsequently occurs through the rest of ETM2. Two other genera, *Pelecocythere* and *Cytherella*, are also relatively common both before and after ETM2, and are present sporadically through ETM2, particularly towards the end. The remaining 3 taxa, *Argilloecia*, *Pennyella*, and an unidentifiable genus of Xestoleberidae, are present, albeit rarely, before, during, and after ETM2. With the exception of the four more common genera, most taxa, although they are present in samples after ETM2, stay relatively rare and are more concentrated in the samples immediately following ETM2, and largely absent from the latest samples in the picked interval.

Discussion

There are many similarities between the two sites, despite their difference in latitude. In particular, the patterns of diversity and abundance are similar between the two sites, as

are the genera that are present at each. At both sites ostracode accumulation rate

decreased through the duration of ETM2 in concert with the carbon and oxygen isotope

excursions relative to the time periods before and after. The decrease at ETM2 is less

variable than in the surrounding time periods at both sites; however, there is noticeably

more variation in ostracode accumulation rate throughout the picked interval in the

equatorial (1258) record than in north Atlantic (U1409) record. As a result, the pattern

of decrease at ETM2 is less clear, but there does still seem to be a sustained relative

decrease that co-occurs with the isotope excursions. Another difference is that there are

samples in the U1409 record with no ostracodes preserved. This is not true of the 1258

record, but there are multiple samples with only a few ostracodes preserved.

Neither site shows evidence of an extinction event or extirpation in ostracodes at the

genus level during ETM2. With the exception of *Herrigocythere*, a rare genus at 1258, at

both sites, the genera that are present before ETM2 are also eventually found again in

samples after ETM2. So, while some taxa may have become so rare as to either not be

preserved in the fossil record or have temporarily left the area for the duration of the

hyperthermal, these scenarios were relatively short-lived and not extreme enough to

rise to the level of an extinction or permanent extirpation from the sites. Only a few

new-to-the-site genera appear either during or after ETM2 at either site, so there also

does not appear to be much difference between pre- and post-ETM2 assemblages at the

study sites. This is particularly true of ODP Site 1258, where there is very little change

even in how common the different genera are before and after ETM2. It is also still

largely true of U1409, but some genera at that site do become less common after ETM2

than they were before.

Both sites are also characterized by the same two dominant genera, *Krithe* and

Neonesidea before, during, and after ETM2. Beyond this, there is also clear overlap

between the other genera present at the sites. Seven genera are present at both sites,

and only four genera are only present at 1258 and seven at U1409. Site U1409 has a

higher diversity than 1258. It seems likely that this also may be an artefact of the slightly

higher sampling resolution at U1409, but it is worth noting that this is in contrast to

evidence that suggests, at least in the Quaternary, ostracode assemblages have higher

diversity during warmer, interglacial time periods (Cronin et al., 1999; Yasuhara et al.,

2009). Yasuhara et al. (2009) suggest that this pattern, at a single site, is likely related to

shifting species distributions up or down slope as temperature changes, which would

not necessarily explain diversity differences between sites at very different latitudes.

Importantly, both studies reiterate the clear response that ostracodes show to rapidly

changing environments (Cronin et al., 1999; Yasuhara et al., 2009). Overall diversity is

also decreased at ETM2 relative to before and after the hyperthermal at both sites. Like

the decrease in ostracode accumulation rates, this drop in diversity is closely tied

temporally to the isotope excursions. It is likely that drop in diversity is mostly

controlled by the decreased abundance of ostracodes during ETM2, particularly

because, in most samples, many of the genera present are represented by only one or two specimens. The more dominant genera, *Krithe* and *Neonesidea*, are also the ones that persist most consistently throughout ETM2. In the same vein, it is also possible that the higher diversity observed at IOPD Site U1409 might be related to the higher numbers of ostracodes found at that site in general.

Notes on Preservation

These sites had relatively large proportions of juvenile ostracodes to adults, which might indicate that the ostracode assemblages are mostly *in-situ*. A relatively large percentage (~34%) of the ostracodes recovered from ODP site 1258 were articulated, which may also be indicative of little to no transport of the ostracodes at that site. Preservation of the ostracodes themselves was moderate. There is some evidence of dissolution, and while the ostracodes were not especially well preserved, preservation was largely good enough to identify genera. While not many fragmented-beyond-identification ostracodes were found during picking, the ostracodes from both sites were fragile enough that attempts to clean sediment off of the carapaces or out from the inside of the valves often resulted in broken valves.

It is worth noting that the lower resolution of the 1258 record may have impacted some of the patterns we found. For instance, some of the differences observed, such as the differences in ostracode accumulation rate variability may be artefacts of the lower

resolution of the 1258 record. There were also fewer ostracodes preserved at that site

in general, and the low sample sizes may have impacted our results, but it is unlikely

that the overall patterns would be different with more specimens. Furthermore,

ostracodes are not present in particularly large abundances at either of these deep-sea

sites, so the differences in abundances are not extreme.

Comparison to PETM

Several authors have reported marked decreases in ostracode abundance (*e.g.*

Yamaguchi and Norris, 2012), and even ostracode extinction events (*e.g.* Boomer and

Whatley, 1995; Steineck and Thomas, 1996; Yamaguchi and Norris, 2015) at the PETM.

Decreases in ostracode abundance and taxonomic diversity at the PETM have been

found at sites worldwide, including the North Atlantic (Yamaguchi and Norris, 2012;

Yamaguchi et al., 2017a), the Southern Ocean (Steineck and Thomas, 1996; Webb et al.,

2009), and the Tethys (Speijer and Morsi, 2002; Morsi and Speijer, 2003), spanning a

wide range of paleodepths. These records also show recoveries in ostracode abundance

to varying degrees following the PETM (see Yamaguchi and Norris, 2015). Although

these results are largely reported in abundance (as opposed to accumulation rates) and

the resolution varies, it is clear that ostracodes at sites around the world were greatly

impacted by the environmental changes they experienced at the PETM. In comparison,

the decreases in ostracode accumulation rate at ETM2 described here, while still

noticeable, are relatively lower than those observed at the PETM. Additionally, we do

not find evidence for an ostracode extinction event at ETM2. Like the PETM however, the presence of the decrease at both the north and equatorial site indicates that ostracodes at different locations were impacted by ETM2. While more data from other sites and at different paleodepths is needed to make more definitive conclusions, this seems to indicate that ostracodes do respond to smaller environmental perturbations such as ETM2, but not to the same degree that they responded to the PETM.

Ostracode Response to Other Environmental Factors

The direct cause of the decrease in ostracode accumulation rate is still unclear, but may be related to changes in food supply, temperature, acidification, or a combination of these factors. Some work has been done to investigate how ostracodes respond to these and other environmental factors, but our knowledge particularly of deep-sea taxa is limited.

Hyperthermal events such as ETM2 are often associated with the shoaling of the CCD, which can result in the dissolution of deep-sea carbonates (*e.g.* Zachos et al., 2005; Stapp et al., 2009). It has been shown that the relative increase in acidity of water below the CCD impacts not only the preservation of deep-sea ostracode valves, but also their biogeographic distribution (Yasuhara et al., 2008; Boomer, 1999), but some taxa have been found able to survive these conditions. As might be expected, some of the most abundant genera at our sites, *Krithe* and *Pennyella*, are taxa that have been found able

to survive in relatively acidic water (Yasuhara et al., 2008; Ayress et al., 1997). Both of

these are genera that do relatively well during ETM2. In fact, *Pennyella* appears at

U1409 only right before ETM2 and remains continuously present throughout ETM2 and

for a while after, but disappears from the site noticeably before the end of the picked

section. It is possible that its resistance to more acidic waters allowed it to temporarily

outcompete other taxa, allowing *Pennyella* to thrive during ETM2. It is also likely that

shoaling of the CCD and relatively higher acidity are at least partially responsible for the

relatively poor preservation of our ostracodes.

Export productivity is an important factor for deep-sea benthic life, but has proven

difficult to model and analyze in the paleo record (Paytan and Griffith, 2007; Winguth et

al., 2012; Norris et al., 2013). Nevertheless, a change in the food supply to the deep-sea

is often thought to be at least a contributing factor to changes to benthic microfossil

assemblages, including ostracodes and foraminifera (*e.g.* Steineck and Thomas, 1996;

Thomas, 2003; Yamaguchi et al., 2012). In ostracode assemblages, the presence and/or

dominance of *Krithe* has been linked to low to intermediate levels of food supply (Didie

et al., 2002; Stepanova and Lyle, 2014). Alvarez Zarikian et al. (2009) found that

assemblages that included *Argilloecia*, *Pelecocythere*, and *Pennyella* were associated

with environmental conditions that included higher food supplies. Here, we find

assemblages that are composed of a mix of these taxa. *Argilloecia* and *Pelecocythere* are

both less common during ETM2, particularly at U1409, which could suggest that the

relative increase in dominance of *Krithe* during ETM2 might be associated with changes

to food supply, but *Pennyella* is relatively more common during ETM2, which suggests

that the relationships between ostracode taxa and food supply are still unclear.

Similarly, Yasuhara et al. (2012) found comparable complications with associations of

Krithe and *Henryhowella*, another genus previously associated with higher food supply,

at Shatsky Rise.

Ostracodes have also been shown to be negatively impacted by decreases in oxygen

content, in some cases even moreso than benthic foraminifera (Braeckman et al., 2013),

but little is known about the different tolerances to low oxygen conditions among

different ostracode taxa. Huang et al. (2019) found that *Krithe* opportunistically became

dominant genus during a time of oxygen depletion. Maiorano et al. (2008) also found

that *Krithe* seemed to be relatively resistant to low-oxygen conditions, whereas

Cytherella were more vulnerable. *Krithe* and *Cytherella* were both relatively common at

U1409 and 1258, although *Krithe* was slightly more common, particularly during ETM2.

Based on this, it seems unlikely that oxygen depletion was the driving factor in the

changes we observed, but the oxygen tolerances of other specific taxa are unclear.

Based on this evidence, it is difficult to determine a single specific environmental change

that could be responsible for the changes that we find in this study. Rather, it seems

more likely that a combination of environmental changes occurred during ETM2 that

impacted different taxa in different ways. It was likely the rapidity of these changes that most impacted these taxa.

Conclusions

A variety of ostracode genera are present at both sites before, during, and after Eocene Thermal Maximum 2. Several of the same genera are present at both sites, despite the large latitudinal difference. At both sites, the assemblages before and after ETM2 are very similar. While most taxa are not present in all of the samples during ETM2, and some disappear for most of the duration of ETM2, all but one of the same genera are present again by the end of ETM2. Two genera total, one from each 1258 and U1409, are present after ETM2, but not before.

Ostracode accumulation rate at both sites shows a sustained relative decrease during ETM2. Fewer ostracodes are present during the isotope excursions than before and after. At U1409 in the North Atlantic, multiple samples at the height of the excursion did not contain any ostracodes, but all of the 1258 samples had at least one ostracode. As could be expected with the decrease in abundance, the number of genera present per sample also decreases at both sites during ETM2.

Generating a more global record of these patterns is one of the best ways we have to understand the impact of environmental changes associated with increases of carbon to

the ocean and atmosphere systems. Connecting and comparing the past environments of localities around the world is the way to put these environmental changes in a global context and is the approach that will lead to the most comprehensive understanding of the environment and the life of the time period. This research represents a relatively unique investigation of a biotic response to changing environmental conditions similar to those we are experiencing today. By using ostracodes, we are able to utilize ocean drill core material to analyze the response of a multicellular animal group from what is now the largest animal phylum on earth in high-resolution. Although continued research is required to determine the definitive causes behind these changes, by choosing to investigate ETM2, we are also able to show that these organisms show a marked response even to a smaller hyperthermal perturbation.

References

Algeret, L., Ortiz, S., Arenillas, L., Molina, E., 2010, What happens when the ocean is overheated? The foraminiferal response across the Paleocene-Eocene Thermal Maximum at the Alamedilla section (Spain): Geological Society of America Bulletin, v. 122, p. 1616-1624.

Alvarez Zarikian, C.A., Stepanova, A.Yu., Grütner, J., 2009, Galcial-interglacial variability in deep sea ostracod assemblage composition at IODP Site U1314 in the subpolar North Atlantic: Marine Geology, v. 258, p. 69-87.

Ayress, M., Neil, H., Passlow, V., Swanson, K., 1997, Benthonic ostracods and deep watermasses: a qualitative comparison of Southwest Pacific, Southern and Atlantic Oceans: Palaeogeography, Palaeoclimatology, Palaeoecology, v. 131, p. 287-302.

Benson, R.H., 1981, Form, function, and architecture of ostracode shells: Annual Review of Earth and Planetary Sciences, v. 9, p. 59-80.

Boomer, I., 1999, Late Cretaceous and Cainozoic bathyal Ostracoda from Central Pacific (DSDP Site 463): Marine Micropaleontology, v. 37, p. 131-147.

Boomer, I., 2002, Environmental Applications of Marine and Freshwater Ostracoda, *in* Haslett, S.K., ed., Quaternary Environmental Micropaleontology: New York, Oxford University Press, 340 p.

Boomer, I., and Whatley, R., 1995, Cenozoic ostracode from guyots in the western Pacific: Holes 865B and 866B (Leg 143), *in* Winterer, E.L., Sager, W.W., Firth, J.V., and Sinton, J.M., eds., Proceedings of the Ocean Drilling Program, Scientific Results, v. 143, p. 75-86.

Braeckman, U., Vanaverbeke, J., Vincx, M., Oevelen, D. van, and Soetaert, K., 2013, Meiofauna metabolism in suboxic sediments: currently overestimated: PLoS One, v. 8, e59289.

Cramer, B.S., Wright, J.D., Kent, D.V., Aubry, M-P., 2003, Orbital climate forcing of $\delta^{13}C$ excursions in the Paleocene-early Eocene (chrons C24n-C25n): Paleoceanography, v. 18, p. 21-1-21-25.

Cronin, T.M., DeMartino, D.M., Dwyer, G.S., Rodriguez-Lazaro, J., 1999, Deep-sea ostracode species diversity: response to late Quaternary climate change: Marine Micropaleontology, v. 37, p. 231-249.

DeConto, R.M, Galeotti, S., Pagani, M., Tracy, D., Schaefer, K., Zhang, T., Pollard, D., and Beerling, D.J., 2012, Past extreme warming events linked to massive carbon release from thawing permafrost, Nature, v. 484, p. 87-92.

Dickens, G.R., Castillo, M.M., Walker, J.C.G., 1997, A blast of gas in the latest Paleocene: Simulating first-order effects of massive dissociation of oceanic methane hydrate: Geology, v. 25, p. 259-262.

Dickens, G.R., O'Neil, J.R., Rea, D.K., Owen, R.M., 1995, Dissoociation of oceanic methane hydrate as a cause of the carbon isotope excursion at the end of the Paleocene: Paleoceanography, v. 10, p. 965-971.

Didie, C., Bauch, H.A., and Helmke, J.P., 2002, Late Quaternary deep-sea ostracodes in the polar and subpolar North Atlantic: paleoecological and paleoenvironmental implications: Palaeogeography, Palaeoclimatology, Palaeoecology, v. 184, p. 195-212.

Dunkley Jones, T., Lunt, D.J., Schmidt, D.N., Ridgwell, A., Sluijs, A., Valdes, P.J., and Maslin, M., 2013, Climate model and proxy data constraints on ocean warming across the Paleocene-Eocene Thermal Maximum: Earth-Science Reviews, v. 125, p. 123-145.

Erbacher, J., Mosher, D.C., Malone, M.J., et al., 2014, Proceedings of ODP, Initial Reports, 207: College Station, TX, Ocean Drilling Program.

Expedition 342 Scientists, 2012, Paleogene Newfoundland sediment drifts. IODP Preliminary Reports, v. 342.

Gutjahr, M., Ridgwell, A., Sexton, P.F., Anagnostou, E., Pearson, P.N., Pälike, H., Norris, R.D., Thomas, E., and Foster, G.L., 2017, Very large release of mostly volcanic carbon during the Palaeocene-Eocene Thermal Maximum, Nature, v. 548, p. 573-580.

Higgins, J.A., and Schrag, D.P., 2006, Beyond methane: Towards a theory for the Paleocene-Eocene thermal maximum: Earth and Planetary Science Letters, v. 245, p. 523-537.

Horne, D.J., Cohen, A., and Martens, K., 2002, Taxonomy, morphology, and biology of Quaternary and living ostracodes, *in* Holmes, J., and Chivas, A, eds., The Ostracoda: Applications in Quaternary Research: Washington, D.C., American Geophysical Union, 313 p.

Horne, D.J., and Martens, K., editors, 2000, Evolutionary biology and ecology of Ostracoda: Theme 3 of the 13th International Symposium on Ostracoda (ISO97): Dordrecht, The Netherlands, Kluwer Academic Publishers, 197 p.

Huang, H.M., Yasuhara, M., Iwatani, H., Yamaguchi, T., Yamada, K., and Mamo, B., 2019, Deep-sea ostracod faunal dynamics in a marginal sea: biotic response to oxygen variability and mid-Pleistocene global changes: Paleobiology, v. 45, p. 85-97.

Kennett, J.P., and Stott, L.D., 1991, Abrupt deep-sea warming, palaeoceanographic changes and benthic extinctions at the of the Palaeocene: Nature, v. 353, p. 225-229.

Kirtland Turner, S., 2018, Constraints on the onset duration of the Paleocene-Eocene Thermal Maximum: Philosophical Transactions of the Royal Society A, v. 376, p. 1-16.

Kirtland Turner, S., Hull, P.M., Kump, L.R., and Ridgwell, A., 2017, A probabilistic assessment of the rapidity of PETM onset: Nature Communications, v. 8, p. 1-10.

Kirtland Turner, S., Sexton, P.F., Charles, C.D., Norris, R.D., 2014, Persistence of carbon release events through the peak of early Eocene global warmth: Nature Geoscience, v. 7, p. 748-751.

Littler, K., Rohl, U., Westerhold, T., and Zachos, J.C., 2014, A high-resolution benthic stable-isotope record for the South Atlantic: Implications for orbital-scale changes in Late Paleocene-Early Eocene climate and carbon cycling: Earth and Planetary Science Letters, v. 401, p. 18-30.

Lauretano, V., Littler, K., Polling, M., Zachos, J.C., and Lourens, L.J., 2015, Frequency, magnitude and character of hyperthermal events at the onset of the Early Eocene Climatic Optimum: Climate of the Past, v. 11, p. 1313-1324.

Maiorano, P., Aiello, G., Barra, D., Di Leo, P., Joannin, S., Lirer, F., Marino, M., Pappalardo, A., Capotondi, L., Ciaranfi, N., and Stefanelli, S., 2008, Paleoenvironmental changes during sapropel 19 (i-cycle 90) deposition: evidences from geochemical, mineralogical and micropaleontological proxies in the mid-Pleistocene Montalbano Jonico land section (southern Italy): Palaeogeography, Palaeoclimatology, Palaeoecology, v. 257, p. 308-334.

McInerney, F.A., and Wing, S.L., 2011, The Paleocene-Eocene Thermal Maximum: A perturbation of carbon cycle, climate, and biosphere with implications for the future: Annual Reviews of Earth and Planetary Science, v. 39, p. 489-516.

Morsi, A.-M.M., and Speijer, R.P., 2003, High-resolution ostracode records of the Paleocene/Eocene transition in the South Eastern Desert of Egypt-taxonomy, biostratigraphy, paleoecology, and paleobiogeography: Senckenbergiana Lethaea, v. 83, p. 61-93.

Norris, R.D., Kirtland Turner, S., Hull, P.M., and Ridgwell, A., 2013, Marine ecosystem responses to Cenozoic global change: Science, v. 341, p. 492-498.

Norris, R.D., Wilson, P.A., Blum, P., and the Expedition 342 Scientists, 2014, Proceedings of IODP, 342: College Station, TX, Integrated Ocean Drilling Program.

Paytan, A., and Griffith, E.M., 2007, Marine barite: Recorder of variations in ocean export productivity: Deep-Sea Research II, v. 54, p. 687-705.

Penman, D.E., Keller, A., D'haenens, S., Kirtland Turner, S., and Hull, P.M., 2019, Atlantic deep-sea cherts associated with Eocene Hyperthermal Events: Paleoceanography and Paleoclimatology, v. 34, p. 1-13.

Sexton, P.N., Norris, R.D., Wilson, P.A., Palike, H., Westerhold, T., Rohl, U., Bolton, C.T., and Gibbs, S., 2011, Multiple Eocene 'hyperthermal' events driven by ocean ventilation: Nature, v. 471, p. 349-353.

Sexton, P.F., Wilson, P.A., and Norris, R.D., 2006, Testing the Cenozoic multisite composite $\delta^{18}O$ and $\delta^{13}C$ curves: New monospecific Eocene records from a single locality, Demerara Rise (Ocean Drilling Program Leg 207): Palaeoceanography, v. 21, PA2019.

Shipboard Scientific Party, 2004, Site 1258, *in* Erbacher, J., Mosher, D.C., Malone, M.J., et al., Proceedings of ODP, Initial Reports, 207: College Station, TX, Ocean Drilling Program, p. 1-117.

Speijer, R.P., and Morsi, A-M.M., 2002, Ostracode turnover and sea-level changes associated with the Paleocene-Eocene thermal maximum: Geology, v. 30, p. 23-26.

Stap, L., Sluijs, A., Thomas, E., Lourens, L., 2009, Patterns and magnitude of deep sea carbonate dissolution during Eocene Thermal Maximum 2 and H2, Walvis Ridge, southeastern Atlantic Ocean: Paleoceanography, v. 24, p. PA1211.

Steineck, P.L., and Thomas, E., 1996, The latest Paleocene crisis in the deep sea: Ostracode succession at Maud Rise, Southern Ocean: Geology, v. 24, p. 583-586.

Stepanova, A., and Lyle, M., 2014, Deep-sea ostracoda from the eastern equatorial Pacific (ODP Site 1238) over the last 460 ka.: Marine Micropaleontology, v. 111, p. 100-117.

Storey, M., Duncan, R.A., and Swisher, C.C., 2007, Paleocene-Eocene thermal maximum and the opening of the northeast Atlantic: Science, v. 316, p. 587-589.

Thomas, E., 2003, Extinction and food at the sea floor: A high-resolution benthic foraminiferal record across the initial Eocene thermal maximum, Southern Ocean Site 690, *in* Wing, S., Gingerich, P., Schmitz, B., and Thomas, E., eds., Causes and Consequences of Globally Warm Climates of the Paleogene, v. 369, p. 319-332.

Thomas, E., 2007, Cenozoic mass extinctions in the deep sea: What perturbs the largest habitat on Earth? *in* Monechi, S., Coccioni, R., and Rampino, M., eds., Large ecosystem perturbations: causes and consequences: Geological Society of America Special Paper, v. 424, p. 1-23.

Tucholke, B.E., and Vogt, P.R., et al., 1979, Western North Atlantic: Sedimentary evolution and aspects of tectonic history, *in* Tucholke, B.E., Vogt, P.R., et al., eds., Initial Reports of the Deep Sea Drilling Project, v. 43, p. 791-825.

Webb, A.E., Leighton, L.R., Schellenberg, S.A., Landau, E.A., Thomas, E., 2009, Impact of the Paleocene-Eocene thermal maximum on deep-ocean microbenthic community structure: Using rank-abundance curves to quantify paleoecological response: Geology, v. 37, p. 783-786.

Winguth, A.M.E., Thomas, E., and Winguth, C., 2012, Global decline in ocean ventilation, oxygenation, and productivity during the Paleocene-Eocene Thermal Maximum: implications for the benthic extinction: Geology, v. 40, p. 263-266.

Yamaguchi, T., Bornemann, A., Matsui, H., and Nishi, H., 2017a, Latest Cretaceous/Paleocene deep-sea ostracode fauna at IOPD Site U1407 (western North Atlantic) with special reference to the Cretaceous/Paleogene boundary and the Latest Danian Event: Marine Micropaleontology, v. 135, p. 32-44.

Yamaguchi, T., Matsui, H., and Nishi, H., 2017b, Taxonomy of Maastrichtian-Thanetian deep-sea ostracodes from U1407, IODP Exp 342, off Newfoundland, Northwestern Atlantic, part 1: Families Cytherellidae, Bairdiidae, Pontocyprididae, Bythocytheridae, and Cytheruridae: Paleontological Research, v. 21, p. 54-75.

Yamaguchi, T., Matsui, H., and Nishi, H., 2017c, Taxonomy of Maastrichtian-Thanetian deep-sea ostracodes from U1407, IODP Exp 342, off Newfoundland, Northwestern Atlantic, part 2: Families Eucytheridae, Krithidae, Thaerocytheridae, Trachyleberididae, and Xestoleberididae: Paleontological Research, v. 21, p. 97-121.

Yamaguchi, T. and Norris, R.D., 2012, Deep-sea ostracode turnovers through the Paleocene-Eocene thermal maximum in DSDP Site 401, Bay of Biscay, North Atlantic: Marine Micropaleontology, v. 86-78, p. 32-44.

Yamaguchi, T., and Norris, R.D., 2015, No place to retreat: Heavy extinction and delayed recovery on a Pacific guyot during the Paleocene-Eocene Thermal Maximum: Geology, v. 43, p. 443-446.

Yamaguchi, T., Norris, R.D., and Bornemann, A., 2012, Dwarfing of ostracodes during the Paleocene-Eocene Thermal Maximum at DSDP Site 401 (Bay of Biscay, North Atlantic) and its implication for changes in organic carbon cycle in deep-sea benthic ecosystem: Palaeogeography, Palaeoclimatology, Palaeoecology, v. 346-347, p. 130-144.

Yasuhara, M., Cronin, T.M., Martínez Arbizu, P., 2008, Abyssal ostracods from the South and Equatorial Atlantic Ocean: Biological and paleoceanographic implications: Deep-Sea Research Part I, v. 55, p. 490-497.

Yasuhara, M., Hunt, G., Cronin, T.M., Hokanishi, N., Kawahata, H., Tsujimoto, A., and Ishtake, M., 2012, Climatic forcing of Quaternary deep-sea benthic communities in the North Pacific Ocean: Paleobiology, v. 38, p. 162-179.

Yasuhara, M., Hunt, G., Cronin, T.M., Okahashi, H., 2009, Temporal latitudinal-gradient dynamics and tropical instability of deep-sea species diversity: PNAS, v. 106, p. 21717-21720.

Zachos, J.C., Bohaty, S.M., John, C.M., McCarren, H., Kelly, D.C., and Nielsen, T., 2007, The Paleocene-Eocene carbon isotope excursion: constraints from individual shell planktonic foraminifer records: Philosophical Transactions of the Royal Society A, v. 365, p. 1829-1842.

Zachos, J.C., Dickens, G.R., and Zeebe, R.E., 2008, An early Cenozoic perspective on greenhouse warming and carbon-cycle dynamics: Nature, v. 451, p. 279-283.

Zachos, J.C., McCarren, H., Murphy, B., Rohl, U., and Westerhold, T., 2010, Tempo and scale of late Paleocene and early Eocene carbon isotope cycles: Implications for the origin of hyperthermals: Earth and Planetary Science Letters, v. 299, p. 242-249.

Zachos, J.C., Röhl, U., Schellenberg, S.A., Sluijs, A., Hodell, D.A., Kelly, D.C., Thomas, E., Nicolo, M., Raffi, I., Lourens, L.J., McCarren, H., and Kroon, D., 2005, Rapid Acidification of the ocean during the Paleocene-Eocene Thermal Maximum: Science, v. 308, p. 1611-1615.

CHAPTER 3: CHANGES IN OSTRACODE BODY SIZE ACROSS EOCENE THERMAL

MAXIMUM 2 AT TWO DEEP-SEA SITES FROM THE NORTH AND EQUATORIAL ATLANTIC

Abstract

Earth's environment has changed continuously throughout its history. One example of a

smaller, but rapid and global, environmental change is Eocene Thermal Maximum 2

(ETM2, ~54 Ma). This event was one of several hyperthermal events that characterized

the early Cenozoic. It is distinguished by carbon and oxygen isotope excursions roughly

half the magnitude of the Paleocene-Eocene Thermal Maximum (PETM), and likely

lasted about half as long. Ostracodes (small, bivalved crustaceans) represent an

opportunity to examine how animal life responded to changes in the environment

associated with this smaller hyperthermal event. This study investigates changes in the

body sizes of four ostracode species from two different genera (*Neonesidea* and *Krithe*)

at two deep marine sites (ODP Site 1258 and IODP Site U1409) before, during, and after

ETM2. All species show a decrease in average body size from before ETM2 to during

ETM2, and most species also show in increase in average body size from ETM2 to after

ETM2, although some decrease further. Generally, the trends for the different species at

the different sites are all fairly similar. While small sample sizes somewhat hinder the

analyses, these changes in body size are likely at least partially related to the changes in

temperature associated with the ETM2 hyperthermal event, but may also be related to

other factors. Regardless, the changes observed as a result of this relatively smaller event indicate that ostracodes, even today, may be adversely impacted by even small changes to their environments.

Introduction

One of the many concerns with climate change today is that changes to their environments will impact the organisms that live in them. In the ocean, these changes will impact things such as temperature, primary production, ocean acidification, and sea level- all of which can, in turn, impact organisms in a variety of ways. During the early Cenozoic, changing environmental conditions resulting from the relatively rapid addition of carbon to ocean-atmosphere system were triggering changes to the ocean environment similar to those which we would expect to occur as a result of anthropogenic carbon release today (Hönisch et al., 2012). Thus, this time period in Earth's history represents an opportunity to investigate what effect these changes had on marine organisms in the past, potentially providing insight into what we can expect for the future of our marine organisms and ecosystems.

One of the events that has been identified in the early Cenozoic as an addition of isotopically light carbon to the ocean and atmosphere systems is Eocene Thermal Maximum 2 (ETM2). ETM2 was an event similar to the more well-known Paleocene-Eocene Thermal Maximum (PETM) hyperthermal event that occurred roughly two

million years after it, between 53-54 million years ago (Kirtland Turner et al., 2014; Lauretano et al., 2015; Westerhold et al., 2007; Zachos et al., 2010). Like the PETM, ETM2 has been identified globally in the geologic record based on the presence of negative carbon and oxygen isotope excursions (Cramer et al., 2003; Lourens et al. 2005; Stap et al., 2010;). The negative carbon isotope excursion is indicative of a release of isotopically light carbon to the ocean-atmosphere system, and the isotopically lighter oxygen observed in these records is associated with the warmer temperatures indicated by the 'hyperthermal' designation of these events (Bradley, 1999; Smart, 2002). Relative to the PETM, records from ETM2 indicate that this was a smaller and shorter hyperthermal event, with a negative carbon isotope excursion of about 1‰ and approximately 2°C of warming (Cramer et al., 2003; Kirtland Turner et al., 2014; Lauretano et al., 2015; Littler et al., 2014).

One way that changes in temperature have been shown to impact organisms is in their body sizes. Temperature effects on body size have been extensively studied in a variety of animal groups. For instance, Bergmann's Rule describes the inclination for organisms living in colder areas to be larger than their same-species or otherwise similar counterparts that live in warmer regions (Blackburn et al., 2008; Millien et al., 2006). Bergmann's Rule was originally identified in and described from large, homeothermic animals, particularly mammals, leading to the hypothesis that the observed trends in body size could be explained through the heat-conserving nature of a low surface area

to volume ratio (Mayr, 1956; Rensch, 1938). Since then, however, Bergmann's Rule has also been found to hold true for many poikilotherms (*e.g.* Ray, 1960), indicating that there are likely other or additional factors that influence this trend.

While Bergmann's Rule has traditionally been applied to organisms living at the same time but in different geographic areas characterized by different climates, it has been suggested that taxa that follow Bergmann's Rule should also show changes in their body sizes as they deal with temporal changes in climate (Hunt et al., 2010). In the case of hyperthermal events, if Bergmann's Rule holds true, the increasing temperatures should be correlated with the presence of organisms with smaller body sizes. This study tests the hypothesis that ostracode (small, bivalved crustaceans) species experienced body size changes during or after the ETM2 hyperthermal event by analyzing body sizes of adults from multiple species of ostracodes from two ocean sediment drill cores in the Atlantic ocean.

Sites

ODP Site 1258

Ocean Drilling Program (ODP) Leg 207 (Figure 3.1) captured a high-resolution Paleogene oceanographic record from tropical latitudes for the purpose of evaluating paleoenvironmental changes and the biotic response to them (Erbacher et al., 2004). Site 1258 of Leg 207 is located on the western slope of the Demerara Rise, about 380 km

north of Suriname in the tropical Atlantic, at about 9°N, 54°W (Shipboard Scientific

Party, 2004), and was recovered from a present sea floor water depth of 3192 m

(Erbacher et al., 2004). The paleodepth of the site during the Eocene was around 2500-

3200 m (Sexton et al., 2006). The material recovered from this site ranges from early

Albian to Miocene in age, though there are some hiatuses in the record (Shipboard

Scientific Party, 2004). The five distinct hiatuses may represent periods of slow

deposition or erosion, and, based on biostratigraphic evidence, appear to range from

approximately 1-32 million years in duration (Shipboard Scientific Party, 2004). Five

lithostratigraphic sequences were recognized from the cores. The Paleocene- and

Eocene-aged material is in a 325 m thick unit, and is greenish gray sequence composed

of nannofossil and calcareous chalk with foraminifera (Shipboard Scientific Party, 2004).

Late Paleocene- middle Eocene sedimentation rates are described as average for

pelagic chalks and oozes, at about 1.5 cm/ kyr (Shipboard Scientific Party, 2004).

Preservation of foraminifera in the Paleocene and Eocene sediments ranges from poor

to good (Shipboard Scientific Party, 2004).
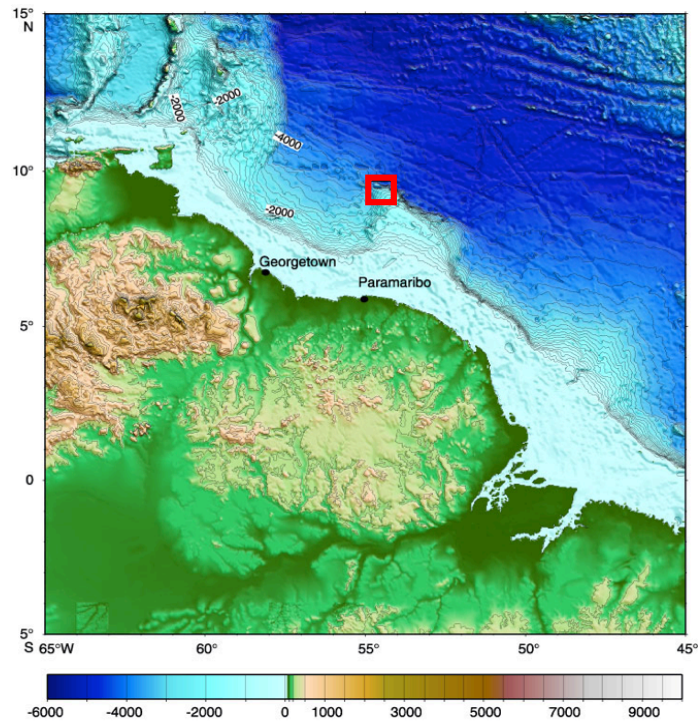
Figure 3.1. ODP Site 1258. Map showing location of ODP Site 1258. Modified from Erbacher et al., 2004.

IODP Site U1409

Expedition 342 of the Integrated Ocean Drilling Program (IODP) targeted Paleogene-aged sedimentary sequences from a range of paleodepths with high deposition and microfossil accumulation rates (Expedition 342 Scientists, 2012). Site U1409 is located on the Southeast Newfoundland Ridge off the coast of Newfoundland, Canada, around 41°N, 49°W (Figure 3.2). The core was recovered from a present sea floor water depth of 3503 m (Norris et al., 2014), and the paleodepth of the site is about 3050 meters below sea level (Tucholke and Vogt, 1979), placing it more shallow than the Paleogene carbonate compensation depth. Coring at the site recovered deep-sea pelagic sediment

ranging from the Pleistocene to the early Paleocene (Norris et al., 2014). The

sedimentary sequence recovered is approximately 200 m thick and is composed of four

lithostratigraphic units (Norris et al., 2014). Sedimentation rates for the Paleocene and

Eocene sections of the core range from 0.47-1.80 cm/kyr (Norris et al., 2014). While the

preservation of the benthic foraminifera tests that are found in the core are typically

good, benthic foraminifera are mostly rare in the Paleocene and Eocene sediments

(Norris et al., 2014).
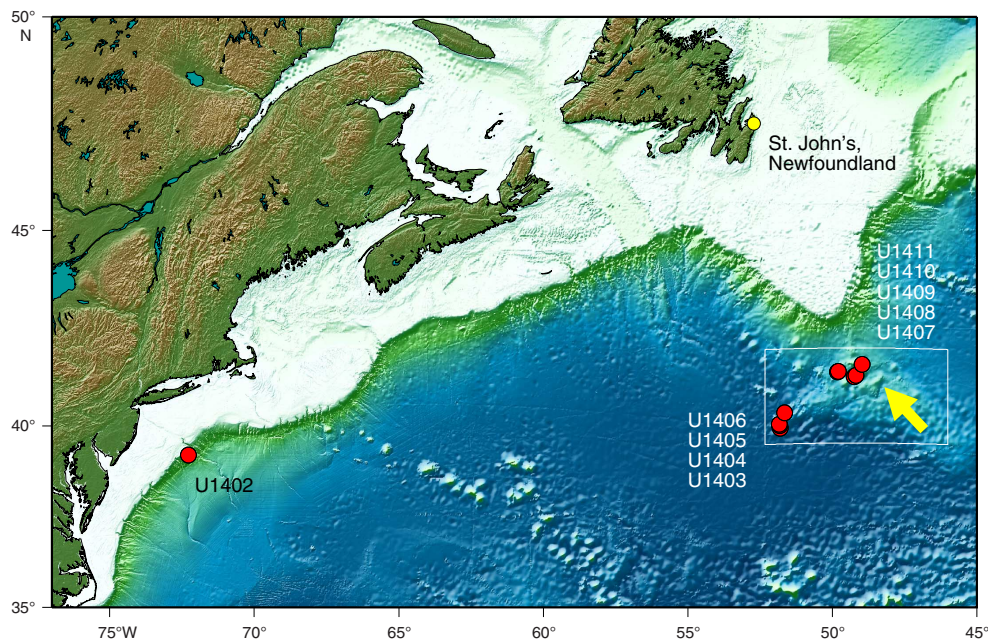
Figure 3.2. IODP Site U1409. Map of sites from IODP expedition 342, including U1409.
Modified from Expedition 342 Scientists, 2012.

This study uses records from both of these sites to directly compare conditions during

ETM2 at different latitudes of the Atlantic Ocean. By comparing data from the North

Atlantic to that of the equatorial region, we begin to create a more global record of the early Eocene time period, and it becomes possible to begin to determine whether life in different locations responded to changes in the same way.

Methods

Sample Processing and Picking

Core sediments from both sites were washed and sieved through a 63 μm mesh with deionized water, dried, and weighed to obtain the coarse fraction. ETM2-aged sediments were identified based on bulk carbonate $\delta^{13}C$ and $\delta^{18}O$ isotope records from the cores. Kirtland Turner et al. (2014) generated bulk $\delta^{13}C$ and $\delta^{18}O$ isotope records for about 4.25 million years of carbonate core sediment spanning the Early Eocene Climate Optimum for Site 1258. This record includes the negative isotope excursions (~1.56‰ in carbon; ~0.61‰ in oxygen) that identify ETM2 between 133.42 and 132.12 mcd.

For IODP Site U1409, bulk carbonate $\delta^{13}C$ and $\delta^{18}O$ isotope records for late Paleocene and early Eocene were run on a Kiel IV carbonate perception device coupled to a DELTA V dual-inlet mass spectrometer. Samples were run with known standard, and the results converted into delta values internally and reported relative to Vienna PeeDee Belemnite (VPBD). At this site, the ETM2 event is located between 174.46 and 172.26 mcd, with a negative carbon isotope excursion of ~0.62‰ and a negative oxygen isotope excursion of ~0.6‰.

For both sites, ostracodes were picked from samples across the identified isotope

excursions in order to develop the ostracode record across the ETM2 hyperthermal

event. All of the ostracodes in the greater than 180 μm size fraction were picked using a

binocular microscope. Ostracodes were picked from samples representing time before,

during, and after ETM2. A high level of sample resolution was used to get as many

ostracodes as possible. At IODP Site U1409, the samples picked were at a resolution of

about every 3 cm; At ODP Site 1258, the samples picked were at a resolution of about

every 9 cm.

Ostracode Specimens

After they were picked, all of the ostracodes were identified to the genus level.

Ostracodes from the two most abundant genera at both sites, *Neonesidea* and *Krithe*,

were identified to the species level (Figure 3.3). Species determinations were made

based on morphological continuity of features commonly used to identify ostracode

species, including valve outline, marginal pore positions, and inner lamella features,

without regard to body size. While some of the species found at these sites are the

same as those encountered by Yamaguchi et al. (2017a and b), deep-sea ostracode taxa

from the Paleocene and especially the Eocene have received relatively little attention,

so some of the species here remain in open nomenclature.
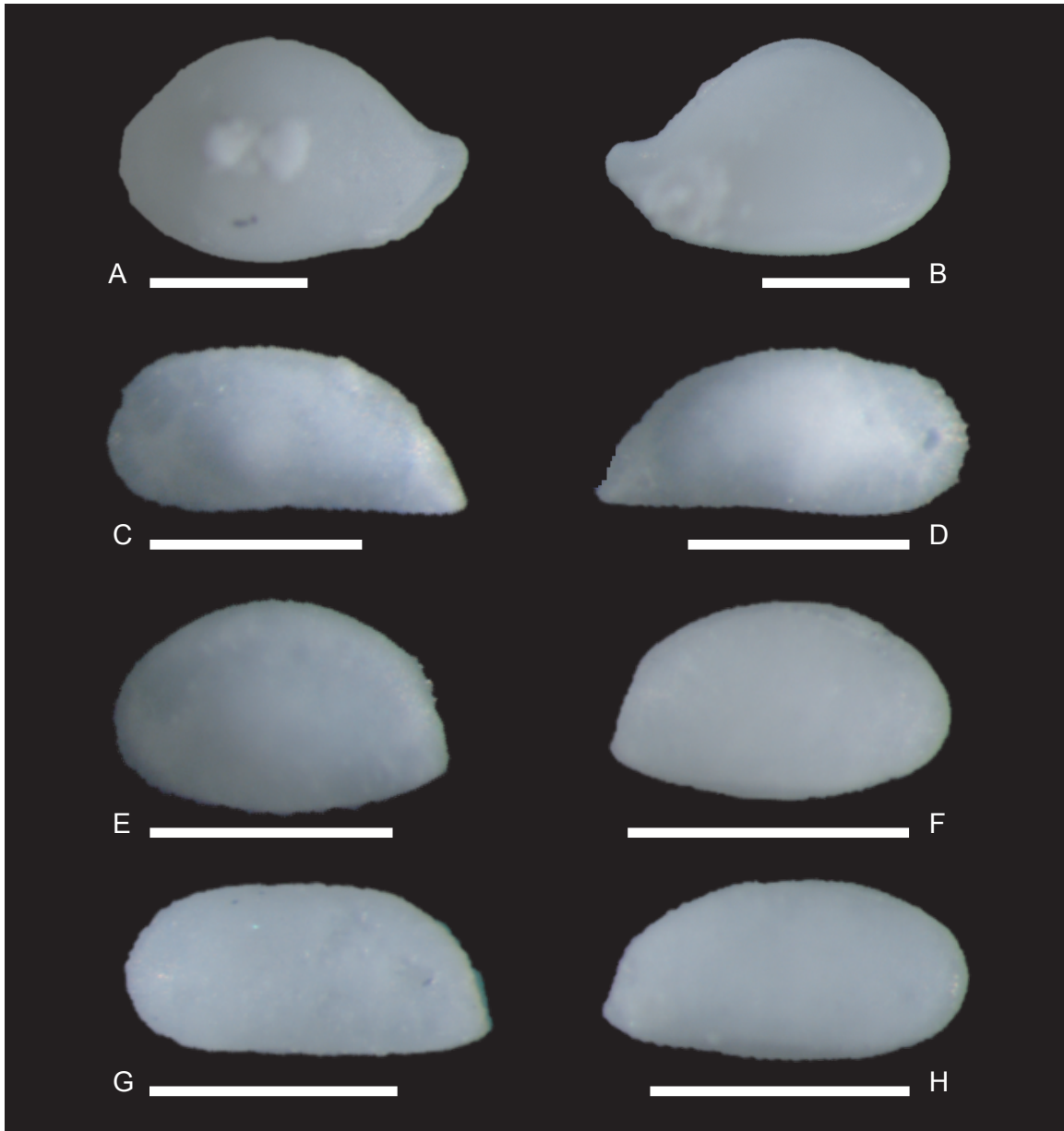
Figure 3.3. Light microscope images of ostracode species used for analyses. All scale bars are 500 µm. A-B: *Neonesidea*; A. *Neonesidea* sp.1 left valve; B. *Neonesidea* sp.1 right valve; C-H: *Krithe*; C. *K. trinidadensis* left valve; D. *K. trinidadensis* right valve; E. *K. crassicaudata* left valve; F. *K. crassicaudata* right valve; G. *K. dolichodeira* left valve; H. *K. dolichodeira* right valve.

As arthropods, ostracodes grow by molting. Particularly in deep-sea settings with low

levels of transport, many of the ostracode valves and carapaces that are preserved in

the fossil record come from juveniles (Yamaguchi et al., 2012). While juvenile ostracodes

were picked, only adults were used for analyses. This was done to ensure that any

observed trends in ostracode body size would be biologically meaningful, and not the

result of higher or lower proportions of preserved juveniles. To identify the adults in

each species, the presence of morphological features typical of adults, such as well-

developed hingements and inner margins, was sought, starting with the largest

specimens of each species in each sample. This continued going by size in descending

order until a 'cut-off' of the largest individuals that clearly did not exhibit adult traits

was reached. All specimens in a sample of that species larger than that were considered

adults. Using this technique helped to ensure that poor preservation or partial

dissolution did not exclude adult ostracodes from the analysis.

Morphometrics and Analysis

For this study, valve area was used as a proxy for body size. To determine valve area,

digital photographs were taken of each specimen using a Leica MZ16 stereomicroscope

with a Leica DFC420 digital camera. The length and height of each valve were measured

using the Fiji distribution of the ImageJ software (Schindelin et al., 2012; Schneider et

al., 2012). Valve length was determined to be the longest distance from the anterior to

the posterior of the valve and valve height was the longest distance from the dorsal to

ventral margin of the valve; the two measurements were taken perpendicular to one

another (Figure 3.4). In the case of broken or damaged valves, if the damage was minor

enough that the edge of the specimen could be easily and accurately determined (*i.e.* a

small chip or crack), the specimen was included. If the damage was significant enough

that the length, width, or species-level identification was uncertain, the specimen was

excluded from analysis. Ostracode valves are often estimated as ellipses for the purpose

of body size measurements (*e.g.* Fernandes Martins et al., 2017; Hunt et al., 2017).

Here, valve area was estimated as an ellipse using one-half of the length and height

measurements as the radii of major and minor axes, respectively.
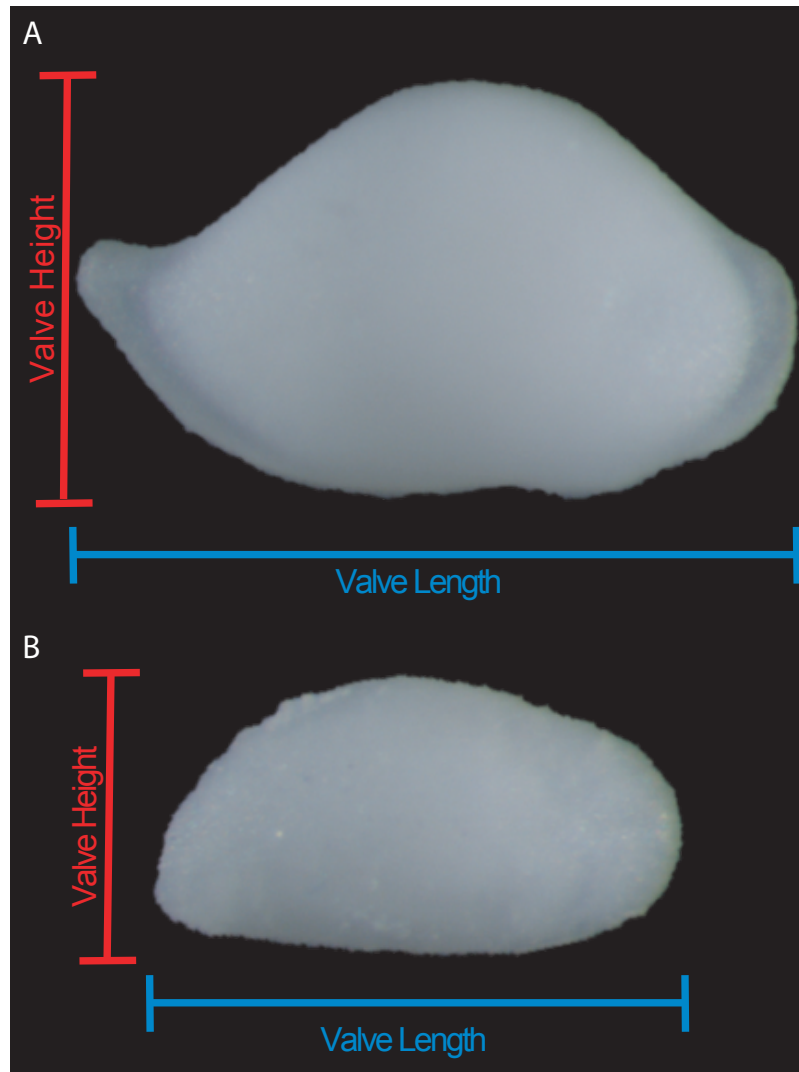
Figure 3.4. Measurement protocol for valve length and height. *Neonesidea* (A) and *Krithe* (B).

Adult ostracodes are often not particularly abundant in deep-sea sediments. In order to increase sample sizes for analysis, the samples from each core were divided into three time bins: Pre-ETM2, ETM2, and Post-ETM2. The ETM2 bin included samples throughout the duration of the carbon and oxygen isotope excursions at each site. The sites have similar magnitude oxygen isotope excursions, so temperature changes at the two sites

should be comparable. The pre- and post-ETM2 samples consisted of the ostracodes in

samples earlier than and later than the ETM2 isotope excursion, respectively. For the

sake of analysis, samples consisted of all of the adult ostracode valves of a single species

in a given time bin. To further maximize sample sizes, both the left and right valves of

each species were included the sample, as has been done by other workers investigating

body size in ostracodes (*e.g.* Hunt et al., 2010; Yamaguchi et al., 2012; Hunt et al., 2017).

Although left and right valves can vary slightly in size, there is no reason that the

proportion of left to right valves should vary with changes in temperature or other

variables, so combining the valves into one sample should not meaningfully impact the

analyses.

The average body size (as determined by valve area) of each sample population was

calculated to determine how body size changed across the three different time bins for

each species at each site. A Kruskal-Wallace analysis, a non-parametric ANOVA which

compares the medians of several (*i.e.* more than two) univariate groups, was run using

the PAleontological STatistics software package (PAST; Hammer et al., 2001) for the

three time binned samples of each species at each site to determine if the observed

changes in valve area were statistically significant.

Results

Ostracode Taxa and Abundances

A single species of *Neonesidea* was identified at both Site 1258 and Site U1409. Five

species of *Krithe* were identified at Site 1258. Two species, *K. crassicaudata* and *K.*

dolichodeira were much more common than the others (Site 1258 *Krithe* are ~31% *K.*

crassicaudata and ~45% *K. dolichodeira*). Of the remaining three, only one species, *K.*

trinidadensis, had adults from at least two of the time bins preserved. Thus, only three

of the species of *Krithe* are included in further analyses for Site 1258 here. A similar

pattern is present in the Site U1409 *Krithe*. There are five species present in the sample,

and, in fact, all but one of the species are the same as those found at Site 1258. Again, *K.*

crassicaudata and *K. dolichodeira* are much more common than the other species (Site

U1409 *Krithe* are ~33% *K. crassicaudata* and ~52% *K. dolichodeira*). Only one other

species, *K. trinidadensis*, included preserved adult specimens.

In total, 21 adult *Neonesidea* sp.1 were preserved at Site 1258, out of a total of 229

usable (preserved well enough to be accurately measured) *Neonesidea* sp.1. At the

same site, out of 205 measurable *Krithe*, 24 were found to be adults. One of those

adults is from a species that had only one adult, and so is largely not included in

analyses. At Site U1409, only 12 of 228 usable *Neonesidea* sp.1 specimens were adults.

The *Krithe* at U1409 represent the largest sample sizes in this study. Of 828 measurable

Krithe at Site U1409, 67 were adults and included in analyses. Thus, the U1409 *Krithe*

analyses generally also had the largest sample sizes.

Ostracode abundances in the ETM2 time bins were much lower than in the pre- and

post-ETM2 time bins, but there were *Neonesidea* and *Krithe* specimens, including adults,

preserved in the ETM2 time bin at each site. Relative abundances of the three *Krithe*

species with multiple preserved adults change slightly, but are largely similar throughout

the different time bins. At Site 1258, *K. dolichodeira* was the dominant *Krithe* species in

each time bin, representing ~45% of *Krithe* in the pre-ETM2 bin and ~38% of *Krithe* in

the ETM2 and post-ETM2 bins. *K. crassicaudata* is slightly more relatively abundant

during ETM2 (~33%) than before (~30%) and after (~25%) ETM2. Of the three species, *K.*

trinidadensis varies the most, ranging from ~4% of the *Krithe* before ETM2 to ~17%

during ETM2, falling back to ~8% after ETM2. There was a little more variation at Site

U1409. *K. dolichodeira* was also the dominant *Krithe* species here, making up about 49%

of *Krithe* before, 67% during, and 57% after ETM2. *K. crassicaudata* was the next-most

relatively abundant species of *Krithe* at all three time bins, despite a noticeable relative

decrease during ETM2 (from ~37% before to ~10% during, and back to ~31% after

ETM2). *K. trinidadensis* was less variable than at Site 1258, ranging less than 5% over all

three bins, from ~6% before and during ETM1 to ~2% after.

Body Size

At these sites, adult *Neonesidea* specimens were among the largest ostracodes

preserved, and were notably larger than *Krithe* (generally about 2.5x larger at Site 1258,

and about 3x larger at Site U1409). Average adult body size, as measured by valve area,

changed in every species with multiple adults observed at the two sites (Table 3.1). In

every population, average adult body size decreases from the before ETM2 time bin to

the ETM2 time bin (with the exception of *K. trinidadensis* at Site 1258, where there were

only adults preserved from samples in the during- and post-ETM2 time bin). In most

populations, there is also at least a modest recovery in body size from the ETM2 time

bin to the post-ETM2 time bin.

Table 3.1. Average body size (valve area) of ostracode populations.

Core	Species	Interval	Average area (in μm^2)	n
1258	*Neonesidea* sp.1	Pre-ETM2	567074	4
	Neonesidea sp.1	ETM2	483010	3
	Neonesidea sp.1	Post-ETM2	495119	14
	K. crassicaudata	Pre-ETM2	228555	1
	K. crassicaudata	ETM2	219911	1
	K. crassicaudata	Post-ETM2	211155	6
	K. dolichodeira	Pre-ETM2	237068	2
	K. dolichodeira	ETM2	194897	2
	K. dolichodeira	Post-ETM2	200462	6
	K. trinidadensis	Pre-ETM2	n/a	0
	K. trinidadensis	ETM2	189433	2
	K. trinidadensis	Post-ETM2	172295	3
U1409	*Neonesidea* sp.1	Pre-ETM2	639798	7
	Neonesidea sp.1	ETM2	635118	2
	Neonesidea sp.1	Post-ETM2	677674	3
	K. crassicaudata	Pre-ETM2	218956	15
	K. crassicaudata	ETM2	167929	2
	K. crassicaudata	Post-ETM2	159791	7
	K. dolichodeira	Pre-ETM2	231695	17
	K. dolichodeira	ETM2	133882	4
	K. dolichodeira	Post-ETM2	170846	11
	K. trinidadensis	Pre-ETM2	220422	8
	K. trinidadensis	ETM2	140567	1
	K. trinidadensis	Post-ETM2	170846	2

At Site 1258, *Neonesidea* sp.1 average body size decreased by ~84,000 μm^2 before

recovering by ~12,000 μm^2 (Figure 3.5a). *K. dolichodeira* body size at the same site

follows a similar pattern, dropping by ~42,000 μm^2 and then increasing again by ~5,500

μm^2. *K. crassicaudata* body size dropped less dramatically (~8,600 μm^2) from the pre-

ETM2 time bin to ETM2, but continued decreasing after ETM2 (~8,800 μm^2). There were

no adult *K. trinidadensis* present in Site 1258 samples before ETM2, but average body

size decreased by ~17,000 μm² following ETM2 (Figure 3.5b).
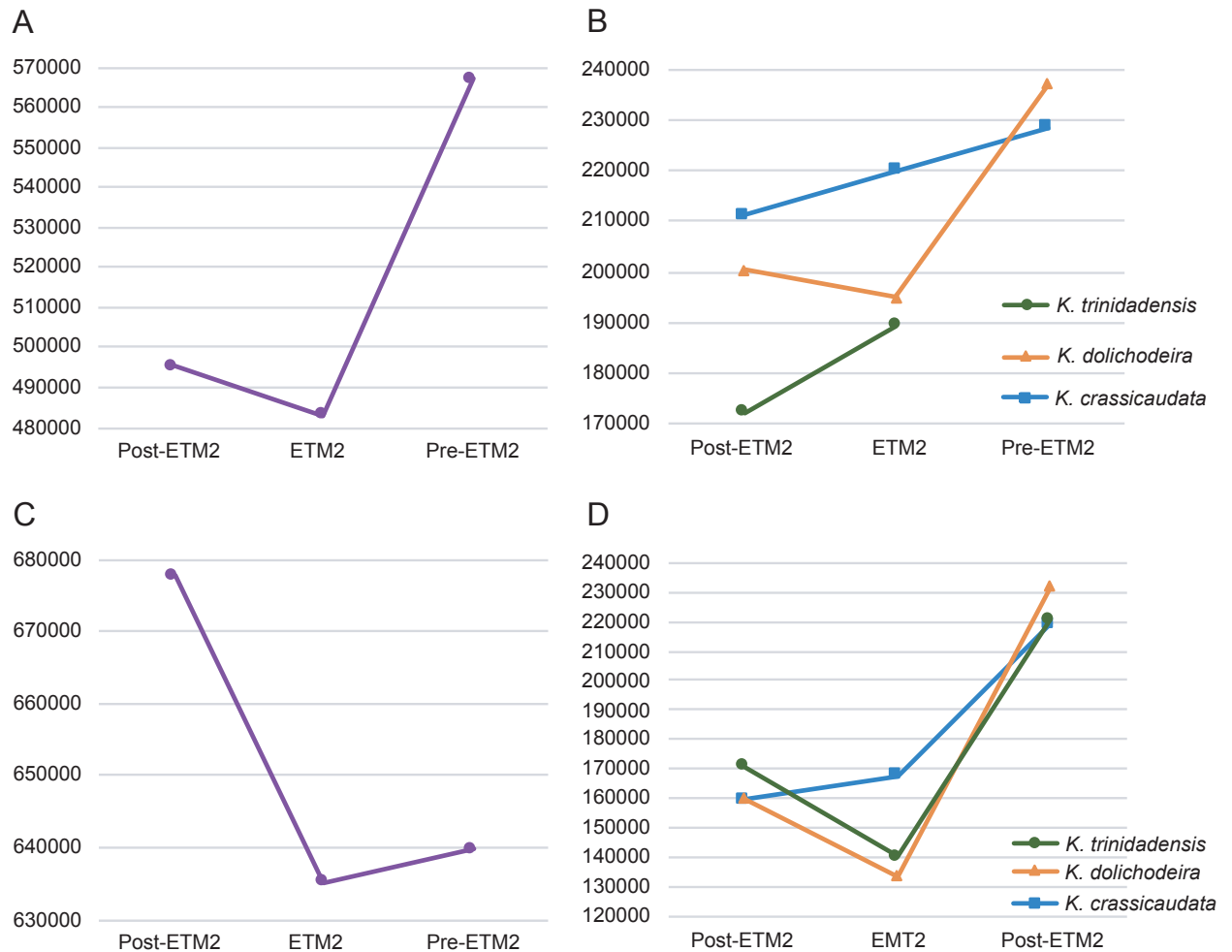
Figure 3.5. Average body sizes (in μm²) for adult ostracodes before, during, and after ETM2. A. Site 1258 *Neonesidea* sp.1; B. Site 1258 *Krithe*; C. Site U1409 *Neonesidea* sp.1; D. Site U1409 *Krithe*.

At Site U1409, average *Neonesidea* sp.1 body size decreased modestly (~4,700 μm²)

going into ETM2, but then increased by ~43,000 μm² following ETM2 (Figure 3.5c). This

is the only population in this study in which body size after ETM2 is larger than it was before the event. Average body size of *K. crassicaudata* at Site U1409 decreases by ~51,000 μm^2 going into ETM2 and continues to decrease by ~8,100 μm^2 after ETM2. Average body sizes of *K. dolichodeira* and *K. trinidadensis* stay very similar to one another throughout the study interval. Average body sizes decrease ~98,000 μm^2 and ~80,000 μm^2 and then increase ~26,000 μm^2 and ~30,000 μm^2, respectively (Figure 3.5d).

Although the various populations investigated here showed generally similar trends in changing body sizes across the intervals, Kruskal-Wallace analyses revealed that the changes in most populations were not statistically significant (Table 3.2). Only the size changes in *Krithe* species at Site U1409 were found to be statistically significant. In all three species, the differences in body size before and after ETM2 were significant. For *K. crassicaudata* and *K. dolichodeira*, but not *K. trinidadensis*, the differences in body size between the pre-ETM2 and ETM2 time bins were also found to be significant. It is worth noting that sample sizes for the *Krithe* populations at U1409, particularly in the pre- and post-ETM2 time bins, represent the largest samples sizes in this study.

Table 3.2. Results of Kruskal-Wallace analyses. *=significant

Core	Species	Comparison	p-value
1258	*Neonesidea* sp.1	Pre-ETM2 vs. ETM2	0.1116
	Neonesidea sp.1	ETM2 vs. Post-ETM2	0.85
	Neonesidea sp.1	Pre-ETM2 vs. Post-ETM2	0.07957
	K. crassicaudata	Pre-ETM2 vs. ETM2	1
	K. crassicaudata	ETM2 vs. Post-ETM2	0.4533
	K. crassicaudata	Pre-ETM2 vs. Post-ETM2	0.4533
	K. dolichodeira	Pre-ETM2 vs. ETM2	0.2453
	K. dolichodeira	ETM2 vs. Post-ETM2	0.2433
	K. dolichodeira	Pre-ETM2 vs. Post-ETM2	0.06675
	K. trinidadensis	Pre-ETM2 vs. ETM2	n/a
	K. trinidadensis	ETM2 vs. Post-ETM2	0.7728
	K. trinidadensis	Pre-ETM2 vs. Post-ETM2	n/a
U1409	*Neonesidea* sp.1	Pre-ETM2 vs. ETM2	0.8836
	Neonesidea sp.1	ETM2 vs. Post-ETM2	0.3865
	Neonesidea sp.1	Pre-ETM2 vs. Post-ETM2	0.4941
	K. crassicaudata	Pre-ETM2 vs. ETM2	0.03065*
	K. crassicaudata	ETM2 vs. Post-ETM2	0.4642
	K. crassicaudata	Pre-ETM2 vs. Post-ETM2	0.00025*
	K. dolichodeira	Pre-ETM2 vs. ETM2	0.0027*
	K. dolichodeira	ETM2 vs. Post-ETM2	0.05835
	K. dolichodeira	Pre-ETM2 vs. Post-ETM2	<0.0001*
	K. trinidadensis	Pre-ETM2 vs. ETM2	0.1752
	K. trinidadensis	ETM2 vs. Post-ETM2	0.5403
	K. trinidadensis	Pre-ETM2 vs. Post-ETM2	0.05*

Discussion

With the exception of two very rare species of *Krithe*, the same species were present at

both sites, and none of the species studied here disappeared completely during any of

the time bins, despite quite low abundances during ETM2. Even the overall relative

abundances of the different species of *Krithe* are similar between the two sites. There

are, however differences in the changes in relative abundances of the two dominant

Krithe species between the two sites. At Site 1258, *K. crassicaudata* becomes slightly more relatively abundant during ETM2 relative to before or after, while the relative abundance of *K. dolichodeira* drops starting at ETM2. Conversely, at Site U1409, *K. crassicaudata* has a lower relative abundance during ETM2 than before or after, and *K. dolichodeira* becomes more relatively abundant during ETM2. At both sites, ostracode abundance is low at ETM2, so the differences may be related to smaller sample sizes. Additionally, while *K. crassicaudata* and *K. dolichodeira* are easily the two most dominant species of *Krithe* at both sites, other species are present, and it is possible that changes in their abundances, particularly during ETM2 when sample sizes are relatively low, are helping to drive these trends. For instance, *K. trinidadensis* becomes more relatively abundant during ETM2 at Site 1258 but not at Site U1409, which might be influencing the differences. Furthermore, one of the rarer *Krithe* species is not present at all during ETM2 at Site 1258, but is at Site U1409, which could also be contributing to the observed differences.

The results of this study indicate that ostracode body size decreased at or after ETM2 for the two most abundant genera at these sites. Every species studied experienced a decrease in body size at ETM2, indicating that Bergmann's Rule was operating in these populations at some level. While the results for the different species at the different sites were very similar in many ways, there were subtle differences between the two sites. At Site 1258 in the equatorial Atlantic, *Neonesidea* average body size decreased

more than *Krithe* species; at Site U1409 in the north Atlantic, the opposite was true, and average *Neonesidea* sp.1 body size actually increased greatly following ETM2. There are a few possible explanations for these results. First, it is possible that the different genera responded differently because of differences in their locations. It is possible that *Neonesidea* generally prefer cooler environments, and so were particularly hard hit when the lower latitude site crossed some threshold during ETM2 and then were not able to grow to their previous size again. Conversely, when temperatures cooled again after EMT2 at the higher latitude site, they were able to grow and thrive again. Another possible explanation is that there were only three adult *Neonesidea* in the U1409 post-ETM2 time bin, and these were from samples fairly far removed from the ETM2 samples. It is possible that the combination of these factors resulted in a slightly skewed representation of overall post-ETM2 *Neonesidea* adult size.

Another possibility is that differences in the magnitude of body size change between the two genera are related to sample size issues. At both sites, the genus with greater changes in body size is also the genus with more specimens. This could indicate that the relatively fewer preserved specimens of the less abundant genus are simply not capturing the full range of sizes that existed in those populations. In both cases, sample sizes are low enough that just a few extreme specimens could easily have an impact on the average body size for those species during the different time bins.

Another similarity between the two sites is the difference in response between *K. crassicaudata* and *K. dolichodeira*. *K. dolichodeira* specimens at both sites begin to increase in body size again following ETM2, but average body size of *K. crassicaudata* specimens continues to decrease in the post-ETM2 time bin. Additionally, at both sites, the decrease in average body size in *K. dolichodeira* both from pre-ETM2 to ETM2, and even the difference between the pre-ETM2 and post-ETM2 size with recovery, are greater than the overall decrease in body sizes of *K. crassicaudata*. This seems to indicate that *K. dolichodeira* is more sensitive to environmental changes than *K. crassicaudata*. It changes more dramatically, and the direction of change shifts more rapidly following a return to prior conditions.

While even the name 'hyperthermal' suggests that the defining characteristic of these events is an increase in temperature, in practice several aspects of the environment change both as a result of and in addition to the changes in temperature during these events. While the results observed here are what would be predicted by Bergmann's Rule, these results do not definitively show that temperature, as opposed to another associated change, was the driving force behind the changes in body size. Some changes, such as a change in productivity and/or metabolic differences in the ostracodes, are particularly hard to rule out. That said, some features of the patterns observed here suggest that temperature was at least a contributing factor in these trends. First, many species not only decreased in size during ETM2, but also began to

increase in size again after the event. As the ETM2 time bins were defined based on the changes in the isotope excursions, with the post-ETM2 time bins beginning following the recoveries in the isotope excursions, the 'recovery' in body size observed here also correlates with recovered isotope excursions, and thus, a return to roughly pre-ETM2 temperatures. Additionally, the magnitudes of the oxygen isotope excursions at the two sites were nearly identical, indicating similar changes in temperature. While this may indicate that changes in things such as productivity were also similar, they may also have been more varied based on other, more regional factors. The generally very similar patterns in ostracode body size at the two sites may indicate that temperature may have been the main, driving factor influencing the body size of the ostracodes. At the very least, it is likely that the same aspect (or combination of aspects) of environmental change was acting at both sites.

Comparison to Other Ostracode Results

Size changes in ostracodes across events of environmental perturbation have been examined in other studies at different time periods and scales. Many of these studies have found that ostracode body size does noticeably change as a result of various environmental perturbations. Chu et al. (2015) found evidence for the Lilliput effect (a reduction in the size of organisms following an extinction event; Urbanek, 1993) in freshwater ostracodes of the genus *Darwinula* during the Permian-Triassic extinction. They found that ostracodes in the stratigraphically higher assemblages from their study

were significantly smaller in all measured parameters (maximum, mean and minimum valve length, height and estimated volume values) than the ostracodes from lower assemblages. They found that this was largely the result of the extinction of large *Darwinula* species, coupled with the arrival of smaller newcomers. Similarly, Forel et al. (2015) found evidence of the Lilliput effect in two marine species of ostracode across the Permian-Triassic extinction.

Hunt and Roy (2006) examined body size changes, as measured by valve length, of the deep-sea ostracode genus *Poseidonamicus* across the Cenozoic. Their results were also consistent with Bergmann's Rule: the *Poseidonamicus* specimens from colder water environments are correspondingly larger than their warmer water counterparts. They also note that, because they did not find anomalously large specimens from sites where they expect higher annual productivity, temperature is more likely to be controlling size changes in these ostracodes; though, their data did not permit direct tests of the influence of primary production on body size. Hunt et al. (2010) found similar results when investigating body size trends in ostracodes from the deep Indian Ocean over the past 40 million years. While a few ostracode lineages in the study showed different patterns, indicating that not all changes in body size can be explained by temperature alone, sizes disproportionately increased only during intervals of sustained cooling. They argued that these results support a view in which the *directionality* in body-size evolution results from trends in temperature or correlated variables.

Moving more precisely to investigations of ostracodes during early Cenozoic hyperthermal events, in one study, deep-sea ostracodes from the North Atlantic decreased in size during the PETM, and, based on the correlation between benthic foraminiferal oxygen isotope data and ostracode body size, measured as biovolume, this decrease was likely the result of increasing temperatures (Yamaguchi et al., 2012). The authors noted that laboratory experiments that report shorter periods of ostracode growth stages as water temperature increases indicate that this correlation is expected (Mezquita et al., 1999; Roca and Wansard, 1997; Martens, 1985). While benthic foraminifera also decreased in body-size during the PETM, the ostracodes had a decrease in lifetime metabolic rate. Conversely, increases in metabolic activity in benthic foraminifera have been correlated with higher temperatures (*e.g.* Alegret et al., 2010; Thomas, 2007). This shows that different benthic taxa exhibited different responses to the changing environmental conditions associated with the PETM.

These previous studies have been focused on larger magnitude and/or longer timescale trends. While each of these studies indicates that ostracodes are impacted by environmental changes, in many cases specifically temperature changes, it is still unclear how dramatic those changes need to be for ostracodes to feel the effect of the change. This work demonstrates that even small temperature changes that are relatively brief in duration are enough to have an impact on ostracode body size. This becomes important as we begin to consider the effects of modern climate change.

Ostracodes are still abundant today, and while specific species often have relatively rigid

environmental tolerances, as a whole they are largely capable of living in any aquatic

environment (Thorp, 2003). As a result, they can play important roles in many

ecosystems. Independent of what direct impacts modern environmental changes may

have for other organisms, if primary consumers such as ostracodes are negatively

impacted, either in terms of abundance or in terms of body mass, those effects may

very well be felt by other, higher-level consumers. While this is only one study on a

limited number of species in only a couple of locations, it does suggest that ostracodes

in different environments show a marked response to even relatively small but rapid

environmental changes.

Notes on Methodologies

One important caveat for this work is that the limited number of adult ostracodes

present in these samples means that the sample sizes for the body size analyses are

relatively low. While this is common for deep-sea ostracodes, and other studies have

run analyses on samples with similarly low abundances (see Hunt et al., 2010;

Yamaguchi et al., 2012), it is not ideal for quantitative analyses. The nature of studying

an event that negatively impacted ostracode abundance further exacerbates this issue,

resulting in particularly low sample sizes during the event of interest. Still, sample sizes

are large enough to statistically distinguish changes in the *Krithe* at Site U1409, and the

similarity in the body size trends of those ostracodes to the others in this study does indicate that the trend might still hold in other populations.

While it is obviously preferable to conduct morphometric analyses on each single species individually, grouping species by genus may be a plausible alternative for increasing sample sizes in morphometric analyses on ostracodes. Because the different species show similar trends, when combined, the changes in body size for all *Krithe* adults at each site closely resemble those of the individual species (Figure 3.6). Furthermore, Kolmogorov-Smirnov analyses indicate that for the pre- and post-ETM2 time bins at Site U1409 the distributions for the body sizes of *K. crassicaudata* and *K. dolichodeira* cannot be statistically distinguished from one another. The ETM2 time bin samples show only a 4.7% chance of coming from the same distribution (enough to reject the null hypothesis), but there are only two *K. crassicaudata* and four *K. dolichodeira* in that time bin, so sample sizes might still be influencing this analysis. At Site 1258, the only time bin with more than one *K. crassicaudata* is the post-ETM2 time bin, and once again the distributions of the two species cannot be distinguished from one another (Table 3.3). While doing genus-level morphometric analyses should certainly be done (if at all) very carefully, on a genus-to-genus basis, and only after multiple confirmations that body size varies very little across species of that genus, the limited number of adult ostracodes preserved in deep-sea sediments may suggest that

such genus-level analyses should be considered more in-depth as a possible solution or

alternative to issues with small sample sizes in these taxa.
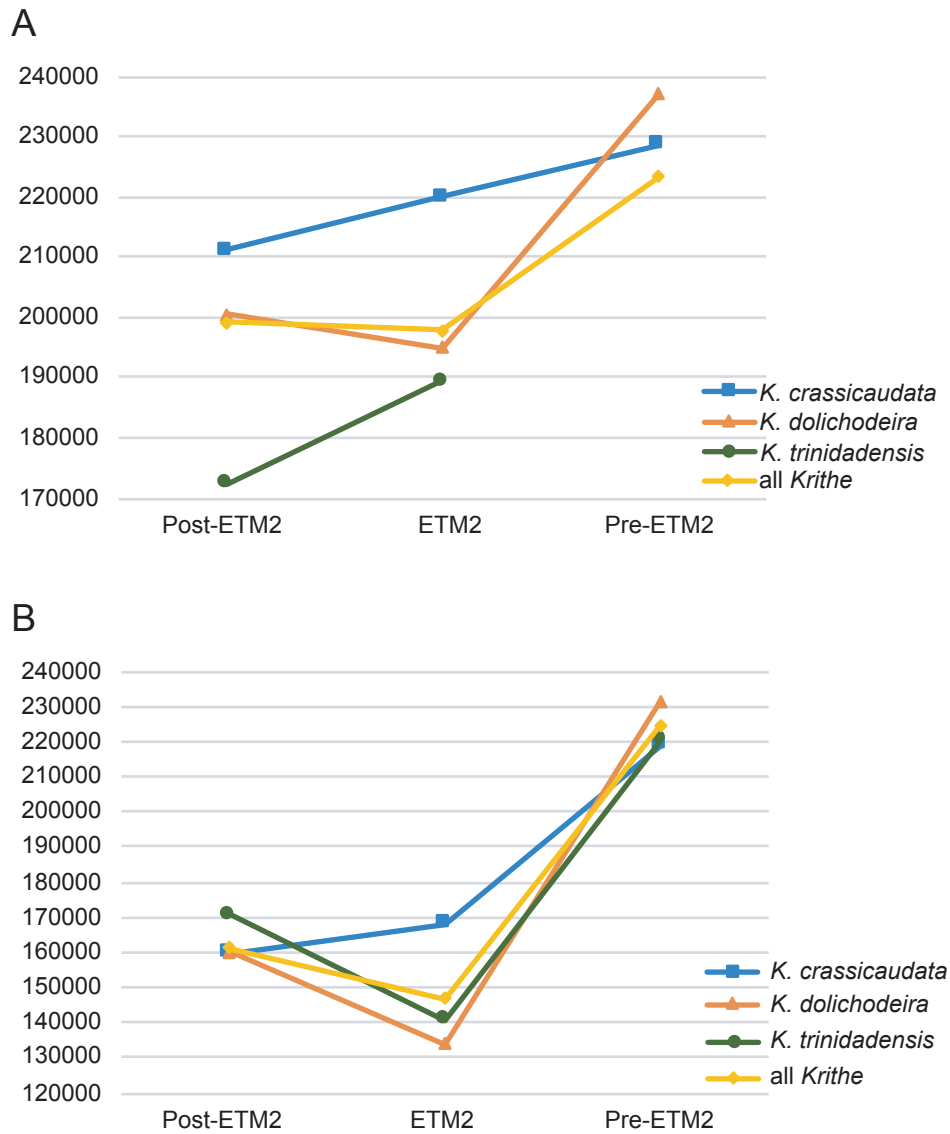

Figure 3.6. Average body sizes including *Krithe* genus grouping. Average body sizes (in µm^2) of adult *Krithe* before, during, and after ETM2, at Site 1258 (A) and Site U1409 (B), including all *Krithe* specimens combined in yellow.

Table 3.3. Results of Kolmogorov-Smirnov analyses for U1409 *K. crassicaudata* and *K. dolichodeira* adults in each time bin.

Time Bin	D	p(same)
Pre-ETM2	0.32941	0.2895
ETM2	1	0.04687
Post-ETM2	0.38961	0.4306

Conclusions

The two ostracode genera studied here, *Neonesidea* and *Krithe*, show evidence of being impacted by environmental changes at the Eocene Thermal Maximum 2 hyperthermal event, even at different locations. The same species are generally present at the two different sites studied here. While the species assemblages of these two genera are relatively unchanged, indicating a lack of species-level turnover or extirpation, species in both genera show changes in body size.

In fact, the various species at both sites showed similar trends in body size change from before ETM2 to ETM2 and from ETM2 to afterwards. All species populations examined this study decreased in size from the pre-ETM2 time bin to the ETM2 time bin. Most populations also showed some amount of increase in body size between the ETM2 and post-ETM2 time bins, but a few continued to decrease. While the trends in the different species remained very similar across the two sites, the observed changes in body size were only found to be statistically significant in *Krithe* species at Site U1409. These were also the populations with the highest sample sizes in this study.

Low sample sizes were an issue in evaluating the results of this study. The limited number of adult ostracodes from deep-sea samples found here is not unique to this study, but does represent a challenge for conducting quantitative morphometric analyses. Binning samples is one method for dealing with this issue, but it will likely continue to be challenging, particularly when specifically investigating events when ostracode abundance is also negatively impacted. Even considering this issue, it does seem that the taxa investigated here did experience changes in body size in response to environmental changes correlated with ETM2. While temperature likely played a role in triggering these changes, other factors such as changes in productivity cannot be ruled out. Whatever the cause(s), the effects were similar both on different species and genera and at different locations. Furthermore, the fact that we see a change at all in response to an event relatively smaller than those that have been previously investigated indicates that ostracodes do respond to smaller environmental changes in the past, and thus, may be likely to do so today.

References

Algeret, L., Ortiz, S., Arenillas, L., Molina, E., 2010, What happens when the ocean is overheated? The foraminiferal response across the Paleocene-Eocene Thermal Maximum at the Alamedilla section (Spain): Geological Society of America Bulletin, v. 122, p. 1616-1624.

Blackburn, T.M., Gaston, K.J., and Loder, N., 2008, Geographic gradients in body size: a clarification of Bergmann's Rule: Diversity and Distributions, v. 5, p. 165-174.

Bradley, R.S., 1999, Paleoclimatology: Reconstructing Climates of the Quaternary. Second Edition: San Diego, Academic Press, 613 p.

Chu, D., Tong, J., Song, H., Benton, M.J., Song, H., Yu, J., Qiu, X., Huang, Y., and Tian, L., 2015, Lilliput effect in freshwater ostracodes during the Permian-Triassic extinction: Palaeogeography, Palaeoclimatology, Palaeoecology, v. 435, p. 38-52.

Cramer, B.S., Wright, J.D., Kent, D.V., and Aubry, M.-P., 2003, Orbital climate forcing of $\delta^{13}C$ excursions in the late Paleocene-early Eocene (chrons C24n-C25n): Paleoceanography, v. 18, 1097.

Dyar, H.G., 1890, The number of molts of lepidopterous larvae: Psyche, v. 5, p. 420-422.

Erbacher, J., Mosher, D.C., Malone, M.J., et al., 2014, Proceedings of ODP, Initial Reports, 207: College Station, TX, Ocean Drilling Program.

Expedition 342 Scientists, 2012, Paleogene Newfoundland sediment drifts. IODP Preliminary Reports, v. 342.

Fernandes Martins, M.J., Hunt, G., Lockwood, R., Swaddle, J.P., and Horne, D.J., 2017, Correlation between investment in sexual traits and valve sexual dimorphism in *Cyprideis* species (Ostracoda): PLoS ONE, v. 12, e0177791.

Forel, M.B., Crasquin, S., Chitnarin, A., Angiolini, L., and Gaetani, M., 2015, Precocious sexual dimorphism and the Lilliput effect in Neo-Tethyan ostracoda (Crustacea) through the Permian-Triassic Boundary: Palaeontology, v. 58, p. 409-454.

Hammer, Ø., Harper, D.A.T., and Ryan, P.D., 2001, PAST: paleontological statistics software package for education and data analysis: Palaeontologia electronica, v.4, p. 9.

Hönisch, B., Ridgwell, A., Schmidt, D.N., Thomas, E., Gibbs, S.J., Sluijs, A., Zeebe, R., Kump, L., Martindale, R.C., Greene, S.E., Kiessling, W., Ries, J., Zachos, J.C., Royer, D.L., Barker, S., Marchitto Jr., T.M., Moyer, R., Pelejero, C., Ziveri, P., Foster, G.L., and Williams, B., 2012, The Geological record of ocean acidification: Science, v. 335, p. 1058-1063.

Hunt, G., Fernandes Martins, M.J., Puckett, T.M., Lockwood, R., Swaddle, J.P., Hall, C.M.S., and Stedman, J., Sexual dimorphism and sexual selection in cytheroidean ostracodes from the Late Cretaceous of the U.S. Coastal Plain: Paleobiology, v. 43, p. 620-641.

Hunt, G., and Roy, K., 2006, Climate change, body size evolution, and Cope's Rule in deep-sea ostracodes: Proceedings of the National Academy of Sciences, v. 103, p. 1347-1352.

Hunt, G., Wicaksono, S.A., Brown, J.E., Macleod, K.G., 2010, Climate-driven body-size trends in the ostracod fauna of the deep Indian Ocean: Palaeontology, v. 53, p. 1255-1268.

Kesling, R.V., 1953, A slide rule for determination of instars in ostracod species: Contributions from the Museum of Paleontology, University of Michigan, v. 11, p. 97-109.

Kirtland Turner, S., Sexton, P.F., Charles, C.D., Norris, R.D., 2014, Persistence of carbon release events through the peak of early Eocene global warmth: Nature Geoscience, v. 7, p. 748-751.

Lauretano, V., Littler, K., Polling, M., Zachos, J.C., and Lourens, L.J., 2015, Frequency, magnitude and character of hyperthermal events at the onset of the Early Eocene Climatic Optimum: Climate of the Past, v. 11, p. 1313-1324.

Littler, K., Röhl, U., Westerhold, T., and Zachos, J.C., 2014, A high-resolution benthic stable-isotope record for the South Atlantic: Implications for orbital-scale changes in Late Paleocene-Early Eocene climate and carbon cycling: Earth and Planetary Science Letters, v. 401, p. 18-30.

Lourens, L.J., Sluijs, A., Kroon, D., Zachos, J.C., Thomas, E., Röhl, U., Bowles, J., and Raffi, I., 2005, Astronomical pacing of late Paleocene to early Eocene global warming events: Nature, v. 435, p. 1083-1087.

Martens, K., 1985, Effects of temperature and salinity on postembryonic growth in *Mytilocypris henricae* (Chapman) (Crustacea, Ostracoda): Journal of Crustacean Biology, v. 5, p. 258-272.

Mayr, E., 1956, Geographical character gradients and climatic adaptation: Evolution, v. 10, p. 105-108.

Mezquita, F., Roca, J.R., and Wansard, G., 1999, Moulting, survival and calcification: The effects of temperature and water chemistry on an ostraod crustacean (*Herpetocypris intermedia*) under experimental conditions: Archiv fur Hydrobiologie, v. 146, p. 219-238.

Millien, V., Lyons, S.K., Olson, L., Smith, F.A., Wilson, A.B., and Yom-Tov, Y., 2006, Ecotypic variation in the context of global climate change: revisiting the rules: Ecology Letters, v. 9., p. 853-869.

Norris, R.D., Wilson, P.A., Blum, P., and the Expedition 342 Scientists, 2014, Proceedings of IODP, 342: College Station, TX, Integrated Ocean Drilling Program.

Ray, C., 1960, The application of Bergmann's and Allen's rules to the poikilotherms: Journal of Morphology, v. 106, p. 85-108.

Rensch, B., 1938, Some problems of geographical variation and species-formation: Proceedings of the Linnean Society of London, v. 150, p. 275-285.

Roca, J.R., and Wansard, G., 1997, Temperature influence on development and calcification of *Herpetocypris brevicaudata* Kaufmann, 1990 (Crustacea: Ostracoda) under experimental conditions. Hydrobiologia, v. 347, p. 91-95.

Schindelin, J., Arganda-Carreras, I., Frise, E., Kaynig, V., Longair, M., Pietzsch, T., Preibisch, S., Rueden, C., Saalfeld, S., Schmid, B., Tinevez, J.Y., White, D.J., Hartenstein, V., Eliceiri, K., Tomancak, P., and Cardona, A., 2012, Fiji: an open-source platform for biological-image analysis: Nature Methods, v. 9, p. 676-682.

Schneider, C.A., Rasband, W.S., and Eliceiri, K.W., 2012, NIH Image to ImageJ: 25 years of image analysis: Nature Methods, v. 9, p. 671-675.

Sexton, P.F., Wilson, P.A., and Norris, R.D., 2006, Testing the Cenozoic multisite composite $\delta^{18}O$ and $\delta^{13}C$ curves: New monospecific Eocene records from a single locality, Demerara Rise (Ocean Drilling Program Leg 207): Paleaeoceanography, v. 21, PA2019.

Shipboard Scientific Party, 2004, Site 1258, *in* Erbacher, J., Mosher, D.C., Malone, M.J., et al., Proceedings of ODP, Initial Reports, 207: College Station, TX, Ocean Drilling Program, p. 1-117.

Smart, C.W., 2002, Environmental applications of deep-sea benthic foraminifera, *in* Haslett, S.K., ed., Quaternary Environmental Micropaleontology: New York, Oxford University Press, 340 p.

Stap, L., Lourens, L.J., Thomas, E., Sluijs A., Bohaty, S., Zachos, J.C., 2010, High-resolution deep-sea carbon and oxygen isotope records of Eocene Thermal Maximum 2 and H2: Geology, v. 38, p. 607-610.

Thomas, E., 2007, Cenozoic mass extinctions in the deep sea: What perturbs the largest habitat on Earth? *in* Monechi, S., Coccioni, R., and Rampino, M., eds., Large ecosystem perturbations: causes and consequences: Geological Society of America Special Paper, v. 424, p. 1-23.

Thorp, J.H., 2003, Arthropoda and related groups, *in* Resh, V.H., and Carde, R.T., eds., Encyclopedia of Insects: New York, Elsevier Science, 1266 p.

Tucholke, B.E., and Vogt, P.R., et al., 1979, Western North Atlantic: Sedimentary evolution and aspects of tectonic history, *in* Tucholke, B.E., Vogt, P.R., et al., eds., Initial Reports of the Deep Sea Drilling Project, v. 43, p. 791-825.

Urbanek, A., 1993, Biotic crises in the history of Upper Silurian graptoloids: A palaeobiological model: Historical Biology, v. 7, p. 29-50.

Westerhold, T., Röhl, U., Laskar, J., Raffi, I., Bowles, J., Lourens, L.J., Zachos, J.C., 2007, On the duration of magentochrons C24r and C25n and the timing of early Eocene global warming events: implications from the Ocean Drilling Program Leg 208 Walvis Ridge depth transect: Paleoceanography, v. 22, PA2201.

Yamaguchi, T., Matsui, H., and Nishi, H., 2017a, Taxonomy of Maastrichtian-Thanetian deep-sea ostracodes from U1407, IODP Exp 342, off Newfoundland, Northwestern Atlantic, part 1: Families Cytherellidae, Bairdiidae, Pontocyprididae, Bythocytheridae, and Cytheruridae: Paleontological Research, v. 21, p. 54-75.

Yamaguchi, T., Matsui, H., and Nishi, H., 2017b, Taxonomy of Maastrichtian-Thanetian deep-sea ostracodes from U1407, IODP Exp 342, off Newfoundland, Northwestern Atlantic, part 2: Families Eucytheridae, Krithidae, Thaerocytheridae, Trachyleberididae, and Xestoleberididae: Paleontological Research, v. 21, p. 97-121.

Yamaguchi, T., Norris, R.D., and Bornemann, A., 2012, Dwarfing of ostracodes during the Paleocene-Eocene Thermal Maximum at DSDP Site 401 (Bay of Biscay, North Atlantic) and its implication for changes in organic carbon cycle in deep-sea benthic ecosystem: Palaeogeography, Palaeoclimatology, Palaeoecology, v. 346-347, p. 130-144.

CONCLUSIONS

The research herein has provided insight into two times of remarkable environmental change in Earth's history, albeit at very different scales. First, in the Ediacaran, when early complex animal life was evolving, I investigated a suite of tri-radial taxa to determine both their relatedness and to try to understand why similar organisms are not found at any other point in the geologic or modern record. After conducting various morphological and ecological analyses on multiple tri-radial genera, it seems likely that these organisms were members of a unique clade, beginning to establish some amount of relatedness among these taxa. Ediacaran tri-radial taxa share multiple morphological features, including branching, radiating features and disc- or node-like features, all superimposed over conical- to disc-shaped bodies with tri-radial symmetry. In addition, these taxa seem to fill similar ecological niches. Many are found in similar environments and seem to be living in similar ways. These niches seem to also commonly focus around being environmental generalists, able to survive, and at times even thrive, in a variety of environments and in association with a variety of other taxa. This makes it perhaps more shocking that tri-radial organisms were not ultimately successful enough to survive past the Ediacaran, nor do other similar organisms take their place in later times. It seems clear that a significant environmental shift would have been needed to disrupt them to the point of extinction. A change in global oxygen levels seems a likely contender for the disappearance of these and other otherwise successful taxa of the White Sea assemblage.

The early Cenozoic was characterized by multiple hyperthermal events of a variety of magnitudes. Eocene Thermal Maximum 2 (ETM2) was the second largest of these events, clocking in at around half the magnitude and duration of the Paleocene-Eocene Thermal Maximum. Bulk carbonate isotope records at two deep-sea ocean drill core sites, ODP Site 1258 on the Demerara Rise in the equatorial Atlantic and IODP Site U1409 off the coast of Newfoundland in the north Atlantic, indicate negative oxygen isotope excursions of ~0.6‰ in association with negative carbon isotope excursions. High-resolution records revealed that despite the great difference in latitude between the two sites, they shared several similar trends in the ostracode response to the ETM2 hyperthermal event. Both sites were represented by a taxonomically diverse assemblage of ostracodes, and several of the same genera and species were present at the two sites, generally with very similar relative abundances. Ostracodes at both sites experience a marked decrease in ostracode accumulation rate during ETM2, but the assemblages of ostracodes present before and after ETM2 are very similar. There is no evidence for an ostracode extinction or origination event at either locality, although some taxa do disappear temporarily during ETM2, resulting in generally lower diversity during the hyperthermal event. The main difference in ostracode abundance trends between the two sites is that at the height of the isotope excursions, multiple samples at Site U1409 completely lacked ostracodes. This was not the case at Site 1258, where all samples had at least one ostracode.

At both sites, the two most abundant genera were *Neonesidea* and *Krithe*. The same

species of these two genera were found at the two sites. As is typical in deep-sea

ostracodes assemblages, which are generally characterized by a relative lack of

transport, the large majority of specimens were from juvenile ostracodes. However,

there were enough adults to do morphometric analyses that are comparable to similar

studies. By separating samples into pre-ETM2, ETM2, and post-ETM2 time bins, I was

able to analyze ostracode body size trends as they related to the ETM2 hyperthermal

event. Similar trends were generally conserved across both the different sites and the

different genera. While there was some variation, the general trend was a decrease in

body size during the ETM2 time bin, followed by a smaller recovery of body size after

ETM2. While there could be multiple environmental factors influencing this trend, this is

consistent with the hypothesis that animal body sizes tend to be smaller in warmer

conditions. Similar results have been found in other ostracodes from the Cenozoic as a

whole, demonstrating that this effect is present both over short and long time scales.

Final Thoughts and Future Directions

Ostracode studies are valuable because ostracodes represent a unique opportunity to

do microfossil-scale quantitative analyses on multicellular animals, which may provide

more relevant comparisons to other complex animal taxa, relative to other single-celled

taxa such as foraminifera. For this reason, it is worth investigating how we conduct

these studies and how to get the most, and most meaningful, use of our samples. An

issue that became important for Cenozoic chapters of this dissertation is relatively low

sample sizes. The consistency of the trends, despite the low abundances, seems to

indicate that these results are likely representative of real trends, and so it would be a

shame to disregard them only because of low sample sizes. While it is important to

proceed carefully, this research also suggests that there are possibilities in proceeding

with samples such as these. Here, the different species of *Krithe* were similar enough in

size that the results for the genus overall did not differ greatly from individual species.

This, and other similar possibilities, are very worth investigating to help us to best utilize

these records in meaningful ways.

Perhaps most importantly what this research shows is that the scales of changes are

important in determining the responses that organisms will have to them. As we have

seen in the fossil record, life has responded in very many different ways to different

environmental perturbations, and these differences are often due to the nature and

scale of the change they experience. Otherwise very successful groups may simply be

unable to cope with change at a certain point. On the other hand, evidence also

suggests that even relatively small changes are enough to result in detectable

differences in abundances, diversity, and other species or organism-level traits. These

lessons from the fossil record should be critically evaluated as we work to proceed

forward mindfully in world facing the prospect of significant environmental changes in

the near future.

REFERENCES

Algeret, L., Ortiz, S., Arenillas, L., Molina, E., 2010, What happens when the ocean is overheated? The foraminiferal response across the Paleocene-Eocene Thermal Maximum at the Alamedilla section (Spain): Geological Society of America Bulletin, v. 122, p. 1616-1624.

Alvarez Zarikian, C.A., Stepanova, A.Yu., Grütner, J., 2009, Galcial-interglacial variability in deep sea ostracod assemblage composition at IODP Site U1314 in the subpolar North Atlantic: Marine Geology, v. 258, p. 69-87.

Ayress, M., Neil, H., Passlow, V., Swanson, K., 1997, Benthonic ostracods and deep watermasses: a qualitative comparison of Southwest Pacific, Southern and Atlantic Oceans: Palaeogeography, Palaeoclimatology, Palaeoecology, v. 131, p. 287-302.

Benson, R.H., 1981, Form, function, and architecture of ostracode shells: Annual Review of Earth and Planetary Sciences, v. 9, p. 59-80.

Blackburn, T.M., Gaston, K.J., and Loder, N., 2008, Geographic gradients in body size: a clarification of Bergmann's Rule: Diversity and Distributions, v. 5, p. 165-174.

Boag, T.H., Darroch, S.A.F., and Laflamme, M., 2016, Ediacaran distributions in space and time: testing assemblage concepts of earliest macroscopic body fossils: Paleobiology, v. 42, p. 574–594.

Boomer, I., 1999, Late Cretaceous and Cainozoic bathyal Ostracoda from Central Pacific (DSDP Site 463): Marine Micropaleontology, v. 37, p. 131-147.

Boomer, I., 2002, Environmental Applications of Marine and Freshwater Ostracoda, *in* Haslett, S.K., ed., Quaternary Environmental Micropaleontology: New York, Oxford University Press, 340 p.

Boomer, I., and Whatley, R., 1995, Cenozoic ostracode from guyots in the western Pacific: Holes 865B and 866B (Leg 143), *in* Winterer, E.L., Sager, W.W., Firth, J.V., and Sinton, J.M., eds., Proceedings of the Ocean Drilling Program, Scientific Results, v. 143, p. 75-86.

Braeckman, U., Vanaverbeke, J., Vincx, M., Oevelen, D. van, and Soetaert, K., 2013, Meiofauna metabolism in suboxic sediments: currently overestimated: PLoS One, v. 8, e59289.

Bradley, R.S., 1999, Paleoclimatology: Reconstructing Climates of the Quaternary. Second Edition: San Diego, Academic Press, 613 p.

Brierley, A.S., and Kingsford, M.J., 2009, Impacts of climate change on marine organisms and ecosystems: Current Biology, v. 19, R602-R614.

Budd, G.E. and Jensen, S., 2015, The origin of the animals and a 'Savannah' hypothesis for early bilaterian evolution: Biological Reviews, v. 92, p. 446-473.

Canfield, D.E., Poulton, S.W., and Narbonne, G.M., 2007, Late-Neoproterozoic deep-ocean oxygenation and the rise of animal life: Science, v. 315, p. 92-95.

Chu, D., Tong, J., Song, H., Benton, M.J., Song, H., Yu, J., Qiu, X., Huang, Y., and Tian, L., 2015, Lilliput effect in freshwater ostracodes during the Permian-Triassic extinction: Palaeogeography, Palaeoclimatology, Palaeoecology, v. 435, p. 38-52.

Clites, E.C., Droser, M.L., and Gehling, J.G., 2012, The advent of hard-part structural support among the Ediacara biota: Ediacaran harbinger of a Cambrian mode of body construction: Geology, v. 40, p. 307–310.

Cramer, B.S., Wright, J.D., Kent, D.V., Aubry, M-P., 2003, Orbital climate forcing of δ^{13}C excursions in the Paleocene-early Eocene (chrons C24n-C25n): Paleoceanography, v. 18, p. 21-1-21-25.

Cronin, T.M., DeMartino, D.M., Dwyer, G.S., Rodriguez-Lazaro, J., 1999, Deep-sea ostracode species diversity: response to late Quaternary climate change: Marine Micropaleontology, v. 37, p. 231-249.

DeConto, R.M, Galeotti, S., Pagani, M., Tracy, D., Schaefer, K., Zhang, T., Pollard, D., and Beerling, D.J., 2012, Past extreme warming events linked to massive carbon release from thawing permafrost, Nature, v. 484, p. 87-92.

Dickens, G.R., Castillo, M.M., Walker, J.C.G., 1997, A blast of gas in the latest Paleocene: Simulating first-order effects of massive dissociation of oceanic methane hydrate: Geology, v. 25, p. 259-262.

Dickens, G.R., O'Neil, J.R., Rea, D.K., Owen, R.M., 1995, Dissoociation of oceanic methane hydrate as a cause of the carbon isotope excursion at the end of the Paleocene: Paleoceanography, v. 10, p. 965-971.

Didie, C., Bauch, H.A., and Helmke, J.P., 2002, Late Quaternary deep-sea ostracodes in the polar and subpolar North Atlantic: paleoecological and paleoenvironmental implications: Palaeogeography, Palaeoclimatology, Palaeoecology, v. 184, p. 195-212.

Doney, S.C., Ruckelshaus, M., Emmett Duffy, J., Barry, J.P., Chan, F., English, C.A., Galindo, H.M., Grebmeier, J.M., Hollowed, A.B., Knowlton, N., and Polovina, J., 2012, Climate change impacts on marine ecosystems: Annual Review of Marine Science, v. 4, p. 11-37.

Droser, M.L., and Gehling, J.G., 2015, The advent of animals: the view from the Ediacaran: Proceedings of the National Academy of Sciences, v. 112, p. 4865-4870.

Droser, M.L., Tarhan, L.G., and Gehling, J.G., 2017, The rise of animals in a changing environment: global ecological innovation in the Ediacaran: Annual Review of Earth and Planetary Sciences, v. 45, p. 593–617.

Dunkley Jones, T., Lunt, D.J., Schmidt, D.N., Ridgwell, A., Sluijs, A., Valdes, P.J., and Maslin, M., 2013, Climate model and proxy data constraints on ocean warming across the Paleocene-Eocene Thermal Maximum: Earth-Science Reviews, v. 125, p. 123-145.

Dyar, H.G., 1890, The number of molts of lepidopterous larvae: Psyche, v. 5, p. 420-422.

Erbacher, J., Mosher, D.C., Malone, M.J., et al., 2014, Proceedings of ODP, Initial Reports, 207: College Station, TX, Ocean Drilling Program.

Erwin, D.H., 2015, Early metazoan life: Divergence, environment and ecology: Philosophical Transactions of the Royal Society of London B, v. 370(1684), 20150036.

Erwin, D.H., Laflamme, M., Tweedt, S.M., Sperling, E.A., Pisani, D., and Peterson, K.J., 2011, The Cambrian conundrum: Early divergence and later ecological success in the early history of animals: Science, v. 334, p. 1091–1097.

Evans, S.D., Diamond, C.W., Droser, M.L., and Lyons, T.W., 2018, Dynamic oxygen coupled with biological and ecological innovation during the second wave of the Ediacara Biota: Emerging Topics in Life Sciences, v. 2, p. 223-233.

Expedition 342 Scientists, 2012, Paleogene Newfoundland sediment drifts. IODP Preliminary Reports, v. 342.

Fedonkin, M.A., 1984, Promorphology of Vendian Radalia, *in* Ivanovsky, A.B.. and Ivanov, A.B., eds., Stratigraphy and Paleontology of the Most Ancient Phanerozoic: Moscow, Nauka, p. 27–45.

Fedonkin, M.A., 1985a, Precambrian metazoans: the problems of preservation, systematics and evolution: Philosophical Transactions of the Royal Society of London B, v. 311 (1148), p. 27–45.

Fedonkin, M.A., 1985, Systematic description of Vendian metazoan, *in* Sokolov, B.S., and Iwanowski, A.B., eds., The Vendian System, Volume 1 Paleontology: Berlin, Springer-Verlag, p. 71–120.

Fedonkin, M.A., Gehling, J.G., Grey, K., Narbonne, G.M., and Vickers-Rich, P., 2007, The Rise of Animals: Evolution and Diversification of the Kingdom Animalia: Baltimore, Maryland, The Johns Hopkins University Press, 326 p.

Fedonkin, M.A., and Ivantsov, A.Y, 2007, *Ventogyrus*, a possible siphonophore-like trilobozoan coelenterate from the Vendian Sequence (late Neoproterozoic), northern Russia, *in* Vickers-Rich, P. and Komarower, P., eds., The Rise and Fall of the Ediacaran Biota: Geological Society Special Publications, Vol. 286: London: Geological Society, p. 187–194.

Fedonkin, M.A., and Waggoner, B.M., 1997, The Late Precambrian fossil *Kimberella* is a mollusc-like bilaterian organism: Nature, v. 388, p. 868–871.

Fernandes Martins, M.J., Hunt, G., Lockwood, R., Swaddle, J.P., and Horne, D.J., 2017, Correlation between investment in sexual traits and valve sexual dimorphism in *Cyprideis* species (Ostracoda): PLoS ONE, v. 12, e0177791.

Fink, W.L., 1982, The conceptual relationship between ontogeny and phylogeny: Paleobiology, v. 8, p. 254–264.

Forel, M.B., Crasquin, S., Chitnarin, A., Angiolini, L., and Gaetani, M., 2015, Precocious sexual dimorphism and the Lilliput effect in Neo-Tethyan ostracoda (Crustacea) through the Permian-Triassic Boundary: Palaeontology, v. 58, p. 409-454.

Gehling, J.G., 2000, Environmental interpretation and a sequence stratigraphic framework for the terminal Proterozoic Ediacara Member within the Rawnsley Quartzite, South Australia: Precambrian Research, v. 100, p. 65–95.

Gehling, J.G. and Droser, M.L., 2013, How well do fossil assemblages of the Ediacara biota tell time?: Geology, v. 41, p. 447–450.

Gehling, J.G., Narbonne, G.M., and Anderson, M.M., 2000, The first named Ediacaran body fossil, *Aspidella terranovica*: Palaeontology, v. 43, p. 427–456.

Glaessner, M.F. and Daily, B., 1959, The geology and late Precambrian fauna of the Ediacara Fossil Reserve: Records of the South Australia Museum, v. 13, p. 396–401.

Glaessner, M.F. and Wade, M., 1966, The late Precambrian fossils from Ediacara, South Australia: Paleontology, v. 9, p. 599–628.

Greene, S.E., Ridgwell, A., Kirtland Turner, S., Schmidt, D.N., Pälike, H., Thomas, E., Greene, L.K., and Hoogakker, B.A.A., 2019, Early Cenozoic decoupling of climate and carbonate compensation depth trends: Paleoceanography and Paleoclimatology.

Gutjahr, M., Ridgwell, A., Sexton, P.F., Anagnostou, E., Pearson, P.N., Pälike, H., Norris, R.D., Thomas, E., and Foster, G.L., 2017, Very large release of mostly volcanic carbon during the Palaeocene-Eocene Thermal Maximum, Nature, v. 548, p. 573-580.

Hall, C.M.S., Droser, M.L., and Gehling, J.G., 2018, Sizing up *Rugoconites*: A study of the ontogeny and ecology of an enigmatic Ediacaran genus: Australasian Palaeontological Memoirs, v 51, p. 7-17.

Hall, C.M.S., Droser, M.L., Gehling, J.G., and Dzaugis, M.E., 2015, Paleoecology of the enigmatic *Tribrachidium*: New data from the Ediacaran of South Australia: Precambrian Research, v. 269, p. 183–194.

Hammer, Ø., Harper, D.A.T., and Ryan, P.D., 2001, PAST: paleontological statistics software package for education and data analysis: Palaeontologia electronica, v.4, p. 9.

Higgins, J.A., and Schrag, D.P., 2006, Beyond methane: Towards a theory for the Paleocene-Eocene thermal maximum: Earth and Planetary Science Letters, v. 245, p. 523-537.

Hönisch, B., Ridgwell, A., Schmidt, D.N., Thomas, E., Gibbs, S.J., Sluijs, A., Zeebe, R., Kump, L., Martindale, R.C., Greene, S.E., Kiessling, W., Ries, J., Zachos, J.C., Royer, D.L., Barker, S., Marchitto Jr., T.M., Moyer, R., Pelejero, C., Ziveri, P., Foster, G.L., and Williams, B., 2012, The Geological record of ocean acidification: Science, v. 335, p. 1058-1063.

Horne, D.J., Cohen, A., and Martens, K., 2002, Taxonomy, morphology, and biology of Quaternary and living ostracodes, *in* Holmes, J., and Chivas, A., eds., The Ostracoda: Applications in Quaternary Research: Washington, D.C., American Geophysical Union, 313 p.

Horne, D.J., and Martens, K., editors, 2000, Evolutionary biology and ecology of Ostracoda: Theme 3 of the 13th International Symposium on Ostracoda (ISO97): Dordrecht, The Netherlands, Kluwer Academic Publishers, 197 p.

Huang, H.M., Yasuhara, M., Iwatani, H., Yamaguchi, T., Yamada, K., and Mamo, B., 2019, Deep-sea ostracod faunal dynamics in a marginal sea: biotic response to oxygen variability and mid-Pleistocene global changes: Paleobiology, v. 45, p. 85-97.

Hunt, G., Fernandes Martins, M.J., Puckett, T.M., Lockwood, R., Swaddle, J.P., Hall, C.M.S., and Stedman, J., Sexual dimorphism and sexual selection in cytheroidean ostracodes from the Late Cretaceous of the U.S. Coastal Plain: Paleobiology, v. 43, p. 620-641.

Hunt, G., and Roy, K., 2006, Climate change, body size evolution, and Cope's Rule in deep-sea ostracodes: Proceedings of the National Academy of Sciences, v. 103, p. 1347-1352.

Hunt, G., Wicaksono, S.A., Brown, J.E., Macleod, K.G., 2010, Climate-driven body-size trends in the ostracod fauna of the deep Indian Ocean: Palaeontology, v. 53, p. 1255-1268.

IPCC, 2014, Climate change 2014: Synthesis Report. Contribution of Working Groups I, II, and III to the Fifth Assessment Report of the Intergovernmental Panel on Climate Change [Core Writing Team, Pachauri, R.K., and Meyer, L.A., eds.]: Geneva, Switzerland, IPCC, 151 pp.

Ivantsov, A.Yu. and Fedonkin, M.A., 2002, Conulariid-like fossil from the Vendian of Russia: a metazoan clade across the Proterozoic/Palaeozoic boundary: Palaeontology, v. 45, p. 1219–1229.

Ivantsov, A.Yu. and Grazhdankin, D.V., 1997, A new representative of the Petalonamae from the Upper Vendian of the Arkhangelsk Region: Palaeontological Journal, v. 31, p. 1–16.

Jenkins, R.J.F., 1992, Functional and ecological aspects of Ediacaran assemblages, *in* Lipps, J.H. and Signor, P.W., eds., Origin and Early Evolution of the Metazoa: New York, Plenum Press, p. 131–176.

Just, J., Kristensen, R., and Olesen, J., 2014, *Dendrogramma*, new genus, with two new non-bilaterian species from the marine bathyal of Southeastern Australia (Animalia, Metazoa incertae sedis) – with similarities to some medusoids from the Precambrian Ediacara: PLoS ONE, v. 9(9), 1–11.

Keller, B.M. and Fedonkin, M.A., 1977, New organic finds in the Precambrian Valday series along the Syuz'ma River: International Geology Review, v. 19, p. 924–930.

Kennett, J.P., and Stott, L.D., 1991, Abrupt deep-sea warming, palaeoceanographic changes and benthic extinctions at the of the Palaeocene: Nature, v. 353, p. 225-229.

Kesling, R.V., 1953, A slide rule for determination of instars in ostracod species: Contributions from the Museum of Paleontology, University of Michigan, v. 11, p. 97-109.

Kirtland Turner, S., 2018, Constraints on the onset duration of the Paleocene-Eocene Thermal Maximum: Philosophical Transactions of the Royal Society A, v. 376, p. 1-16.

Kirtland Turner, S., Hull, P.M., Kump, L.R., and Ridgwell, A., 2017, A probabilistic assessment of the rapidity of PETM onset: Nature Communications, v. 8, p. 1-10.

Kirtland Turner, S., Sexton, P.F., Charles, C.D., Norris, R.D., 2014, Persistence of carbon release events through the peak of early Eocene global warmth: Nature Geoscience, v. 7, p. 748-751.

Knoll, A.H., 2011, The multiple origins of complex multicellularity: Annual Review of Earth and Planetary Sciences, v. 39, p. 217-239.

Laflamme, M., Darroch, S.A.F., Tweedt, S.M., Peterson, K.J., and Erwin, D.H., 2013, The end of the Ediacara: extinction, biotic replacement, or Cheshire Cat?: Gondwana Research, v. 23, p. 558–573.

Lauretano, V., Littler, K., Polling, M., Zachos, J.C., and Lourens, L.J., 2015, Frequency, magnitude and character of hyperthermal events at the onset of the Early Eocene Climatic Optimum: Climate of the Past, v. 11, p. 1313-1324.

Littler, K., Rohl, U., Westerhold, T., and Zachos, J.C., 2014, A high-resolution benthic stable-isotope record for the South Atlantic: Implications for orbital-scale changes in Late Paleocene-Early Eocene climate and carbon cycling: Earth and Planetary Science Letters, v. 401, p. 18-30.

Lourens, L.J., Sluijs, A., Kroon, D., Zachos, J.C., Thomas, E., Röhl, U., Bowles, J., and Raffi, I., 2005, Astronomical pacing of late Paleocene to early Eocene global warming events: Nature, v. 435, p. 1083-1087.

Lyons, T.W., Reinhard, C.T., and Planavsky, N.J., 2014, The rise of oxygen in Earth's early ocean and atmosphere: Nature, v. 506, p. 307-315.

Maiorano, P., Aiello, G., Barra, D., Di Leo, P., Joannin, S., Lirer, F., Marino, M., Pappalardo, A., Capotondi, L., Ciaranfi, N., and Stefanelli, S., 2008, Paleonvironmental changes during sapropel 19 (i-cycle 90) deposition: evidences from geochemical, mineralogical and micropaleontological proxies in the mid-Pleistocene Montalbano Jonico land section (southern Italy): Palaeogeography, Palaeoclimatology, Palaeoecology, v. 257, p. 308-334.

Martens, K., 1985, Effects of temperature and salinity on postembryonic growth in *Mytilocypris henricae* (Chapman) (Crustacea, Ostracoda): Journal of Crustacean Biology, v. 5, p. 258-272.

Martin, M.W., Grazhdankin, D.V., Bowring, S.A., Evans, D.A.D., Fedonkin, M.A., and Kirschvink, J.L., 2000, Age of Neoproterozoic bilaterian body and trace fossils, White Sea, Russia: implications for metazoan evolution: Science, v. 288, p. 841–845.

Mayr, E., 1956, Geographical character gradients and climatic adaptation: Evolution, v. 10, p. 105-108.

McCall, G.J.H., 2006, The Vendian (Ediacaran) in the geological record: Enigmas in geology's prelude to the Cambrian explosion: Earth-Science Reviews, v. 77, p. 1–229.

McInerney, F.A., and Wing, S.L., 2011, The Paleocene-Eocene Thermal Maximum: A perturbation of carbon cycle, climate, and biosphere with implications for the future: Annual Reviews of Earth and Planetary Science, v. 39, p. 489-516.

McMenamin, M.A.S., 2000, The garden of Ediacara: Discovering the first complex Life: New York, Columbia University Press.

Mezquita, F., Roca, J.R., and Wansard, G., 1999, Moulting, survival and calcification: The effects of temperature and water chemistry on an ostraod crustacean (*Herpetocypris intermedia*) under experimental conditions: Archiv fur Hydrobiologie, v. 146, p. 219-238.

Millien, V., Lyons, S.K., Olson, L., Smith, F.A., Wilson, A.B., and Yom-Tov, Y., 2006, Ecotypic variation in the context of global climate change: revisiting the rules: Ecology Letters, v. 9., p. 853-869.

Morsi, A.-M.M., and Speijer, R.P., 2003, High-resolution ostracode records of the Paleocene/Eocene transition in the South Eastern Desert of Egypt-taxonomy, biostratigraphy, paleoecology, and paleobiogeography: Senckenbergiana Lethaea, v. 83, p. 61-93.

Narbonne, G.M., 2005, The Ediacara biota: Neoproterozoic origin of animals and their ecosystems: Annual Review of Earth and Planetary Sciences, v. 33, p. 421–442.

Narbonne, G.M. and Hofmann, H.J., 1987, Ediacaran biota of the Wernecke Mountains, Yukon, Canada: Palaeontology, v. 30, p. 647–676.

Norris, R.D., Kirtland Turner, S., Hull, P.M., and Ridgwell, A., 2013, Marine ecosystem responses to Cenozoic global change: Science, v. 341, p. 492-498.

Norris, R.D., Wilson, P.A., Blum, P., and the Expedition 342 Scientists, 2014, Proceedings of IODP, 342: College Station, TX, Integrated Ocean Drilling Program.

Paytan, A., and Griffith, E.M., 2007, Marine barite: Recorder of variations in ocean export productivity: Deep-Sea Research II, v. 54, p. 687-705.

Penman, D.E., Keller, A., D'haenens, S., Kirtland Turner, S., and Hull, P.M., 2019, Atlantic deep-sea cherts associated with Eocene Hyperthermal Events: Paleoceanography and Paleoclimatology, v. 34, p. 1-13.

Rahman, I.A., Darroch, S.A.F., Racicot, R.A., and Laflamme, M., 2015, Suspension feeding in the enigmatic Ediacaran organism *Tribrachidium* demonstrates complexity of Neoproterozoic ecosystems: Science Advances, v. 1(10), e1500800.

Ray, C., 1960, The application of Bergmann's and Allen's rules to the poikilotherms: Journal of Morphology, v. 106, p. 85-108.

Reid, L.M., García-Bellido, D.C., Payne, J.L., Runnegar, B., and Gehling, J.G., 2017, Possible evidence of primary succession in a juvenile-dominated Ediacara fossil surface from the Flinders Ranges, South Australia: Palaeogeography, Palaeoclimatology, Palaeoclimatology, v. 476, p. 68–76.

Rensch, B., 1938, Some problems of geographical variation and species-formation: Proceedings of the Linnean Society of London, v. 150, p. 275-285.

Retallack, G.J., 2013, Ediacaran life on land: Nature, v. 493, p. 89–92.

Roca, J.R., and Wansard, G., 1997, Temperature influence on development and calcification of *Herpetocypris brevicaudata* Kaufmann, 1990 (Crustacea: Ostracoda) under experimental conditions. Hydrobiologia, v. 347, p. 91-95.

Schindelin, J., Arganda-Carreras, I., Frise, E., Kaynig, V., Longair, M., Pietzsch, T., Preibisch, S., Rueden, C., Saalfeld, S., Schmid, B., Tinevez, J.Y., White, D.J., Hartenstein, V., Eliceiri, K., Tomancak, P., and Cardona, A., 2012, Fiji: an open-source platform for biological-image analysis: Nature Methods, v. 9, p. 676-682.

Schneider, C.A., Rasband, W.S., and Eliceiri, K.W., 2012, NIH Image to ImageJ: 25 years of image analysis: Nature Methods, v. 9, p. 671-675.

Seilacher, A., 1989, Vendozoa: Organismic construction in the Proterozoic biosphere: Lethaia, v. 22, p. 229–239.

Seilacher, A., 1992, Vendobionta and Psammocorallia: Lost constructions of Precambrian evolution: Journal of the Geological Society, v. 149, p. 607–613.

Seilacher, A., 1999, Biomat-related lifestyles in the Precambrian: Palaios, v. 14, p. 86–93.

Sepkoski, J.J., 1981, A factor analytic description of the Phanerozoic marine fossil record: Paleobiology, v. 7, p. 36-53.

Sexton, P.N., Norris, R.D., Wilson, P.A., Palike, H., Westerhold, T., Rohl, U., Bolton, C.T., and Gibbs, S., 2011, Multiple Eocene 'hyperthermal' events driven by ocean ventilation: Nature, v. 471, p. 349-353.

Sexton, P.F., Wilson, P.A., and Norris, R.D., 2006, Testing the Cenozoic multisite composite δ^{18}O and δ^{13}C curves: New monospecific Eocene records from a single locality, Demerara Rise (Ocean Drilling Program Leg 207): Paleaeoceanography, v. 21, PA2019.

Shipboard Scientific Party, 2004, Site 1258, in Erbacher, J., Mosher, D.C., Malone, M.J., et al., Proceedings of ODP, Initial Reports, 207: College Station, TX, Ocean Drilling Program, p. 1-117.

Smart, C.W., 2002, Environmental applications of deep-sea benthic foraminifera, in Haslett, S.K., ed., Quaternary Environmental Micropaleontology: New York, Oxford University Press, 340 p.

Speijer, R.P., and Morsi, A-M.M., 2002, Ostracode turnover and sea-level changes associated with the Paleocene-Eocene thermal maximum: Geology, v. 30, p. 23-26.

Stap, L., Lourens, L.J., Thomas, E., Sluijs A., Bohaty, S., Zachos, J.C., 2010, High-resolution deep-sea carbon and oxygen isotope records of Eocene Thermal Maximum 2 and H2: Geology, v. 38, p. 607-610.

Stap, L., Sluijs, A., Thomas, E., Lourens, L., 2009, Patterns and magnitude of deep sea carbonate dissolution during Eocene Thermal Maximum 2 and H2, Walvis Ridge, southeastern Atlantic Ocean: Paleoceanography, v. 24, p. PA1211.

Steineck, P.L., and Thomas, E., 1996, The latest Paleocene crisis in the deep sea: Ostraocde succession at Maud Rise, Southern Ocean: Geology, v. 24, p. 583-586.

Stepanova, A., and Lyle, M., 2014, Deep-sea ostracoda from the eastern equatorial Pacific (ODP Site 1238) over the last 460 ka.: Marine Micropaleontology, v. 111, p. 100-117.

Storey, M., Duncan, R.A., and Swisher, C.C., 2007, Paleocene-Eocene thermal maximum and the opening of the northeast Atlantic: Science, v. 316, p. 587-589.

Tarhan, L.G., Droser, M.L., Gehling, J.G., and Dzaugis, M.P., 2017, Microbial mat sandwiches and other anactualistic sedimentary features of the Ediacara Member (Rawnsley Quartzite, South Australia): Implications for interpretation of the Ediacaran sedimentary record: Palaios, v. 32, p. 181–194.

Thomas, E., 2003, Extinction and food at the sea floor: A high-resolution benthic foraminiferal record across the initial Eocene thermal maximum, Southern Ocean Site 690, *in* Wing, S., Gingerich, P., Schmitz, B., and Thomas, E., eds., Causes and Consequences of Globally Warm Climates of the Paleogene, v. 369, p. 319-332.

Thomas, E., 2007, Cenozoic mass extinctions in the deep sea: What perturbs the largest habitat on Earth? *in* Monechi, S., Coccioni, R., and Rampino, M., eds., Large ecosystem perturbations: causes and consequences: Geological Society of America Special Paper, v. 424, p. 1-23.

Thorp, J.H., 2003, Arthropoda and related groups, *in* Resh, V.H., and Carde, R.T., eds., Encyclopedia of Insects: New York, Elsevier Science, 1266 p.

Tucholke, B.E., and Vogt, P.R., et al., 1979, Western North Atlantic: Sedimentary evolution and aspects of tectonic history, *in* Tucholke, B.E., Vogt, P.R., et al., eds., Initial Reports of the Deep Sea Drilling Project, v. 43, p. 791-825.

Urbanek, A., 1993, Biotic crises in the history of Upper Silurian graptoloids: A palaeobiological model: Historical Biology, v. 7, p. 29-50.

Wade, M., 1969, Medusae from uppermost Precambrian or Cambrian sandstones, central Australia: Palaeontology, v. 12, p. 351–365.

Wade, M., 1972, Hydrozoa and Scyphozoa and other medusoids from the Precambrian Ediacara fauna, South Australia: Palaeontology, v. 15, p. 197–225.

Waggoner, B., 2003, The Ediacaran biotas in space and time. Integrative and Comparative Biology: v. 43, p. 104–113.

Webb, A.E., Leighton, L.R., Schellenberg, S.A., Landau, E.A., Thomas, E., 2009, Impact of the Paleocene-Eocene thermal maximum on deep-ocean microbenthic community structure: Using rank-abundance curves to quantify paleoecological response: Geology, v. 37, p. 783-786.

Westerhold, T., Röhl, U., Laskar, J., Raffi, I., Bowles, J., Lourens, L.J., Zachos, J.C., 2007, On the duration of magentochrons C24r and C25n and the timing of early Eocene global warming events: implications from the Ocean Drilling Program Leg 208 Walvis Ridge depth transect: Paleoceanography, v. 22, PA2201.

Winguth, A.M.E., Thomas, E., and Winguth, C., 2012, Global decline in ocean ventilation, oxygenation, and productivity during the Paleocene-Eocene Thermal Maximum: implications for the benthic extinction: Geology, v. 40, p. 263-266.

Xiao, S. and Laflamme, M., 2009, On the eve of animal radiation: phylogeny, ecology, and evolution the Ediacara biota: Trends in Ecology and Evolution, v. 24, p. 31-40.

Yamaguchi, T., Bornemann, A., Matsui, H., and Nishi, H., 2017a, Latest Cretaceous/Paleocene deep-sea ostracode fauna at IOPD Site U1407 (western North Atlantic) with special reference to the Cretaceous/Paleogene boundary and the Latest Danian Event: Marine Micropaleontology, v. 135, p. 32-44.

Yamaguchi, T., Matsui, H., and Nishi, H., 2017b, Taxonomy of Maastrichtian-Thanetian deep-sea ostracodes from U1407, IODP Exp 342, off Newfoundland, Northwestern Atlantic, part 1: Families Cytherellidae, Bairdiidae, Pontocyprididae, Bythocytheridae, and Cytheruridae: Paleontological Research, v. 21, p. 54-75.

Yamaguchi, T., Matsui, H., and Nishi, H., 2017c, Taxonomy of Maastrichtian-Thanetian deep-sea ostracodes from U1407, IODP Exp 342, off Newfoundland, Northwestern Atlantic, part 2: Families Eucytheridae, Krithidae, Thaerocytheridae, Trachyleberididae, and Xestoleberididae: Paleontological Research, v. 21, p. 97-121.

Yamaguchi, T. and Norris, R.D., 2012, Deep-sea ostracode turnovers through the Paleocene-Eocene thermal maximum in DSDP Site 401, Bay of Biscay, North Atlantic: Marine Micropaleontology, v. 86-78, p. 32-44.

Yamaguchi, T., and Norris, R.D., 2015, No place to retreat: Heavy extinction and delayed recovery on a Pacific guyot during the Paleocene-Eocene Thermal Maximum: Geology, v. 43, p. 443-446.

Yamaguchi, T., Norris, R.D., and Bornemann, A., 2012, Dwarfing of ostracodes during the Paleocene-Eocene Thermal Maximum at DSDP Site 401 (Bay of Biscay, North Atlantic) and its implication for changes in organic carbon cycle in deep-sea benthic ecosystem: Palaeogeography, Palaeoclimatology, Palaeoecology, v. 346-347, p. 130-144.

Yasuhara, M., Cronin, T.M., Martínez Arbizu, P., 2008, Abyssal ostracods from the South and Equatorial Atlantic Ocean: Biological and paleoceanographic implications: Deep-Sea Research Part I, v. 55, p. 490-497.

Yasuhara, M., Hunt, G., Cronin, T.M., Hokanishi, N., Kawahata, H., Tsujimoto, A., and Ishtake, M., 2012, Climatic forcing of Quaternary deep-sea benthic communities in the North Pacific Ocean: Paleobiology, v. 38, p. 162-179.

Yasuhara, M., Hunt, G., Cronin, T.M., Okahashi, H., 2009, Temporal latitudinal-gradient dynamics and tropical instability of deep-sea species diversity: PNAS, v. 106, p. 21717-21720.

Zachos, J.C., Bohaty, S.M., John, C.M., McCarren, H., Kelly, D.C., and Nielsen, T., 2007, The Paleocene-Eocene carbon isotope excursion: constraints from individual shell planktonic foraminifer records: Philosophical Transactions of the Royal Society A, v. 365, p. 1829-1842.

Zachos, J.C., Dickens, G.R., and Zeebe, R.E., 2008, An early Cenozoic perspective on greenhouse warming and carbon-cycle dynamics: Nature, v. 451, p. 279-283.

Zachos, J.C., McCarren, H., Murphy, B., Rohl, U., and Westerhold, T., 2010, Tempo and scale of late Paleocene and early Eocene carbon isotope cycles: Implications for the origin of hyperthermals: Earth and Planetary Science Letters, v. 299, p. 242-249.

Zachos, J.C., Röhl, U., Schellenberg, S.A., Sluijs, A., Hodell, D.A., Kelly, D.C., Thomas, E., Nicolo, M., Raffi, I., Lourens, L.J., McCarren, H., and Kroon, D., 2005, Rapid Acidification of the ocean during the Paleocene-Eocene Thermal Maximum: Science, v. 308, p. 1611-1615.